Automated Assessment of Defects in Bridge Structures

Final Report
April 2025

IOWA STATE UNIVERSITY
Institute for Transportation

Sponsored by
Iowa Department of Transportation
and Federal Highway Administration
(SPR-RE-222(014)-8H-00,
InTrans Project 22-798)

The preparation of this report was financed in part through funds provided by the Iowa Department of Transportation through its "Second Revised Agreement for the Management of Research Conducted by Iowa State University for the Iowa Department of Transportation" and its amendments.

Technical Report Documentation Page

1. Report No.	2. Government Accession No.	3. Recipient's Catalog No.
InTrans Project 22-798		

4. Title and Subtitle	5. Report Date
Automated Assessment of Defects in Bridge Structures	April 2025
	6. Performing Organization Code
7. Author(s)	**8. Performing Organization Report No.**
Behrouz Shafei (orcid.org/0000-0001-5677-6324) and Ibrahim Odeh (orcid.org/0009-0004-1553-829X)	InTrans Project 22-798
9. Performing Organization Name and Address	**10. Work Unit No. (TRAIS)**
Bridge Engineering Center Iowa State University 2711 South Loop Drive, Suite 4700 Ames, IA 50010-8664	**11. Contract or Grant No.**
12. Sponsoring Organization Name and Address	**13. Type of Report and Period Covered**
Iowa Department of Transportation 800 Lincoln Way Ames, IA 50010 Federal Highway Administration 1200 New Jersey Avenue, SE Washington, DC 20590	Final Report
	14. Sponsoring Agency Code
	SPR-RE22(014)-8H-00

15. Supplementary Notes

Visit https://bec.iastate.edu for color pdfs of this and other research reports.

16. Abstract

Effective and timely bridge inspections are crucial for extending bridge lifespans and preventing catastrophic failures. Traditional inspection methods often involve manual visual assessments and can be time-consuming, labor-intensive, and prone to human error. Recent technological advancements in unmanned aerial vehicles (UAVs), artificial intelligence (AI), and machine learning (ML) offer promising solutions to these challenges. When high-quality images captured by UAVs are analyzed using AI and ML algorithms, structural defects can be detected and quantified with greater precision and efficiency than manual inspections.

The primary objective of this research was to enhance the accuracy and efficiency of structural inspections by integrating UAV technology for image capture and AI-based detection models for analysis. High-resolution images of bridge components were collected using UAVs operating at various distances and angles and were then processed through a custom-developed convolutional neural network (CNN) to detect critical defects such as cracking and spalling. The model's performance was assessed through multiple case studies, and its ability to detect and quantify defects under different conditions was validated against field data. This approach yielded significant improvements over traditional bridge inspection methods in terms of the precision with which structural vulnerabilities were identified and accurately quantified defect dimensions.

Furthermore, the research incorporated the development of three-dimensional (3D) models of bridge structures using commercially available software to enable detailed structural assessments. High-resolution UAV imagery was successfully integrated into 3D modeling software to generate detailed models of bridge structures enabling comprehensive structural assessments and allowing for the quantification of detected defects. The results demonstrate the potential of UAV-based inspections combined with AI-powered detection models to revolutionize bridge inspection practices by offering a more reliable, efficient, and cost-effective approach to infrastructure maintenance and supporting more informed decision-making for infrastructure safety and longevity.

17. Key Words		18. Distribution Statement	
artificial intelligence—bridge inspection—convolutional neural network—unmanned aerial vehicles—machine learning		No restrictions.	
19. Security Classification (of this report)	**20. Security Classification (of this page)**	**21. No. of Pages**	**22. Price**
Unclassified.	Unclassified.	112	NA

Form DOT F 1700.7 (8-72) **Reproduction of completed page authorized**

AUTOMATED ASSESSMENT OF DEFECTS IN BRIDGE STRUCTURES

Final Report
April 2025

Principal Investigator
Behrouz Shafei, Associate Professor
Bridge Engineering Center, Iowa State University

Research Assistant
Ibrahim Odeh

Authors
Behrouz Shafei and Ibrahim Odeh

Sponsored by
Iowa Department of Transportation and
Federal Highway Administration
(SPR-RE22(014)-8H-00)

Preparation of this report was financed in part
through funds provided by the Iowa Department of Transportation
through its Research Management Agreement with the
Institute for Transportation
(InTrans Project 22-798)

A report from
Bridge Engineering Center
Iowa State University
2711 South Loop Drive, Suite 4700
Ames, IA 50010-8664
Phone: 515-294-8103 / Fax: 515-294-0467
https://bec.iastate.edu

TABLE OF CONTENTS

LIST OF FIGURES

LIST OF TABLES

ACKNOWLEDGMENTS

The research team would like to acknowledge the Iowa Department of Transportation (DOT) for sponsoring this research and the Federal Highway Administration (FHWA) for the state planning and research (SPR) funds used for this project. The research team would also like to thank the Iowa DOT technical advisory committee (TAC) members on this project, including James Hauber, Joseph Stanisz, Michael Todsen, Brian Johnson, and Curtis Carter.

EXECUTIVE SUMMARY

Background and Problem Statement

Bridges play a critical role in transportation infrastructure, providing essential connections for economic and social activities. Due to constant exposure to environmental stressors, traffic loads, and natural wear, bridges are vulnerable to deterioration, including the development of cracks, corrosion, spalling, and other structural defects. Effective and timely inspection of bridges is crucial for ensuring safety, extending bridge lifespans, and preventing catastrophic failures. Traditional inspection methods, which often involve manual visual assessments, can be time-consuming, labor-intensive, and prone to human error. These limitations necessitate more advanced, reliable, and efficient techniques for bridge inspection and maintenance. Recent technological advancements, particularly in the fields of unmanned aerial vehicles (UAVs), artificial intelligence (AI), and machine learning (ML), offer promising solutions to the challenges posed by traditional inspection methods. UAVs, commonly known as drones, provide the ability to capture high-resolution images of bridge structures from various angles and distances, making them an invaluable tool for structural health monitoring. When combined with AI and ML algorithms, these images can be analyzed to detect and quantify structural defects with greater precision and efficiency than manual inspections.

Research Description

This research project developed advanced models for detecting and quantifying structural defects in bridge infrastructure using UAVs and machine learning algorithms. The primary objective was to enhance the accuracy and efficiency of structural inspections by integrating drone technology for image capture and AI-based detection models for analysis. To ensure comprehensive data coverage, high-resolution images of bridge components were collected using UAVs operating at various distances and angles. The captured images were then processed through a custom-developed convolutional neural network (CNN) to detect critical defects such as cracks and spalling. The model's performance was assessed through multiple case studies, and its ability to detect and quantify defects under different conditions was validated against field data. This approach yielded significant improvements over traditional bridge inspection methods in terms of the precision with which structural vulnerabilities were identified and provided accurate quantification of defect dimensions.

Furthermore, the research incorporated the development of three-dimensional (3D) models of bridge structures using software such as Bentley iTwin Capture, Pix4D, and Autodesk ReCap Pro. These 3D models enabled detailed structural assessments and laid a foundation for predictive maintenance strategies. The results demonstrated the potential of UAV-based inspections combined with AI-powered detection models to revolutionize bridge inspection practices, offering a more reliable, efficient, and cost-effective approach to infrastructure maintenance.

Key Findings

- The developed model, integrating UAV technology with ML/AI algorithms, demonstrated significant improvements over traditional bridge inspection methods in the detection of structural defects such as cracks and spalling. The developed models were particularly effective in identifying fine cracks and distinguishing them from natural concrete segmentation lines. Their accuracy was validated by comparing the predictions with field data, which resulted in a low margin of error and demonstrated the reliability of the developed framework as a tool for bridge inspections.
- The research highlighted the importance of optimal drone positioning during image capture. Drones operated at closer distances provided more detailed and accurate images, which enhanced the model's ability to detect smaller defects. Conversely, greater distances, though useful for capturing the overall structure, led to lower detail in defect detection. This finding emphasizes the need to balance safety and detail when conducting aerial inspections.

The study successfully integrated high-resolution drone imagery into 3D modeling software, such as Bentley iTwin Capture and Pix4D, to generate detailed models of bridge structures. These models enabled comprehensive structural assessments and allowed for the quantification of detected defects. The use of these models can facilitate predictive maintenance strategies, supporting more informed decision-making for infrastructure safety and longevity.

CHAPTER 1: INTRODUCTION

1.1 Background

The task of inspecting and detecting damage in bridges has traditionally been a challenging aspect of civil infrastructure management. Historically, these duties have primarily been executed manually, often involving physical attendance by the inspector. This conventional approach presents various obstacles to inspection, such as the lack of accessibility to difficult/far areas, safety risks for inspectors, and the time-consuming nature of the whole process. The need for routine inspections to ensure structural integrity and public safety further compounds these obstacles. Moreover, the regular inspection process could be influenced by subjective judgments and varying environmental conditions, potentially affecting the consistency and reliability of the assessments.

The introduction of drone technology marked a significant enhancement and shift in this field. Unmanned aerial vehicles (UAVs), or drones, have rapidly spread and developed, offering innovative solutions to the limitations and challenges of regular inspection processes. With advanced sensors and high-quality cameras, drones can easily access hard-to-reach areas and provide more detailed images and data for assessing the condition of bridge components. This technology enhances safety by reducing the need for inspectors' direct involvement in risky and unreachable areas, which enables a more comprehensive and less intrusive inspection process. The mobility of drones has thus positioned them as a valuable tool for bridge inspections.

Integrating artificial intelligence (AI) and machine learning (ML) in data analysis is the final step in automating bridge inspections. AI and ML algorithms are adept at processing a massive amount of complex data, such as the imagery and sensor readings collected by phones, satellites, or drones. These technologies can detect damage, patterns, and potential structural issues more accurately and rapidly than inspector analysis. The ability of AI to learn and improve over time and with more training means that the system becomes more efficient and accurate with each inspection.

1.2 Research Objectives

The study aimed to leverage and identify opportunities to adopt UAVs to enhance the damage detection, inspection, and three-dimensional (3D) modeling of bridge infrastructure, thereby benefiting the department of transportation (DOT) and digital construction sectors. Additional objectives of the study included the following:

- **Development of an integrated system**. The primary goal of this research was to develop a comprehensive and integrated system that combines drone technology with advanced AI and ML algorithms. The system resulting from this research was designed specifically for the inspection of bridge structures and the detection of damage. By leveraging the capabilities of drones for data collection and AI/ML for data analysis, the system provided a more efficient and accurate solution compared to traditional bridge inspection methods, ensuring the timely identification of structural issues and enhancing the overall reliability of inspections.

- **Accuracy and efficiency in damage detection**. A key aim of this study was to significantly improve the accuracy and speed with which structural defects and potential issues within bridge structures are identified. Traditional inspection methods are often time-consuming and prone to human error. By utilizing automated systems driven by AI and ML, the outcome of this research helped detect and classify defects with higher precision while greatly reducing the time required for inspections. This enhanced accuracy and efficiency allowed for quicker identification of critical issues, ultimately contributing to improved safety and maintenance practices.
- **Predictive maintenance and decision-making**. Another essential objective was to enable predictive maintenance and support informed decision-making through continuous data analysis over time. By monitoring changes in the structural health of bridges, this system showed promise to forecast potential deterioration before it reaches critical levels. This predictive approach will not only extend the lifespan of bridges but also reduce maintenance costs and ensure that interventions are planned proactively, thereby minimizing the risks associated with unexpected structural failures.

1.3 Research Benefits

Incorporating drone technology with AI and ML for bridge inspections offers many benefits, such as improving the efficiency and accuracy of damage detection. By utilizing drones, the need for manual, physically demanding inspections will be highly reduced, lowering the risk of accidents and ensuring the safety of inspectors. This approach is also far more cost-effective than traditional inspection methods, decreasing labor costs and the time needed for routine inspections through fast, detailed, and comprehensive data processing and analysis.

The developed system's AI and ML component allows for advanced data processing and the identification of structural defects and potential issues with precision and speed unattainable by traditional methods. This will not only control the inspection process but also enable predictive maintenance, allowing for the early detection and rectification of problems ultimately extending the lifespan of bridges.

Finally, the data-driven nature of this technology supported informed decision-making, providing a robust foundation for infrastructure management and planning. This innovative method can revolutionize bridge maintenance, ensuring safer and more reliable infrastructure across varied environments and conditions.

CHAPTER 2: DAMAGE DETECTION ALGORITHMS AND TECHNOLOGIES

2.1 Overview

Maintaining the functionality of bridge structures is critical to ensuring public safety and avoiding costly repairs and closures. Over time, bridges can suffer from various forms of damage that compromise their structural integrity and performance. Therefore, the detection and quantification of damage in a timely and cost-effective manner is of great importance for the management of transportation networks.

Traditionally, bridge components are evaluated through visual inspections, during which engineers in charge physically inspect the component(s) of concern. Visual inspections involve meticulous scrutiny by human inspectors to detect signs of deterioration and damage. This time-consuming practice primarily relies on the inspector's expertise to identify anomalies as much as access permits. Nevertheless, direct inspections involve inherent limitations that affect their accuracy and efficiency (Mirzazade et al. 2022).

Subjectivity in human interpretation introduces inconsistencies in damage identification and categorization, potentially affecting condition assessment and rating. For instance, in detecting hairline cracks or subsurface defects that are often missed by visual inspections, AI models trained on large datasets can identify patterns and anomalies that are not easily discernible to the human eye. A case study involving the inspection of a concrete bridge deck showed that an AI-based crack detection model identified 30% more microcracks than a team of experienced inspectors, highlighting the technology's enhanced sensitivity and precision (Saseethar and Narkhede 2024). Meanwhile, adverse environmental conditions, such as poor lighting, can similarly reduce the accuracy of evaluations by human inspectors.

Difficulties in access to certain bridge elements, such as those at high elevations or submerged in water, can also hamper thorough examinations. For example, an underwater inspection using autonomous underwater vehicles (UUVs) equipped with AI-based sonar imaging can safely and effectively identify structural issues in submerged bridge components, an area traditionally difficult and dangerous for divers to access (Ioannou et al. 2024).

The outlined constraints underscore the need for innovative strategies, such as capturing images using drones and processing them through AI and ML algorithms, to enhance accuracy, efficiency, and objectivity in bridge condition assessment (Ayele et al. 2020, Kebig et al. 2021). In particular, advancements in AI/ML have introduced the potential to transform how bridge structures are inspected and evaluated. Automated inspections can also generate vast amounts of data that can be analyzed to identify trends, prioritize maintenance, and optimize inspection intervals.

The structural integrity of bridges is crucial for ensuring public safety and infrastructure longevity. Figure 2.1 depicts the prevalence of cracks in bridge components.

Figure 2.1. Examples of cracks in bridge components: (a) abutment, (b) concrete girder, (c) pier, (d) steel girder, (e) deck, and (f) column

Figure 2.2 provides a comprehensive view of the diverse types of damage observed in these critical structures, emphasizing the multifaceted challenges engineers and maintenance teams must address to mitigate risks and uphold the resilience of bridge infrastructure.

(a)

(b)

(c)

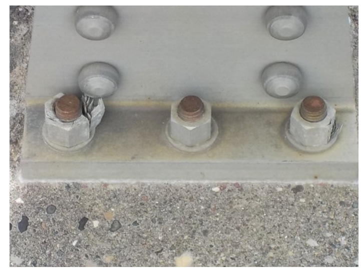

(d)

(e)

(f)

(g)

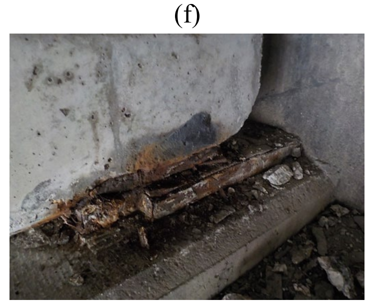

(h)

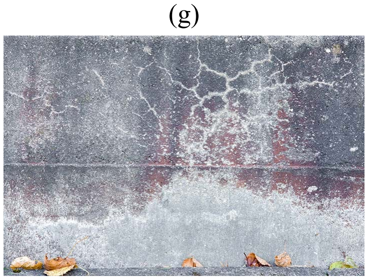

(i)

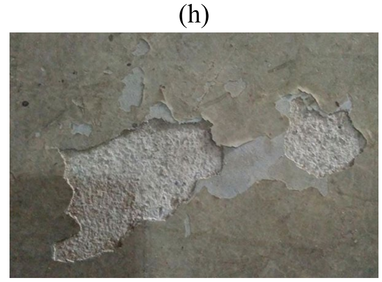

(j)

Figure 2.2. Examples of other types of damage observed in bridge components: (a) concrete spalling, (b) efflorescence, (c) girder corrosion, (d) galvanic corrosion in bolts, (e) rebar exposure, (f) rebar corrosion, (g) concrete column spalling, (h) bed corrosion, (i) concrete discoloration, and (j) concrete delamination

Bridge structures are commonly prone to a wide variety of damage types. Table 2.1 compiles various types of damage that are investigated in the available literature, while Figure 2.3 presents the percentage frequencies of damage that are discussed in the literature.

Table 2.1. Main damage types investigated in the available literature

Damage Type	References
Crack	Kun et al. 2022, Perry et al. 2022, Seo et al. 2022, Mir et al. 2022, Munawar et al. 2022, Jeong et al. 2022, Mirzazade et al. 2022, Guo et al. 2021, Savino and Tondolo 2021, Montaggioli et al. 2021, Qin et al. 2021, Chun et al. 2021, Kim et al. 2021, Fan 2021, Deng et al. 2021, Quqa et al. 2022, Yang et al. 2020, Abdelkader et al. 2020, Li et al. 2020, Kong et al. 2020, Liu and El-Gohary 2020, Perry et al. 2020, Arong et al. 2020, Bhowmick et al. 2020, Zhu et al. 2020, Zhou et al. 2019, Morgenthal et al. 2019, Song et al. 2019, Medhi et al. 2019, Elbeheri and Zayed 2018, Gulgec et al. 2019, Modarres et al. 2018, Seo et al. 2018, Reagan et al. 2017, Khaloo et al. 2018, Cha and Choi 2017, Aliakbar et al. 2016, Miyamoto et al. 2014, Miyamoto 2013, Kusunose et al. 2003, Liu and Gao 2022, Meng et al. 2022, Malek et al. 2022, Zhai et al. 2022
Corrosion, rust, and coating erosion	Chun et al. 2021, Elbeheri and Zayed 2018, Arong et al. 2020, Bianchi et al. 2022, Munawar et al. 2022, Jeong et al. 2022, Arong et al. 2020
Spalling and peeling	Seo et al. 2022, Jeong et al. 2022, Chun et al. 2021, Fan 2021, Arong et al. 2020, Zhu et al. 2020, Elbeheri and Zayed 2018, Galdelli et al. 2022
Exposed reinforcing bars; uncovered/oxidized metal bar	Chun et al. 2021, Arong et al. 2020, Zhu et al. 2020, Fan 2021, Belcore et al. 2022
Expansion joints damage	Kim et al. 2021, Reagan et al. 2017, Chun et al. 2021
Connection damage; loose bolt; fracture of steel bolts; failure of joint; moisture-related damage at joints	Reagan et al. 2017, Reagan et al. 2017, Zhou et al. 2019, Chun et al. 2021, Arong et al. 2020, Seo et al. 2018
Water leakage; water damage caused by water coming from the deck; drainage issues	Arong et al. 2020, Chun et al. 2021, Seo et al. 2018, Belcore et al. 2022
Efflorescence; free lime	Arong et al. 2020, Chun et al. 2021, Jeong et al. 2022, Fan 2021
Weathering of wood	Seo et al. 2022
Discoloration	Jeong et al. 2022, Seo et al. 2018, Galdelli et al. 2022, Chun et al. 2021
Floating	Arong et al. 2020
Exposed anchorage zone	Arong et al. 2020
Damaged truss chord	Reagan et al. 2017
Prestressing of fix section	Arong et al. 2020
Displacement and frequency responses	Medhi et al. 2019, Chun et al. 2021
Delamination	Savino and Tondolo 2021, Chun et al. 2021

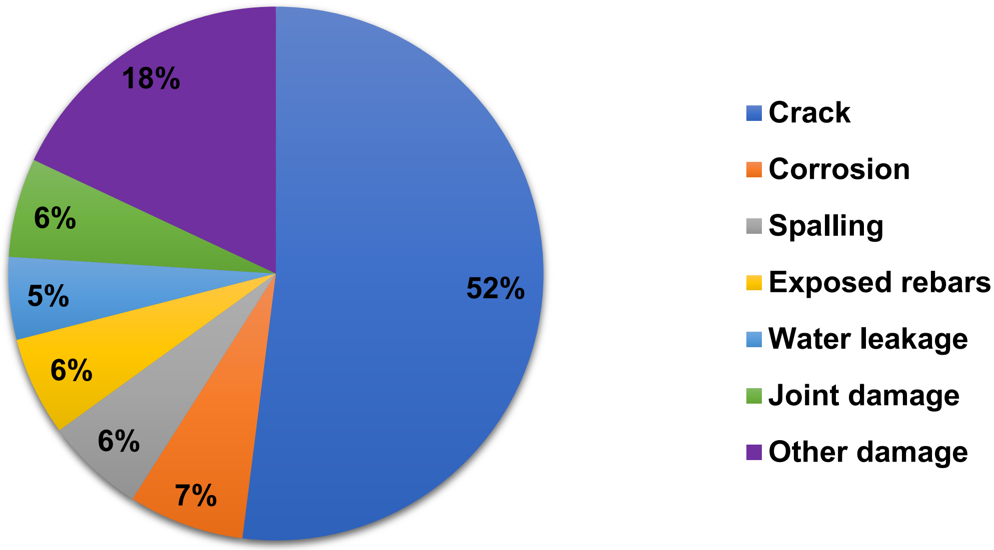

Figure 2.3. Percentage of studies dedicated to each damage type in the current literature

As mentioned above, the types of damage observed in bridges varies depending on the mechanical and environmental stressors they are exposed to (Shafei et al. 2012, 2013). Mechanical stressors originating from traffic loads and dynamic forces can induce structural fatigue, excessive deformation, and cracking (Alipour and Shafei 2016a, Alipour and Shafei 2016b, Alipour and Shafei 2022, Shi et al. 2020, Aldemir and Turer 2021). On the other hand, environmental stressors, such as temperature, moisture, freeze-thaw cycles, and exposure to aggressive chemicals, can initiate steel corrosion, crack formation, and concrete spalling (Chen et al. 2018, Tran et al. 2020, Shi et al. 2020).

To ensure that bridge components meet the expected strength and serviceability requirements, regular condition assessments are devised (Khatami et al. 2016, 2021, 2023). Such assessments include detecting and quantifying the extent of damage to the bridge structure (Kulkarni and Shafei 2018, Zhang and Yuen 2022, Azad and Shafei 2025). This is a crucial task for various transportation agencies, as damage can accumulate over time and cause sudden failure if it remains undetected. The collapse of the Silver Bridge over the Ohio River in 1967, which was attributed to hidden corrosion in suspension chain links, serves as a stark reminder of the consequences of overlooked deterioration. More than half a century later, the failure of the Morandi Bridge in Genoa, Italy, in 2018, was found to be due to a combination of factors, including corrosion and faulty concrete, which had not been detected through regular inspections (Piscitelli et al. 2020). Most recently, the Tretten Bridge, a 10-year-old wooden road bridge in southern Norway, collapsed and fell into the river in August 2022 due to a block shear failure at the junction between the wooden and steel/dowel components. The referenced bridge was subject to a thorough inspection in 2021 and a rapid inspection in June 2022 with no faults reported. The consequences of bridge failures illustrate the critical need for advanced inspection strategies that address the limitations of traditional visual assessments. Furthermore, the early detection and repair of defects can significantly help reduce direct and indirect costs while extending the service life of bridges (Malekloo et al. 2021).

To improve the efficiency and accuracy of damage detection, visual inspection techniques are often paired with nondestructive evaluation (NDE) methods. NDE represents a suite of methods designed to assess the integrity and health of structural materials and systems without causing any physical damage or disruption to their functionality. These methods are capable of finding hidden defects, anomalies, and signs of deterioration that may not be detected during visual inspections. NDE methods encompass diverse approaches, such as ultrasonic testing (Zhang et al. 2023), impact echo testing (Hafiz et al. 2022), ground-penetrating radar (Zhang et al. 2023), infrared thermography (Sakagami et al. 2014), radiographic testing (Uesaka et al. 2018), eddy current testing (Ichinose et al. 2007), and acoustic emission testing (Nair and Cai 2010). NDE methods, however, often require specialized skills and equipment, which can impose constraints on how large-scale civil infrastructure, such as bridges, can be scanned in real-world applications.

With imaging technologies and AI/ML algorithms, new capabilities have emerged for bridge damage detection. In particular, image-based inspection has received growing attention, as it provides a visual representation of the bridge structure, facilitating the process of identifying and quantifying damage (Qiao et al. 2021). Various strategies can be used to collect high-quality images from bridges, including the use of cameras by human inspectors, UAVs, and UUVs (Jeong et al. 2022, Perry et al. 2020, Kun et al. 2022). Despite the benefits introduced by using high-resolution cameras, which can capture several thousands to millions of images from bridge components, real advantages to the bridge industry remain limited without methods in place for automated damage detection and quantification.

To address this gap, AI/ML algorithms have been rapidly developed in recent years to automatically identify and classify different types of damage (Dipankar and Suman 2023, Ai et al. 2023). With proper training, such algorithms have proved to be promising in making the condition assessment process more accurate and efficient, especially by reducing the risk of human error. The available algorithms span various deep learning algorithms, such as convolutional neural networks (CNNs) (Pantoja-Rosero et al. 2022, Qin et al. 2021), support vector machines (SVMs) (Arong et al. 2020, Fan 2021), random forests (Belcore et al. 2022), and decision trees (Allah Bukhsh et al. 2020, Naser 2021). While the listed algorithms offer several features, there are certain tradeoffs in their computational efficiency, accuracy, and ease of implementation. Hence, choosing appropriate algorithms that can meet the damage detection and assessment needs of bridge inspections is often a critical task, requiring significant AI/ML experience. Given that most bridge engineers and inspectors do not have a computer vision background, there is a need for comparative studies to systematically evaluate and recommend the algorithms of choice for a variety of bridge assessment tasks.

Considering the outlined questions and gaps, this literature review first provides a detailed perspective on the types of damage that can be automatically detected in bridge structures. The damage types span from surface cracks, which are frequently investigated, to those deemed as signs of abnormal conditions. The literature review then discusses how the identified damage types can be assessed not only qualitatively but also quantitatively. This is critical to ensure that the outputs of advanced damage detection strategies are guided to deliver what is needed for real-world bridge maintenance and management (Section 2.2). With the wealth of information obtained, image-based data collection techniques are investigated. Given that recorded images are often the inputs for AI/ML algorithms, the properties expected from image databases, in terms of resolution, number, and quality, are examined (Section 2.3). After determining the necessary inputs, the applications of various AI/ML algorithms are explored. This is one of the unique contributions of the current study, as it establishes not only input and output requirements but also algorithms appropriate for damage detection and quantification in each of the main bridge components (Section 2.4). This section also includes a rigorous assessment of the advantages and limitations of various AI/ML algorithms employed to date. The literature review concludes with a set of recommendations covering data collection, preprocessing, feature extraction, model selection, and prediction validation (Section 2.5). The outcome serves as a holistic reference for researchers and practitioners not only in the bridge engineering domain but also in other engineering domains that can equally benefit from a transition from traditional to new inspection and condition assessment strategies.

2.2 Bridge Damage Types and Characteristics

Bridge structures are prone to damage from two broad categories of causes: (1) damage due to sudden extreme events, such as earthquakes and vehicle/vessel collisions, and (2) damage due to continuous deterioration processes, such as corrosion and fatigue. Despite the importance of both categories, this study's investigations are mainly focused on the instances of damage incurred by the latter category of causes, while the findings remain applicable to the former category of causes as well. Various measurements and units have been used to express damage both qualitatively and quantitatively for the condition assessment of bridges. Features, including color, texture, and size, are widely used to classify various types of damage, such as cracking, rust, and peeling paint.

Among the most common damage types is the formation and propagation of cracks. This has been explored by a number of AI/ML-related research studies, including Li et al. (2020), Yang et al. (2020), Wang et al. (2020), Adel et al. (2021), Deng et al. (2021), Guo et al. (2021), Montaggioli et al. (2021), Qin et al. (2021), Savino and Tondolo (2021), Galdelli et al. (2022), Mir et al. (2022), Mirzazade et al. (2022), Perry et al. (2020 and 2022), Quqa et al. (2022), and Zhai et al. (2022). Crack detection models in the cited studies cover various sizes, patterns, and types of cracks in different materials. For example, in steel components, cracks can be a result of imperfections in welded connections, fatigue due to repetitive traffic loads, or corrosion caused by environmental stressors (Quqa et al. 2022). On the other hand, cracks in concrete components can be due to a completely different set of causes, including curing issues, shrinkage and creep, temperature fluctuations, and freeze-thaw cycles. Such a variety has required the detection models to capture cracks with a width of 1 mm (or even less), depending on the components of interest and their serviceability requirements.

In Adel et al. (2021), pits were defined as small concrete fragments that fall out of cracks formed in reinforced concrete (RC) deck slabs subjected to moving wheel loads. The referenced study explored the detection of pits along with surface cracks. In Perry et al. (2020), structural defects, such as cracking and spalling, were detected, and the defect width and area were quantified. Perry et al. (2022) transformed the pixel information of cracks identified in images into a Cartesian coordinate system to find crack dimensions through measuring the length of corresponding line segments. Galdelli et al. (2022) identified defects, such as holes, bumps, and color variations, by pixel detection. The outputs were a set of regions and bounding boxes capturing the expected locations of defects. In Savino and Tondolo (2021), a deep learning-based algorithm was employed to classify exterior concrete surfaces into undamaged, cracked, and delaminated surfaces. Relevant details used for delaminated surfaces included the oxide color, texture of aggregates, and width and depth of cracks. The referenced study primarily established the classification but did not measure the extent of damage further.

Morgenthal et al. (2019) presented a framework for automated crack detection in concrete structures using an unmanned aircraft system. This study captured the continuous path of cracks with different widths and angles. Similarly, Bhowmick et al. (2020) proposed a computer vision-based framework to utilize a set of high-quality images of randomly selected cracks to train the necessary algorithms and determine the crack width and length on various concrete surfaces. For this purpose, a pixel-level identification class was used to quantify the crack size. The length, area, maximum width, mean width, and orientation of individual cracks were measured after locating the cracks. In separate studies, Aliakbar et al. (2016) detected cracks in real-time images from structural sites, and Reagan et al. (2017) detected sub-millimeter cracks in abutment walls and other bridge components. Liu and Gao (2022) and Meng et al. (2022) introduced methods for crack detection in concrete structures, with the latter utilizing a drone-based system for real-time detection. The referenced study located the cracks and worked toward the quantification of maximum crack width. Xu et al. (2022) proposed a concrete crack segmentation network, while Malek et al. (2022) used augmented reality for crack detection.

ML methods have also been employed for damage assessment in bridge components, as indicated in past studies, including Song et al. (2019), Kun et al. (2022), and Mir et al. (2022). Specifically, Cha and Choi (2017), Modarres et al. (2018), Yang et al. (2020), Li et al. (2020), Guo et al. (2021), Qin et al. (2021), Mirzazade et al. (2022), and Tang et al. (2023) used ML techniques for crack detection. Among them, Mir et al. (2022) evaluated the degree of damage by focusing on the range of the crack width. Low-brightness regions were extracted using a dynamic threshold method and divided into cracked and non-cracked regions. Crack width classification was performed, and the datasets were divided into three classes, based on the crack widths, spanning from 0 to 9, 9 to 12, and 12 to 16 pixels, as Classes 1, 2, and 3, respectively. Kun et al. (2022) located the cracks on bridge decks and quantified the extent of cracks through pixel-level segmentation of crack paths. Liu and Gao (2022) detected cracks with the ability to determine their associated areas and edges at the pixel level. In Mirzazade et al. (2022), the presence of cracks was evaluated by detecting features based on the texture and color of each surface. The study included a binary classification (not cracked and cracked) and a multiclass classification (intact, simple, and complex). Tang et al. (2023) measured the crack width by utilizing a computer vision method. This method involved crack segmentation and backbone refinement to capture the crack skeleton.

Fatigue-induced crack detection has been studied by Wang et al. (2020). The study was performed on a steel box girder of a 20-year-old suspension bridge. For similar damage detection purposes, Kong et al. (2020) and Zhai et al. (2022) used a combination of real-world and synthetic images while utilizing image processing techniques. Wang et al. (2020) proposed a computer vision-based methodology for monitoring fatigue cracks in U-rib-to-deck weld seams.

Due to the cumulated effects of heavy vehicle loads and initial welding defects, bridge decks made with orthotropic steel-box girders (OSGs) often experience fatigue-induced cracks. These cracks tend to be predominantly situated in the vicinity of U-ribs. The crack length, width, and average width were extracted by Wang et al. (2020) after detecting the cracks. The cracked area was determined by counting the pixels within its segmentation mask. Given that the crack's skeleton is a single-pixel width representation of its shape, the crack length was equivalently quantified as the count of pixels within the skeleton. Furthermore, the measurement of the crack width was performed based on the segmentation mask's horizontal dimension.

Corrosion in steel and exposed reinforcing bars in concrete have been the focus of a set of AI/ML-related studies. Fan (2021) detected rebar exposure, while Arong et al. (2020) and Bianchi et al. (2022) investigated corrosion as well. The proposed methods detected the area of corrosion by identifying the key feature points (e.g., location, direction, length, and area) and then measuring the pixels associated with each. Corrosion is known to consist of two main visual characteristics, i.e., rough texture surface and product color. To identify these two features, Munawar et al. (2022) proposed a version-based ML technique for detecting corrosion and water staining on various bridge surfaces. The referenced study performed segmentation through binary image representation and measured the height and width distributions of the corrosion pixels.

A few AI/ML-related studies have investigated concrete spalling. Among them, Seo et al. (2018) used pixel-based methods to determine the spalled area. In a separate effort, Jeong et al. (2022) presented a damage identification and classification approach to detect spalling on railing posts, decks, pier caps, and other bridge components. Chun et al. (2021) detected multiple forms of damage, including spalling. The referenced study used image captioning to describe the damaged bridge components. An attention mechanism was employed to focus on input image pixels when generating a sentence to describe the damage. Zhu et al. (2020) and Fan (2021) also proposed ML-based frameworks to detect spalling. In Fan (2021), the scalar and vector measures of the digital image spectra were evaluated for spalling detection with SVM-based clustering. A quantification of area ratio and deterioration extent was employed to further evaluate damage ranges.

Some AI/ML-related studies have investigated multiple types of damage. Perry et al. (2020) detected the location of defect areas, such as cracks, spalling areas, and delaminated regions on bridge decks, girders, and other components. Belcore et al. (2022) presented geomatics and ML techniques for the automated detection and classification of images into various classes of damage, including drainage issues, uncovered metal bars, and oxidized rebars. A set of features was considered for each damaged object, while the classification datasets were enriched with derivative features, including spectral, textural, and statistical-based details. Zhu et al. (2020) detected the location of various instances of damage through a computer vision-based method. For this purpose, the images were labeled with designation such as crack, spalling, exposed rebar, pockmark, and intact. In a similar effort, Arong et al. (2020) used an ML technique to detect various damage types, including peeling and exposed steel bars, in bridge components. Medhi et al. (2019) developed a contactless, noninvasive alternative for assessing the displacement and frequency responses of vibrating structures by combining high-resolution images with computer vision techniques and real-time image and signal processing methods.

Chun et al. (2021) covered a wide spectrum of damage types, including displacement, flaking, fissures, slanting, scour, missing material, sinking, exposed rebar, clogging, holes in the concrete, concrete spalling, fractures, cracks, corrosion, deformation, discoloration, degradation of anti-corrosive layers, damaged reinforcement, abnormal expansion, degradation, leaking, and potholes.

Overall, different damage types and characteristics have been used to evaluate the condition state of bridge components. Some of the common measurements have been crack width, spalled area, scratch size, and corrosion region. On the other hand, some studies, such as Aliakbar et al. (2016), Modarres et al. (2018), Khaloo et al. (2018), and Kong et al. (2020), did not quantify the damage but primarily aimed to locate it. The following section provides the necessary details on how the damage types and characteristics of interest can be captured through various technology-enabled data collection techniques. Table 2.2 presents the damage types that are determined by using the AI/ML techniques.

Table 2.2. Quantification of the extent of damage detected in bridge components

Damage Quantification	Reference
Cracks	
Crack location	Malek et al. 2022
Crack width	Mir et al. 2022
Crack area	Liu and Gao 2022
Maximum crack width	Meng et al. 2022
Crack width	Xu et al. 2022
Maximum crack width/angle measurement	Zheng et al. 2022
Crack location	Kun et al. 2022
Crack location, crack length, kink length/angle	Perry et al. 2022
Length and width of cracks	Jeong et al. 2022
Crack size	Quqa et al. 2022
Continuous boundary of cracks, crack length and width	Li et al. 2020
Crack location, length, width, and average width	Wang et al. 2020
Crack geometry, length, width, area, and orientation	Bhowmick et al. 2020
Crack location, width	Morgenthal et al. 2019
Corrosion	
Located corrosion, measured corrosion area	Bianchi et al. 2022
Corrosion location, height, width distributions	Munawar et al. 2022
Spalling	
Spalling numbers, area ratios, and deterioration levels	Fan 2021
Spalled area	Seo et al. 2018
Expansion Joint Gap	
Size of the gap in the bridge deck	Jeong et al. 2022
Gap width	Kim et al. 2021
Other Damage Types	
Detection of defects, such as holes, bumps, and color variation	Galdelli et al. 2022
Quantification of defects, in terms of width and area	Perry et al. 2020

2.3 Image and Data Collection for Bridge Damage Detection

Data collection is a critical step for the detection and quantification of damage in bridges. Data obtained from NDE methods and health monitoring systems often provide valuable information about the condition state of bridge structures. Those methods and systems, however, require specialized skills and equipment, limiting their practical application. As an alternative source of data, direct visual observations (during conventional inspections) and camera-recorded images are frequently used to determine the types and extents of damage. With a transition to automated processes for damage detection, it is vital to know the main characteristics of the images required to provide reliable inputs. In particular, image datasets can be produced by various equipment, including that used by human inspectors, UAVs, and UUVs. The images can be captured by digital cameras of various resolutions or generated through image synthesis approaches. The image quality can also significantly differ depending on, for example, distance, angle, and lighting conditions. Given possible variations, in terms of both quality and quantity, it is critical to have a proper understanding of the capabilities required to obtain images useful for postprocessing through AI/ML techniques.

Several studies have used high-resolution cameras to capture images of bridge decks, walls, piers, and other structural components. In Jeong et al. (2022), two UAVs, i.e., DJI Phantom 4 and DJI Matrice 210 equipped with 12.4-megapixel and 20.8-megapixel cameras, respectively, were used. The images captured were used to identify the instances of damage in concrete columns and cross-laminated timber beams. In Perry et al. (2020), the images were taken using four UAVs: DJI Matrice 600 Pro with a Zenmuse X3 camera (12.4-megapixel resolution), DJI Phantom 4 Pro V2.0 (20-megapixel resolution), DJI Mavic 2 Zoom (12-megapixel resolution), and DJI Mavic 2 Pro (20-megapixel resolution). The high-resolution images obtained from piers, pier caps, decks, and beams were used to generate a 3D point cloud and photorealistic model. Bhowmick et al. (2020) used a video recorded by a UAV with a resolution of 2,160×4,096 pixels at 24 frames per second (fps). The video was translated and rotated during parts of the test to simulate real-world inspections. In addition, an iPhone video with a resolution of 720×1,280 pixels was recorded at 30 fps. A comparison of the captured videos showed that the higher resolution and mobility of the UAV enabled more complete footage of cracks on the target concrete beam to be captured from different angles. In Kun et al. (2022), 385 images were collected from bridge cracks using an I-800 Airborne Plane Array Camera and a UAV platform. The images had a 2,560 × 2,560 pixel resolution and were captured using a dual camera with optical zoom and 360-degree non-dead angle detection. The real-time kinematic positioning information was transmitted back to the ground station for data analysis. Overall, the dataset was found to be sufficient for training a deep learning model to achieve the expected crack segmentation accuracy. Munawar et al. (2022) used a UAV to capture 1,300 images of various bridge surfaces with a 4,864×3,648 pixel resolution. After collecting the dataset, preprocessing was performed on the captured images for the removal of unwanted objects and noise by rotating, cropping, and flipping the images. Belcore et al. (2022) used a Raspberry Pi RGB camera module installed on a UAV to capture 495 images of bridge intrados with a 45-degree orientation and a resolution of 1,024×720 pixels.

Seo et al. (2018) used a DJI Phantom 4 UAV to capture high-resolution images of a bridge with low illumination. The bridge had glued-laminated girders with a composite concrete deck. The high-quality imagery was noted to improve the damage identification and facilitate the inspection process. In a separate study, Morgenthal et al. (2019) proposed a framework for automated UAVs to help with the inspection of large bridges. The referenced study obtained 1,250 high-resolution images of bridge piers using a UAV. The images had a resolution of 0.6 mm/pixel. In Aliakbar et al. (2016), a set of 10 images was obtained from a UAV positioned at two different distances from a simulated structure. The target structure consisted of four homogenous metallic cubes placed on each other. Each set included three images taken from the center, left, and right directions. To mitigate the angular displacement caused by the UAV's drift during flight, the left and right views of the structure were included with an angular displacement of approximately 20 degrees. The central image was taken as a reference image, while the other two images were transformed with respect to the reference image. For each set, the three images were then stitched together to form the final image. In Li et al. (2020), the Bridge Substructure Detection 10 (BSD-10) device was used to collect 7,200 images with a resolution of 224×224 pixels from 10 existing bridges (most of which had service ages of less than 20 years). The images were captured under different lighting conditions and distances. Khaloo et al. (2018) used two cameras, i.e., a Sony NEX-7 and a GoPro Hero 3, mounted on a UAV to capture images of a bridge at various pixel sizes. Structural defects, such as cracks and spalling, were then identified. Compared to a regular inspection, the UAV-based inspection was able to detect more defects. Limitations were, however, reported for the UAV-based inspection, including flight time, range of the UAV platform, and processing time for damage detection. In Mirzazade et al. (2022) and Kim et al. (2021), a Sony R10C camera with a 20.1-megapixel resolution and NEXUS equipment with a resolution of 10,000×1,024 pixels were used, respectively, to obtain a set of images from bridge abutments. During the first scanning reported in Mirzazade et al. (2022), 140 images with a resolution of 5,634×3,753 pixels were captured under different perspectives and light conditions. To augment the number of images available for training the damage detection algorithms, the images were sliced into 227×227 pixels. A total of 8,344 cropped images were selected from them to generate the dataset.

Image capturing parameters, such as resolution, distance, angle, and coverage area, are expected to allow for the identification of defects in target structural components. Lighting conditions strongly influence image quality. Therefore, controlled illumination or normalization in postprocessing can become necessary. To improve the efficiency of image processing, captured images are often cropped to smaller sizes and gray-scaled. In the relevant AI/ML studies, 64×64 pixel images were used by Guo et al. (2021) and 224×224 pixel resized images with RGB color channels were employed by Savino and Tondolo (2021). The methods used in these studies were similar to those used in Kim et al. (2021) and Mirzazade et al. (2022), in which the row images were cropped.

Data augmentation through rotation, blurring, and noise injection can synthetically expand datasets. The key is to retain meaningful damage signatures and structural contexts while preparing the images for algorithm objectives like training and run-time performance. Galdelli et al. (2022) used three different multicamera systems to capture different types of images for bridge damage detection. The RGB camera captured color images with a resolution of 4,096×3,000 pixels, the depth camera captured color images with a resolution of 1,280×720 pixels, and the multispectral camera captured images with a resolution of 2,048×1,088 pixels. The third camera was able to capture multispectral images with frequencies across the shortwave infrared, visible, ultraviolet, and electromagnetic spectra, covering the 175 nm to 2500 nm wavelength range. Perry et al. (2022) used three datasets to detect cracks in steel girders, utilizing a total of 250 images with a resolution of 4,928×3,264 pixels. Bianchi et al. (2022) used 288 images with a resolution of 1,920×1,060 pixels and found that images taken from 1.5 to 2.4 m (5 to 8 ft) offsets produce the lowest amount of errors. Reagan et al. (2017) used a set of 2-megapixel acA1600-20um digital cameras. A resolution of 1,626×1,236 pixels was used to inspect the wall and abutment of a 56-year old bridge. In Zheng et al. (2022), the girders and abutments of two bridges that contained cracks were photographed with a high-resolution 24-megapixel camera. The images were 2,560×2,560 pixels and processed by a quadrilateral transformation to convert them to square subblocks. The subblocks were spliced together to restore the investigated surface area. After compiling all subblocks, the model was able to detect the cracks.

Liu and Gao (2022) proposed an image acquisition module composed of area-scan cameras, optical lenses, and infrared light sources. The image resolutions were 5,472×3,648 pixels, while the optical lens offered a focal length of 16 mm and a minimum operating distance of 0.10 m. The study utilized 150 images cropped to different sizes and reported a high crack detection accuracy. Lattanzi et al. (2016) captured a total of 390 images from reinforced concrete bridge columns. All images were analyzed with a resolution of 50 pixels/inch. The developed regression models were found to be capable of predicting the maximum lateral displacement experienced by a damaged reinforced concrete column. In a separate study, Malek et al. (2022) employed a Microsoft HoloLens headset to capture images for crack damage detection. The study utilized two different generations of this headset, with the first generation having a photo resolution of 2,048×1,152 pixels and a video resolution of 1,280×720 pixels, while the second generation had a photo resolution of 3,904×2,196 pixels and a video resolution of 2,272×1,278 pixels. Both headsets were able to detect cracks with a width of 0.7 mm after implementing the Canny algorithm into the headsets, but the second-generation headset was noted to provide a higher level of crack detection accuracy. In Mir et al. (2022), six training images with a resolution of 1,100×500 pixels were extracted from a 2,592×1,944 pixel original image captured for crack detection. Crack classification based on width was found to be valuable in scenarios where adequate image resolution is lacking. Zhai et al. (2022) used 120 real-world images of fatigue-induced cracks from steel box girders with resolutions of 4,928×3,264 and 5,152×3,864 pixels. The images were then augmented by cropping and flipping.

For damage detection purposes, Modarres et al. (2018) utilized 2,400 images of the concrete surfaces of existing bridge structures with a resolution of 96×96 pixels. In a separate effort, Zhu et al. (2020) used 1,180 images with arbitrary sizes and pixel resolutions. The prediction models were then tested on 134 images taken from different bridges that were not part of the training and validation sets. Similarly, Zhou et al. (2019) employed a training dataset of 500 images labeled for damage. Song et al. (2019) used a dataset of 2,068 bridge crack images. The large images were cut into 256×256 pixel images. A total of 5,180 small images were eventually used after blurred images were removed. The dataset was divided into training, validation, and test sets in a ratio of 8:1:1. Cha and Choi (2017) used a database of 20,000 images of cracked concrete and 20,000 images of uncracked concrete. After the original high-resolution images were cropped, 80% of the images were used for training and the remaining 20% for validation.

Xu et al. (2022) used the Bridge Crack Image Data and Crack Forest Dataset for a crack detection model. The Bridge Crack Image Data contained 2,000 bridge crack images with a resolution of 1,024×1,024 pixels, while the Crack Forest Dataset included 118 crack images sized to 480×360 pixels. The main characteristic of the referenced images, which were taken using an iPhone 5, is that they contain noise such as shadows, oil spots, and water stains. To enhance the ability of the models to learn crack features, the training set images were enhanced by cropping, rotating, and flipping. In Meng et al. (2022), two datasets, METUCrack (i.e., images captured from buildings) (Özgenel 2019) and SBGCrack (i.e., images from the First International Project Competition for Structural Health Monitoring) (Bao et al. 2021), were used to train and test the AI/ML algorithms. The METUCrack dataset contained 458 images of concrete surface cracks with a resolution of 3,024×4,032 pixels, while the SBGCrack dataset contained 200 images of fatigue-induced cracks with a resolution of 4,928×3,264 pixels. Both datasets were scaled to 1,024×1,024 pixels and split into training, validation, and test sets in a 7:2:1 ratio.

Focusing on gusset plates, Gulgec et al. (2019) generated a total of 30,000 damaged samples (by simulating different noise levels) and 30,000 intact samples. To generate the sample images, various loading cases, damage scenarios, and noise levels were considered. Four different noise levels were added to the noise-free samples, and a convolution operation with a kernel size of 2×2×2 and a stride of 3 was performed. The outcome of the referenced study was high accuracy in detecting damage in gusset plates. This accuracy was maintained even after introducing up to 16% noise. Abdelkader et al. (2020) worked to filter different types of noise. Among them were Gaussian noise, which mainly affects all of the pixel values; salt and pepper noise, which usually occurs due to errors during the image transmission phase; and speckle noise, which is a granular disturbance that impacts all of the intrinsic attributes of an image. The process began with the conversion of RGB images into grayscale images, with intensity values ranging from 0 to 255. This conversion was to improve image processing while preserving essential distress features. The grayscale images were then standardized to 200×200 pixels to ensure consistency in the training and testing process. The next step was to convert the noise-free images into noisy ones. This was to evaluate how well the noise detection model could identify different types of noise in an image.

A study by Zhu et al. (2020) classified partial defects (e.g., spalling, exposed rebar, cracks, and pockmarks) on bridge surfaces. For this purpose, a transfer learning model was trained on 1,180 images and then tested on 134 images from various bridge components, including decks and walls. The model achieved 97.8% accuracy on the testing set. Savino and Tondolo (2021) applied an automated concrete damage classification scheme to different concrete surfaces, including piers and decks. The referenced study utilized eight pretrained networks and selected GoogLeNet as the best network (with 94% accuracy). Liu and El-Gohary (2020) proposed a semantic image retrieval and clustering method to collect relevant images from the web and cluster them for bridge component and defect detection. The method was evaluated for its ability to predict the condition rating of the decks, superstructures, and substructures of 2,646 bridges in the state of Washington. The performance was evaluated using the silhouette coefficient and showed promising results. In Fan (2021), a dataset of 1,000 damage samples (including rebar exposure, spalling, efflorescence, and cracking) was randomly selected for training and testing purposes. A hybrid model (i.e., cluster analysis followed by SVM classification) performed better than a standalone SVM for detecting all four damage types. Deng et al. (2021) generated a dataset using real-world images of cracks on concrete surfaces that were taken at different angles and distances with a range of background information. Various cameras were used, including RGB, depth, multispectral, and high-resolution cameras, with resolutions ranging from 1,280×720 to 5,152×3,864 pixels. The cracks were successfully detected by the model, but the detection accuracy was noted to be significantly affected by the lighting condition and complexity of the background.

UAVs are commonly used to capture images, while real-time kinematic positioning information is transmitted back to the ground station for data analysis. The images have different sizes and resolutions. They are often cropped, resized, or gray-scaled to improve the efficiency of image processing algorithms. Some studies have used multiple cameras to capture images from different angles, and others have used devices to collect images under different lighting conditions and distances. Among the examples, Cha et al. (2017), Li and Zhao (2019), Feng et al. (2019), and Aliyari et al. (2021) collected high-resolution images suitable for damage detection. Using UAVs and high-resolution cameras has improved the efficiency of image processing, while the standardization of image size/quality and the extraction of important features of distress have helped with noise reduction.

There are, however, some limitations and challenges when using digital cameras or UAVs for collecting images from bridge structures. One is the limited field of view, as cameras and UAVs offer a specific field of view, which means that they may not be able to capture the entire bridge component in a single image. This can result in incomplete datasets, making it challenging to detect damage accurately. A second limitation is that the quality of images captured by cameras and UAVs can be affected by various factors, including lighting conditions, weather, and camera settings. Poor image quality can make it challenging to detect damage accurately. A third limitation is that collecting and storing large numbers of images can be challenging and expensive, particularly if high-resolution images are used. To address the outlined limitations, several strategies can be employed. Using multiple cameras or UAVs can help capture a wide field of view and reduce the risk of missing important data. Furthermore, choosing cameras and sensors specifically designed for aerial photography and bridge inspection can deliver high-resolution images even in constrained environments or under low-light conditions. Image processing techniques, such as image enhancement and noise reduction, can help improve the quality of images, while the use of cloud storage and computing makes it possible to collect and analyze a large inventory of images.

2.4 Automated Damage Detection in Bridge Components

2.4.1 Convolutional Neural Networks

Several AI/ML algorithms have been used for detecting damage in bridge components. Among them, CNNs have been widely considered in the available literature. For example, Xu et al. (2022) proposed a convolution-deconvolution feature fusion holistically nested network (CDFFHNet) for concrete surface crack detection. The architecture of the network was composed of three components: (1) VGG-16 feature extraction with a channel attention mechanism, (2) a convolution-deconvolution feature fusion module, and (3) a multiscale feature fusion holistically nested network. The network improved the accuracy of crack segmentation compared to benchmark networks, such as holistically nested edge detection (HED), fully convolutional network (FCN), segmentation network (SegNet), U-Net convolutional network (U-Net), and richer convolutional features (RCF). The CDFFHNet was found to outperform the other networks in all three metrics of accuracy, recall, and F1 score. This superiority was attributed to the CNN employed to identify surface cracks in bridge components (Qin et al. 2021). The referenced CNN was constructed with four convolutional layers, four pooling layers, and three fully connected layers. It was then trained with the backpropagation stochastic gradient descent method. The results showed that the accuracy of crack identification using the CNN algorithm can be significantly higher than that obtained from traditional image processing methods. A cascade broad neural network (CBNN) was proposed by Guo et al. (2021) for concrete surface crack classification. The classes included not cracked and cracked, as well as intact, simple crack, and complex crack. The cascade structure in each level was an ensemble of different broad learning classifiers to encourage diversity. The CBNN achieved higher accuracy than other methods like ResNet-50 and offered a more straightforward structure and faster training time.

Bhowmick et al. (2020) proposed a method for processing video measurements using a deep neural network image segmentation architecture called U-Net. U-Net segmented the pixels in the crack images and converted the original RGB images of the concrete surface to binary images of cracks. Morphological operations were then performed to compute the geometric properties of the cracks, such as length, width, area, and orientation. The method was validated by carrying out a laboratory experiment on a concrete beam. Bhowmick et al. (2020) found that U-Net successfully detects and segments multiple propagating cracks on the beam surfaces not used for training. Similarly, Guo et al. (2021) showed that the cascade structure and ensemble classification can enable high accuracy after efficient training. Munawar et al. (2022) proposed a modified deep hierarchical CNN (16 convolution layers plus a cycle generative adversarial network [CycleGAN]) for pixel-wise damage segmentation on various steel surfaces. The architecture was optimized for damage specific to critical sections of bridge piers through fine-tuning the main image properties, such as brightness, contrast, and sharpness. The effectiveness model was assessed using 1,300 civil infrastructure images. The results showed that the proposed model outperformed other models, including pyramid scene parsing network (PSPNet), DeepLab, baseline, and SegNet. The referenced method produced a global accuracy of 0.989, class average accuracy of 0.931, mean intersection of union (IoU) of 0.878, precision of 0.849, recall of 0.818, and F-score of 0.833. Guided filtering and conditional random fields methods were used to further refine the prediction results.

CNN algorithms can also identify and detect instances of damage in steel components commonly found in bridge structures. Through synthetic data augmentation, Zhai et al. (2022) used an FCN to detect fatigue-induced cracks in steel box girders. This method involved mapping synthetic textures onto a 3D graphics model to generate synthetic images, which were then used to train the FCN with real data. The outlined method improved crack identification performance from 35% to 40% for IoU and from 49% to 62% for precision. Wang et al. (2020) proposed a machine vision-based methodology for monitoring fatigue-induced cracks in U-rib-to-deck weld seams in OSG bridges. An internet of things (IoT)-based image acquisition device was designed, along with a framework for image rectification and stitching. A cascade crack recognition method was developed, including a crack region detection, crack semantic segmentation, close morphological operation, and skeleton extraction algorithm. A deep convolutional neural network (DCNN)-based crack classifier was employed to distinguish whether the sub-images include cracks. The proposed methodology was applied to 14 fatigue-induced cracks in orthotropic steel box girder bridges and showed promising results, with a root mean square error of 3.0195 mm and 0.003 mm in length and width measurements, respectively.

Perry et al. (2022) developed a U-Net network to determine the pixel-level location of cracks in webs of steel girders (where the crack is far from the flange-to-web interface). This was followed by a surrogate model based on a Gaussian process to estimate stress intensity factors, which served as indicators of fracture for cracks of different sizes. The U-Net architecture is a powerful tool for image segmentation with an encoder-decoder structure. The encoder reduces the size and increases the depth of the input, while the decoder layers are added from the encoder layers to produce the final output. The 10 tested U-Net architectures, 5 with colored inputs and 5 with grayscale inputs, were trained and demonstrated high accuracy when examining the validation dataset. However, a tradeoff was noted between the processing time and accuracy, where smaller U-Nets had a faster processing time but a lower accuracy. Kim et al. (2018) proposed a DCNN-based damage locating method for detecting damage in steel frames. The method achieved 99.3% accuracy, outperforming MobileNet and ResNet, which provided 96.2% and 95.4% accuracy, respectively.

Bianchi et al. (2022) evaluated a combination of images and AI/ML techniques to detect corrosion in steel bridge girders. Specifically, experimental assessments were conducted on three image registration methods, i.e., rigid, deformable, and hybrid. The assessments primarily aimed to evaluate the model's effectiveness in preserving the geometric properties of the source images. The best results were achieved with homography-based transformations. In addition, a semantic damage detection model was trained on 440 annotated bridge inspection images using the DeeplabV3+ architecture. SuperGlue, which is a graph neural network (GNN), matched the feature points. A dense image alignment method, known as image registration or random sample consensus (RANSAC)-flow, was used to geometrically align the newly obtained images with the original inspection images. The aligned images were then examined to detect time-dependent changes in damage as a measure to determine the progression of deterioration. This pretrained deep neural network damage detection model achieved an F1 score of 86.67% on the test dataset. The feature-matching process involved obtaining interest points, computing descriptors, conducting nearest neighbor searches, filtering out incompatible searches, and estimating valid transformations.

To detect, match, and analyze the features that are present in images taken from a bridge component, classical feature-matching techniques often use (1) scale-invariant feature transform (SIFT) for finding feature points, (2) Lowe's ratio test for filtering points, and (3) RANSAC for finding transformations. Kim et al. (2021) detected the instances of damage in bridge expansion joints using a CNN as a feature extractor. Nineteen image patches were created and classified to identify the presence of damage. A U-Net architecture was used as a segmentation model to extract the gap region from the cropped images. The first model was trained to extract metal parts from the line-scan images, and the second model was trained to find the gap region. The gap length was then calculated by converting the minimum gap distance in pixels to millimeters. The developed algorithm had an identification accuracy of more than 95% and reduced the investigation time by more than 95%, i.e., from 1 hour/bridge to 3 minutes/bridge. The accuracy of the gap measurements was also improved from 67.5% to 95.0%. Zhou et al. (2019) used You Only Look Once (YOLO) Version 3 (v3), a CNN-based object detection algorithm, to detect damage in high-strength bolts in long-span steel bridges. The referenced study developed a dataset of 500 labeled images and trained the YOLOv3 model on the dataset. The feasibility of the proposed method was verified by testing the model on two new damage images.

In addition to detecting damage in steel components, CNN algorithms have been used to detect damage in concrete components. Zheng et al. (2022) proposed a convolutional active learning identification-segmentation-measurement (CAL-ISM) framework for crack detection in reinforced concrete bridge piers. The framework included four steps: (1) pretraining of a benchmark classification model, (2) retraining with a semi-supervised active learning model, (3) pixel-level crack segmentation, and (4) crack width measurement. The CAL-ISM framework was applied to two bridges and showed promising results, where the maximum recognition error was limited to less than 10% for narrow cracks and an error range of 0% to 12% for actual bridges. Deng et al. (2021) developed a modified YOLOv2 network for crack identification in reinforced concrete structures. Using real-world images with handwritten text, YOLOv2 served as a single-stage object detection network, predicting the location of objects through bounding boxes. It was then fine-tuned to differentiate concrete cracks from crack-like features. The outcome was found to offer an accuracy level similar to that provided by a region-based CNN (R-CNN). The process, however, was faster, indicating the potential for use in real-time crack detection applications. Modarres et al. (2018) proposed a CNN architecture for damage detection and classification in honeycomb panels. The algorithm's architecture included three stacks of convolutional pooling layers and three fully connected hidden layers. The algorithm used a rectified linear unit (ReLU) activation, a 0.75 dropout rate, adaptive moment estimation optimization, and a softmax cost function. The proposed architecture achieved a predictive accuracy of 99.6% in classifying different types of damage in synthetic honeycomb structures and outperformed other AI/ML algorithms in real-world concrete bridge crack scenarios (with a predictive accuracy of 98.8%).

Kun et al. (2022) captured images of abutments, piers, and box girders from a concrete bridge structure and used the deep bridge crack classification (DBCC)-Net method, a CNN-based neural network, for crack patch classification. This method used a two-stage crack detection strategy for finding cracks and extracting crack morphology from high-resolution images. The first stage realized the coarse extraction of crack position, and the second stage extracted the complete crack morphology from the location suggested by the semantic segmentation network. The postprocessing capability and a two-stage crack detection strategy enabled the network to detect cracks quickly. This method addressed the issue that the target detection network could only detect crack locations and not crack shape features.

Jeong et al. (2022) proposed a CNN algorithm for damage identification and classification in several bridge components, including railing posts, decks, pier caps, columns/piers/piles, and floor beams. A pixel-based algorithm was employed to measure the extent of damage (e.g., cracking, spalling, discoloration, efflorescence, and rust) by counting pixels in an image. The predictive accuracy was validated by comparing the damage measure provided by the image analysis with that from direct measurement. In a separate effort, Chun et al. (2021) combined CNN Inception v3, gated recurrent unit (GRU), and an attention mechanism for explanatory text generation to describe image contexts. It was found that 68.8% of the generated texts were correct and 92.9% were either correct or partially correct. A vision-based method for detecting concrete cracks using a deep CNN was proposed by Cha and Choi (2017). The dataset was generated from images taken under uncontrolled circumstances and fed into the designed CNN, resulting in 98% accuracy in training and validation. Input images were generalized to a vector format with 96 elements in training. The vector was then classified as crack or intact after it was processed through the ReLU, last convolution, and softmax layers. The trained CNN classifier was found to perform well in testing with images taken under uncontrolled situations.

In Mirzazade et al. (2022), a trained CNN algorithm was combined with a sliding window technique and autonomously flying drones. A real-world case study on a simply supported concrete bridge was performed to compare the performance of four different CNNs (i.e., VGG-19, Inception v3, GoogLeNet, and ResNet) for autonomous crack detection in bridges. The models were evaluated based on accuracy, loss (the difference between the predicted values [output] and the actual or target values in the model), computational time, model size, and architectural depth. Inception v3 achieved the highest accuracy (96.2%) but with the longest training time (12 hours). GoogleNet offered a good balance between accuracy (around 90%) and computation time (4 hours). GoogLeNet had the best performance in terms of accuracy and precision, but it only drew a boundary box around the likely damaged regions, not a pixel-level region specifying the crack. The application of pretrained CNN models demonstrated the feasibility of transfer learning in overcoming data scarcity issues common in this domain. Moreover, the comparison of different CNN architectures provided valuable insights into the tradeoffs between accuracy, computational efficiency, and model complexity. Seo et al. (2022) used an ML-based approach coupled with image visibility optimization techniques to improve visual bridge inspection using remote-controlled drones. The approach involved using CNNs as a representative AI/ML algorithm for the analysis of high-resolution images of the deck, superstructure, and substructure. The efficiency was evaluated using remote-controlled drones to detect and measure the damage (in terms of cracking, weathering, and spalling) observed on two bridges in Minnesota. The CNN algorithm was trained with images that contained various damage types but fine-tuned for optimized visibility.

Abdelkader et al. (2020) proposed a two-tier method for automatically detecting noise and restoring bridge defect images. In the first tier, the hybrid Elman neural network-invasive weed optimization (ENN-IWO) model was employed for identifying the type of noise in the image. The model outperformed other classifiers by achieving a 95.28% accuracy, 95.24% sensitivity, 98.07% specificity, 95.25% precision, 95.34% F-measure, and 0.935 Kappa coefficient. In the second tier, the moth-flame optimization-based restoration model was used to improve the degraded image quality of bridge defects. The model outperformed other conventional and optimization-based restoration models. The outcome of the proposed method was a hybrid image filtering protocol that integrated spatial and frequency domain filters. Li et al. (2020) proposed a crack extraction algorithm that used multilayer features extracted from an FCN and a naive Bayes data fusion model. The method showed notable recognition accuracy, computational time, and accuracy rates compared to other CNN algorithms. Gulgec et al. (2019) introduced a deep architecture and training process for CNNs to detect and localize damage. The training phase consisted of two tasks, i.e., detection and localization. Detection was treated as a classification problem (0 for undamaged and 1 for damaged), while localization was treated as a regression problem. Shared front-end layers were used for more efficient learning, shorter training time, and lower computational cost. Song et al. (2019) utilized SegNet, a lightweight end-to-end pixel-wise classification model, to detect and localize cracks in images. The referenced study used data augmentation to improve the generalization ability and performed nonlinear upsampling using pooling indices. The IoU on the bridge crack image dataset reached more than 0.70. The SegNet method outperformed traditional edge detection methods, such as Canny and Sobel, to a margin that it could detect cracks in images with large amounts of noise interference and complex background textures. The trained SegNet model was able to segment the cracks in images at any size with the sliding window scanning feature. Figure 2.4 compiles the CNN algorithms that are discussed in this section.

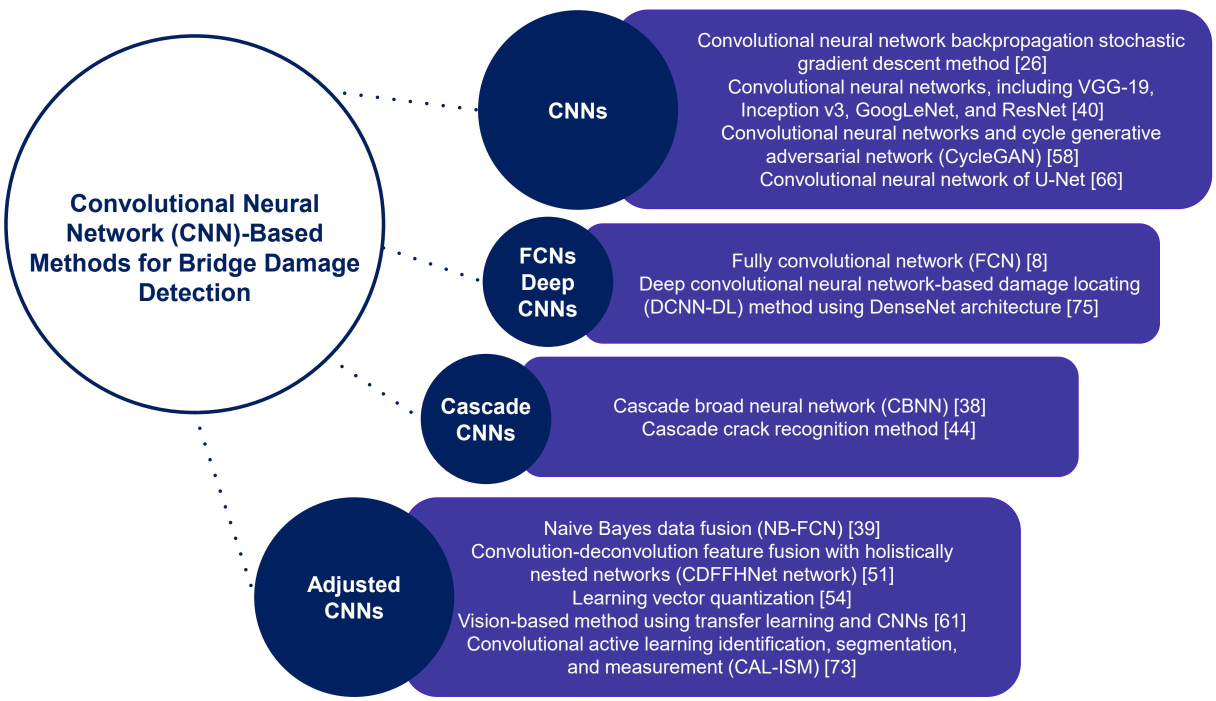

Figure 2.4. Overview of CNN-based algorithms used to detect bridge damage

2.4.2 Support Vector Machines

SVMs have been used for damage detection in different bridge components, including piers and decks. Mir et al. (2022) proposed an SVM-based discriminant generation method for crack detection on concrete surfaces. Semantic segmentation with ResNet-18 (a CNN with 18 layers) was used to detect the crack rate in the images. Three classes were created for crack widths ranging from 0 to 8 pixels, 8 to 12 pixels, and 12 to 16 pixels. Low-brightness regions were divided into cracked and non-cracked regions and trained for feature selection by boosting. This improved the detection rate by 11.7% compared to the arbitrary features method. Fan (2021) proposed a method for detecting four different damage types in reinforced concrete bridges (included rebar exposure, spalling, efflorescence, and cracking) using a hybrid machine learning (HML) approach. The HML combined cluster analyses with an SVM to create SVM-based clustering. Six evaluation indicators were used to compare the classification of SVM and SVM-based clustering. The results indicated that the SVM-based clustering approach had superior detection capability compared to the SVM for multiple types of damage. The highest detection accuracy was for cracks (with an accuracy of 99.3%), followed by rebar exposure, concrete spalling, and efflorescence (with an accuracy of 94.9%). It should be noted that the effectiveness of HML was found to be reliant on image quality. Hence, color changes and environmental noise can limit HML's image recognition effectiveness. Arong et al. (2020) proposed an SVM-based bridge soundness evaluation method using 971 bridge inspection data points. The SVM was used to classify the health of bridge components, where the health rating was classified into the four categories of I (or Good), II, III, and IV (or poor), as one of the outcomes.

2.4.3 Classification Algorithms

Different classification algorithms have been used to identify instances of damage in bridge components. Belcore et al. (2022) proposed a semiautomatic, object-oriented, supervised classification. This classification used a random forest model for damage detection using images captured by a modified UAV equipped with a low-cost camera. The input included an orthoimage and a digital surface model from photogrammetric processing. The algorithm was tested on a bridge made of two separate prestressed concrete structures in Turin, Italy. The outcome showed effectiveness in almost all classes, with an F1 score never below 0.75. The accuracy could be further improved by using infrared-sensitive sensors and correcting for environmental lighting conditions. Meng et al. (2022) proposed an automatic crack detection method using a drone, including lightweight classification and crack segmentation algorithms (LSegModel and CLsModel) and a high-precision crack segmentation algorithm (HSegModel). The method involved obtaining an orthogonal projection of the target image and classifying the crack regions using CLsModel. This was followed by segmentation using LSegModel and HSegModel. The results indicated that the proposed method had high accuracy in detecting cracks, outperforming traditional edge detection and deep learning-based methods. Yang and Cervone (2019) developed a system that used deep learning and multiple classifiers for damage assessment using aerial images. The referenced study manually labeled a small set of images that showed flooded or non-flooded areas and then identified the most characteristic features using several ML classifiers. An ensemble max-voting classifier was also used to classify the unlabeled images. The evaluation results showed an accuracy of 85.6% and an F1 score of 89.1%, demonstrating the effectiveness of combining deep learning and an ensemble max-voting classifier.

Lattanzi et al. (2016) investigated the viability of applying computer vision techniques for estimating the peak displacement of bridge columns subjected to seismic excitations. Correlations were established by using images (of damaged columns) and experimental data from lateral load tests performed on reinforced concrete bridge columns. The proposed computer vision algorithms were based on image segmentation, feature extraction, and nonlinear regression analysis. With the objective of estimating the peak drift, the referenced study reported strong correlations between parameterized crack patterns and structural displacements. Liu and

Gao (2022) proposed a method for crack detection in concrete structures using the baseline model of visual characteristics of images (BMVCI) method. The method involved cropping images into sub-images, denoising, generating visual characteristics, and implementing a kernel principal component analysis (KPCA). A crack detection index and a novel detection method (through an acquisition module composed of area-scan cameras, optical lenses, and infrared light sources) were then used to detect cracks. The results showed excellent performance in detecting cracks in concrete structural components. Compared to CNN-based methods, the proposed method exhibited improved computational efficiency, as it does not require a large training dataset.

As an alternative algorithm, the speeded up robust features (SURF)-based algorithm detects points of interest and extracts features for image stitching and crack identification, helping identify changes in bridge structures. Aliakbar et al. (2016) used a SURF-based algorithm for bridge crack detection. The algorithm was tested on images taken by a stationary UAV and showed successful results in detecting physical changes. Kong et al. (2020) compared the detection and performance of four feature point extraction methods (i.e., FAST, ORB, SIFT, and SURF) for fatigue-induced crack detection. The ORB and SIFT methods performed well in feature point extraction, while the FAST method had a higher matching rate in low-light conditions. The ORB method was reported to be the fastest method among those investigated in the referenced study.

Another approach for damage assessment is using edge detection methods. Among them, the Canny edge detection algorithm offers a pattern recognition technique to recognize the edge pixels in an image. Malek et al. (2022) used the Canny algorithm for bridge damage detection, as it offers low computational demand and fast processing in addition to its ability to detect low-contrast edges. The referenced study processed RGB crack images through a series of steps, including image acquisition, grayscale conversion, noise reduction, gradient evaluation with the Sobel operator, and edge evaluation using hysteresis thresholding for binary image segmentation. The recall-precision analysis showed that the maximum accuracy can range from 7.5% to 9.5% after simplifications. Perry et al. (2020) proposed a defect detection algorithm that relied on computer vision and was optimized for concrete bridge defects. The algorithm used black hat transform, Canny edge detector, Gaussian blur, and OpenCV functions for preprocessing and identifying defects. The system was compared to human-based and UAV-assisted inspections and showed advantages in terms of in-depth data analytics and automated damage quantification and visualization. The algorithms proposed for identifying and tracking defects, along with the element identification algorithm, successfully detected, located, and measured the size of flaws (cracking, spalling, and delamination) in the target structural components. Galdelli et al. (2022) used a flaw detection system for damage detection in the bridge's sub-areas and the deck's lower surface. The system converted RGB and 3D images to grayscale, passed them through a blurring filter (Gaussian or bilateral), performed adaptive thresholding and nonlinear morphological operations, and completed contour searches. Upon removing the outliers, the flaw detection system produced high-quality and robust results, but the identification task remained a challenge in computer vision, requiring large amounts of data.

Lastly, some studies explored photogrammetric techniques for damage detection. Morgenthal et al. (2019) used a combination of tailored point cloud analysis algorithms, a pseudo-algorithm to compute viewpoints on an offset surface, and a structure-from-motion (SfM) algorithm to detect anomalies in concrete bridge structures. To maintain the main geometric properties of images without any distortion, preprocessing was performed on the images before feeding them into the model. Photogrammetric 3D reconstruction and anomaly detection were conducted on cracked piers based on the processed images. The 3D point cloud was converted into a 3D surface model to map anomalies with exact dimensions and locations. The imaging geometry obtained from the photogrammetric analysis allowed the characterization of cracks and localization of anomalies on bridge surfaces. Khaloo et al. (2018) used a multiscale photogrammetric 3D scene reconstruction technique to generate a highly accurate and dense 3D point cloud of a bridge using UAV-acquired images and a hierarchical dense SfM algorithm. The study showed that the developed inspection methodology provided superior 3D models with the accuracy required to detect defects. Among the instances were critical structural defects, including damaged chords, splits in timber elements, and loose bolt connections that were also visually confirmed. Figure 2.5 compiles the SVM and classification-based algorithms discussed in this section.

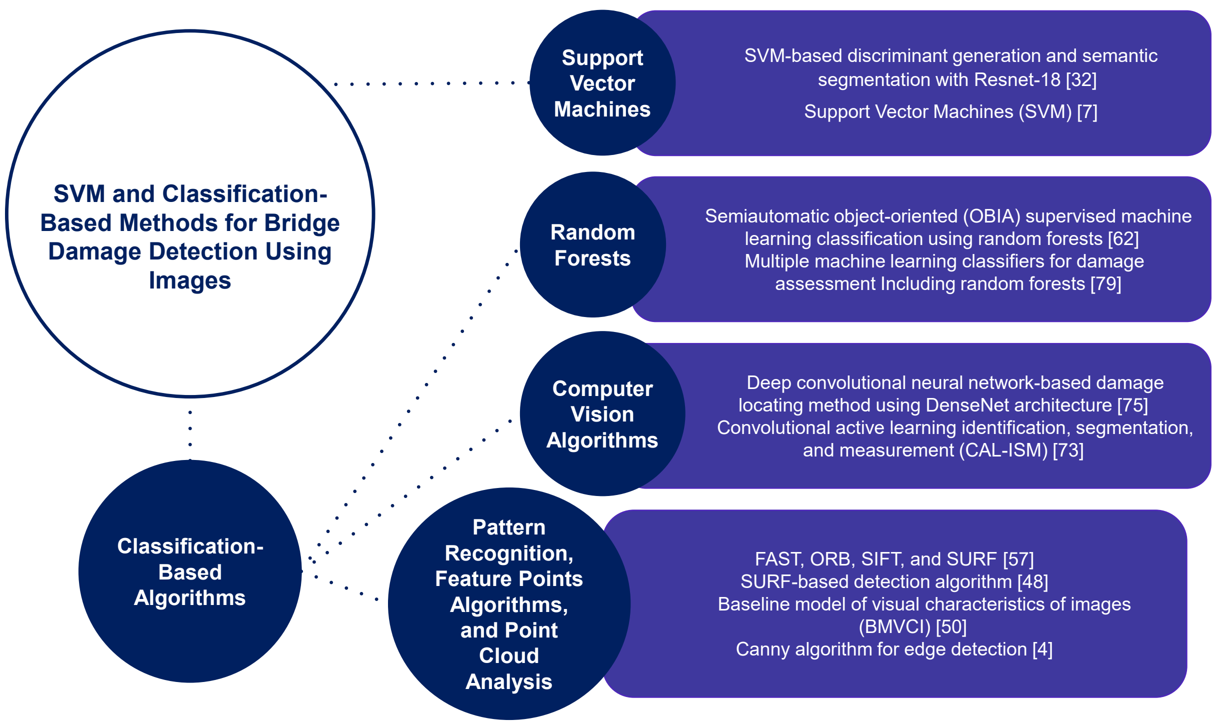

Figure 2.5. Overview of SVM and classification-based algorithms used to detect bridge damage

2.4.4 Classical ML Algorithms

Classical ML-based methods, which include techniques such as artificial neural network (ANN), k-nearest neighbors (KNN), and regression have laid the groundwork for many of the advanced algorithms of deep learning used today. These methods have been instrumental in various structural damage detection tasks over the past decade and have provided significant contributions to the field.

One of the earliest applications of machine learning to image-based crack characterization involved the use of an unsupervised clustering technique, K-means clustering, a method that partitions data points into distinct clusters. Oliveira and Correia (2013) proposed a system that employed unsupervised learning to classify cracks based on their visual attributes. The method involved capturing images and applying K-means clustering to group pixels into distinct clusters representing different crack types. While achieving a relatively high F-measure of 93.5%, the system faced challenges in accurately detecting narrow cracks.

Logistic regression, a statistical classification method, has also been employed in bridge damage detection. Landstrom and Thurley (2012) developed a system for detecting cracks. After applying morphological image processing to extract crack segments, logistic regression was used to classify these segments as cracks or non-cracks. The system achieved an overall accuracy of over 80%.

ANNs have shown promise in overcoming the challenge of fragmented cracks in images (Kankar et al. 2012, Wang and He 2007). Wu et al. (2016) introduced the MorphLink-C method to connect discontinuous crack segments using dilation and thinning operations. An ANN was then employed to classify the resulting connected crack structures as either cracks or non-cracks. This approach demonstrated improved classification accuracy compared to more traditional methods. Unlike deep learning models, classical ML methods do not rely on neural networks but instead use handcrafted features and statistical approaches.

Classical ML models provide transparent decision-making, making it easier to understand their predictions. They often require fewer computational resources and are more straightforward to implement. While these classical algorithms played a crucial role in early bridge damage detection, they faced certain limitations. Most methods had limited crack characterization. They focused on binary classification (crack/non-crack) with limited ability to categorize cracks based on severity or type. They often relied heavily on image preprocessing techniques, which could be sensitive to factors like lighting or noise (Lee and Wei 2010). Supervised learning methods like ANNs typically require large, well-labeled datasets for effective training, which can be expensive and time-consuming to acquire (Feng et al. 2017).

2.5 Recommendations for Real-World Applications

2.5.1 Recommendations Based on Damage Types and Characteristics

Based on the available literature, a main area of research and development in the context of automated bridge condition assessment is crack detection, with many studies that have been dedicated to the use of AI/ML techniques for detecting cracks in various bridge components. Among the measures of interest, the length, width, average width, maximum width, orientation, and continuous centerline of cracks with different widths and angles have been investigated to date. Fatigue-induced crack detection has also been an active area of research, with vision-based methods holding promise for automated inspections over time. Among the relevant studies, Wang et al. (2020) presented a machine vision approach using image processing techniques to locate fatigue-induced cracks in steel bridges. The developed approach was able to detect cracks over 1 mm in length. However, from the current literature, detecting small surface cracks has remained challenging for vision-based methods. Limitations stem from image resolution, lighting conditions, and surface textures, which can obscure hairline cracks. While progress has been made on laboratory samples, real-world conditions introduce further difficulties. As a potential solution, computer vision has been proposed to be combined with NDE methods to improve the detection of surface and subsurface cracks.

In addition to cracks, the available studies have explored the use of computer vision to detect other forms of damage in bridge structures. Concrete spalling, which can expose the embedded rebars, has been investigated through techniques like the texture analysis of surface images. Exposed rebars themselves have been detected by training AI/ML models on rust patterns and rebar shapes. Weathering damage, such as efflorescence, has been investigated using color-based image processing. Capturing water leakage has been another area of study to evaluate this cause of deterioration over time. Similarly, damage to expansion joints and seals can be located by boundary detection and monitoring the changes. While the current methods show promise in controlled laboratory environments, challenges arise in real-world settings due to occlusion, lighting variation, and material inconsistencies. Hence, robust detection and localization of the listed defects still prove difficult. The issue can be magnified given the diversity of structural materials, damage types, and imaging conditions. In the meantime, continued research has yielded practical solutions to address the standing issues and assist human inspectors in bridge condition assessment.

Current studies primarily focus on single defect modes, but a few studies (e.g., Arong et al. 2020, Chun et al. 2021) have investigated multiple instances of damage, such as corrosion and water staining, and multiple forms of damage, including spalling and rebar exposure. While the relevant studies have identified and located different types of damage (with various levels of accuracy), some have quantified the extent of damage, specifically where cracks, spalling, corrosion, and joint gaps are present. Quantification of the damage severity, not just detection, is a critical task for planning maintenance and repair activities. With only a few studies available in this domain, additional effort is needed on capturing the extent of damage in a variety of materials, components, and details that exist in bridge structures. Efforts have also been made to expand the damage types that can be detected (beyond cracks, spalling, corrosion, and leakage). However, progress is still limited, especially when dealing with small-size defects.

For the assessment of damaged regions, some studies have used pixel-based methods and conversion factors from pixels to millimeters/inches or square millimeters/inches. Additional software products, such as ImageJ, have been employed to count the number of pixels in the damaged regions in each image. This has been useful to determine the extent of damage in instances like rebar corrosion and concrete spalling. Corrosion quantification, in particular, has been performed by measuring the height and width distributions of the corrosion pixels or the area of the corroded region. There are also studies that have used image segmentation and deep learning models to measure gap width and size. Such measurements, when used on appropriate images captured from bridge components, help quantify various types of damage and inform repair and maintenance decisions.

2.5.2 Recommendations for Alternative Image and Data Collection

For the automated detection, localization, and measurement of damage using AI/ML techniques, image samples or datasets are required as inputs for AI/ML algorithms. Images are commonly captured by human inspectors, UAVs, and UUVs at different angles and resolutions under different lighting conditions. High-quality image datasets are critical to train and validate the predictive models for damage detection. Hence, access to a variety of images for different defect types is key for robust algorithm training and testing. Overall, standardized datasets collected under diverse real-world conditions enable progress in the vision-based assessment of bridge structures.

From the current literature, image-based inspections have been performed with various cameras, including RGB, depth, multispectral, and high-resolution cameras. RGB cameras are a common and economical option, but they have limitations in capturing subtle surface defects and material conditions. Depth cameras add 3D structural information to aid damage localization and measurement. However, the resolution of such images can be lower than that captured by RGB cameras. High-resolution cameras, especially in real-world settings, are critical to capture fine details like microcracks. On the other hand, very high-resolution pictures can pose challenges in terms of file transfer and storage. Beyond the hardware specifications, factors such as camera stability, calibration, and controlled light contribute to the quality and accuracy of an automated damage analysis. Some studies have used multiple cameras to capture images from different angles. This is to obtain a complete view of the subject or scene being photographed. To cover a full view of a bridge component, overlapping images can provide a wide overall view. Some challenges with using multiple cameras can include the complexity of setup and synchronization, the processing and storage of additional data, and difficulty merging and aligning images from different viewpoints.

It should also be noted that bridges are large structures, and some areas may be hard to reach. Moreover, lighting consistency may not exist across different bridge components, depending on the time and weather conditions. Shadows and glares can also obscure the damaged regions. Hence, advanced cameras and image processing methodologies can become necessary to generate appropriate input for detecting damage in various bridge components.

2.5.3 Recommendations for Damage Detection Algorithms

There are several considerations in using AI/ML techniques to detect damage in bridge components. Object detection algorithms, such as Faster R-CNN, can be used to identify and localize damage in images (Deng et al. 2021), but they require extensive labeled bounding boxes, which can be time-consuming to collect. Data augmentation and generative models, such as generative adversarial networks (GANs), can synthesize damage examples from limited data but at the risk of not mimicking the diversity of damage in real-world instances. Multimodal deep learning methods hold promise for enhanced bridge damage detection, leveraging various image data. They, however, need to be tailored to the available datasets and problem constraints to ensure their overall success. This has introduced several opportunities for additional research and development.

A main aspect to consider with AI/ML algorithms is the availability and quality of training data. An AI/ML algorithm can only learn to detect bridge damage instances if it is trained on a large and diverse dataset of bridge images with labels indicating the location and severity of damage. However, such datasets may not exist, or the quality of the annotations may vary depending on the expertise of the annotator. This can lead to biases in the training data, which can result in inaccurate or unreliable predictions. Additionally, obtaining high-quality annotated datasets can be expensive and time-consuming. Hence, recommendations have been made on using techniques, such as cropping, rotation, color/contrast shifting, and noise addition, to expand the usable training data. In addition, transfer learning from models pretrained on image datasets like ImageNet can be leveraged to extract useful features.

Another aspect to consider is the generalizability of AI/ML models. A model trained on one set of bridge images may not perform well on a different set of images due to variations in lighting, angles, weather conditions, and other contributing factors. This can limit the model's usefulness in real-world scenarios, where new images are regularly captured and added to the bridge inventory. Transfer learning techniques can adapt pretrained models to new datasets, reducing the amount of new data required for training while improving the generalization performance. For bridge damage detection, CNNs pretrained on large image classification datasets like ImageNet can be effectively utilized. Pretrained models provide generalized feature extraction capabilities that transfer well to new domains, as reflected in the relevant studies.

The interpretability of AI/ML models is another key aspect. While deep learning models have shown remarkable accuracy in detecting anomalies, they can be difficult to interpret because of the models' complexities, as the most recent AI/ML models have millions of parameters and use multiple nonlinear processing layers. This makes it hard to intuitively follow all transformations applied to the input, making it challenging to understand the specific features or patterns that AI/ML models use to detect damage. To address this challenge, especially for engineers who need to make informed bridge maintenance or repair decisions, interpretability techniques such as saliency maps, feature visualization, and attention mechanisms can be used to understand how a model makes predictions. Saliency maps help highlight input image regions that were most relevant to the model's prediction. For instance, Zhang et al. (2023) generated gradient-based saliency maps for detecting concrete cracks, revealing visual evidence that supports damage detection. Interactive model inspection tools like ActiVis and CNN Visualizer also allow users to visualize activations and adjust inputs to understand the model's behavior.

Besides algorithm details, computational requirements for AI/ML models are in need of attention. Deep learning models can be computationally expensive and require large amounts of data to complete the training process effectively. This can limit the model's scalability and make it challenging to deploy in resource-constrained environments. Techniques such as model compression, pruning, and quantization can be used to reduce the size and complexity of models while maintaining their accuracy to a reasonable extent. Among the alternatives, model compression techniques like knowledge distillation can reduce a model's size by training a downsized model to mimic an ensemble or large model. By employing this approach, Chen et al. (2023) achieved an F1 score of 85.70% and an IoU of 78.22% in crack detection accuracy.

Past studies have used different types of CNN for concrete crack detection, surface crack identification, concrete surface damage classification, and prediction of the structure's ability to withstand service loads. To improve accuracy, various architectures, such as CDFFHNet, CBNN, U-Net, and modified deep hierarchical CNN, have been considered. The choice of architecture, however, depends on balancing the performance, efficiency, and application requirements. An ensemble combining multiple models can potentially deliver the best overall results. Some CNN models are trained using backpropagation stochastic gradient descent methods and validated using test sets. Weaknesses of CNNs include overfitting and the need for a large amount of data. Transfer learning and synthetic data augmentation have been proposed to improve CNNs' feature extraction and identification performance. In addition, CNNs have been used for detecting damage in various bridge components using techniques such as CAL-ISM, YOLOv2, and DBCC-Net. These techniques often involve benchmark classification model training, crack segmentation, and crack width measurement. The accuracy of these methods varies depending on the technique and the type of bridge component. CNNs have also been applied for image retrieval and clustering, UAV-aided inspection, and explanatory text generation for damage identification and classification in various bridge components. However, some shortcomings of CNNs include difficulties in detecting complex damage patterns and high computational power requirements.

In addition to CNNs, SVMs have been used in several studies for damage detection in different bridge components, such as piers and decks. The relevant studies have utilized different SVM-based methods to detect cracks and other instances of damage using various features, such as semantic segmentation and shape features. The proposed methods have shown improved detection accuracy and reduced false detection rates compared to conventional methods (e.g., CDFFHNet, CBNN, and U-Net). However, some limitations related to image quality and environmental factors should be considered when developing SVM-based bridge damage detection and evaluation methods. While SVMs have shown promise for automated crack and damage detection in bridges, some challenges remain in real-world application. Factors including lighting conditions, image quality, occlusion, and complexity of damage patterns can affect feature extraction and classification performance. Preprocessing techniques, such as image enhancement and segmentation, may be needed to improve image quality. Moreover, different classification algorithms have been used for damage detection, including random forest, CLsModel, LSegModel, HSegModel, and the ensemble max-voting classifier. The results from past studies show that the available algorithms can effectively detect damage in bridge components. Recommendations for further improvement include combining SVM with other techniques like segmentation or feature engineering to improve robustness. The ensemble methods that use SVM and deep learning together also hold promise. Overall, SVMs offer flexible frameworks well-suited for bridge damage detection, but care should be taken to design models that can be generalized to new datasets and conditions. In the meantime, improvements in accuracy can be made by using sensitive sensors and correcting for environmental lighting conditions. This helps provide a rich information representation that can be leveraged by SVMs.

For damage detection purposes, computer vision algorithms that are based on image segmentation, feature extraction, and nonlinear regression analysis can be utilized. SURF-based algorithms have been tested on images taken by a stationary UAV to identify changes in the structural components of bridges. Other approaches include traditional edge detection methods, such as the Canny algorithm and photogrammetric techniques. The Canny algorithm has been used for bridge damage detection, offering low computational demand, high processing speed, and low-contrast edge detection capabilities. The current literature has also explored using photogrammetric techniques for damage detection. For this purpose, a combination of tailored point cloud analysis algorithms and SfM algorithms has been employed to detect anomalies in bridge components. Although these techniques have produced high-quality results, the identification task remains challenging in computer vision, requiring large amounts of data. In addition, variations in camera lighting or structural design details can limit the accuracy of predictions. Nonetheless, these techniques are valuable for improving the inspection process and reducing the reliance on human inspectors.

Figure 2.6 summarizes the steps for bridge damage detection using AI/ML techniques.

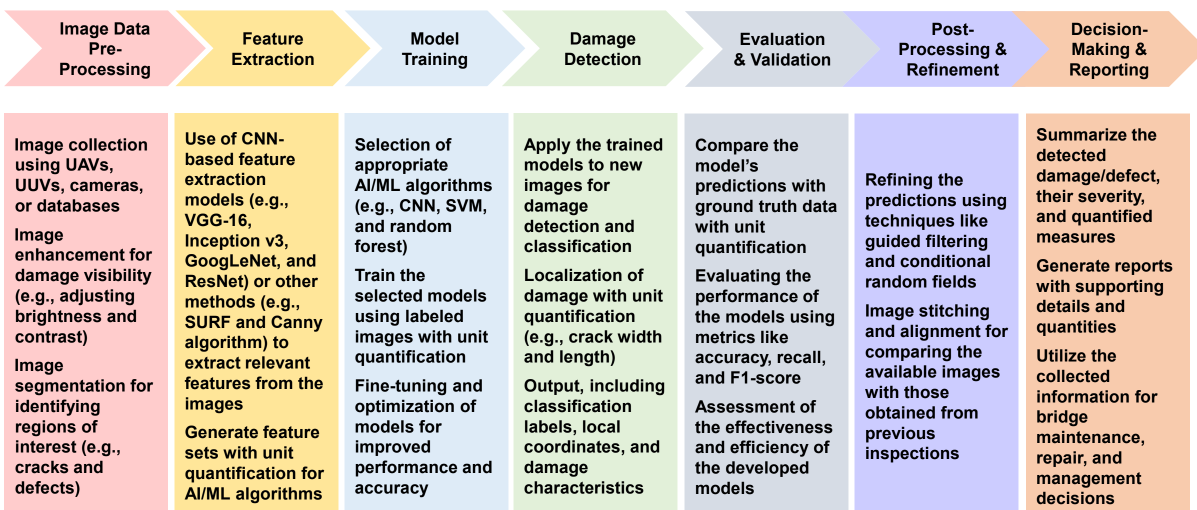

Figure 2.6. Recommended steps for bridge maintenance and management based on the instances of damage/defects detected using AI/ML techniques

2.6 Main Findings

The literature review presented in this chapter provides holistic information about the main bridge damage types and characteristics that can be captured through AI/ML algorithms Table 2.3 summarizes the AI/ML techniques that have been explored in the literature for their ability to detect different damage types in bridge components. Various image collection techniques that have been used to generate useful inputs for such algorithms were discussed, including practical recommendations to address the challenges associated with material characteristics, structural details, and environmental conditions. The main AI/ML algorithms that have been used for bridge damage detection to date were then discussed in terms of their core capabilities and features.

Several promising research and development directions have been identified for automated damage detection in bridges. Among them, the use of UAVs and UUVs presents a great opportunity to improve the inspection of hard-to-reach regions of bridge structures. Current

UAVs utilize basic visual and LiDAR sensors, but integrating advanced technologies like thermal imaging, hyperspectral cameras, and ultrasonic testing can help detect subsurface flaws invisible to the naked eye. Autonomous navigation and collision avoidance capabilities must progress beyond reliance on Global Positioning System (GPS) connectivity to enable the inspection of confined spaces under bridges using onboard sensors. Meanwhile, tethered UUVs show promise for underwater inspection of substructures and foundations. Further development of UUV mobility and waterproofing and of nondestructive testing payloads suited for concrete and steel in turbid waters is critical. Beyond improved sensing, combining UAV and UUV data with other inspection inputs within a single planning and visualization framework is expected to provide a holistic assessment of bridge conditions above and below water.

Table 2.3. AI/ML techniques used to detect different damage types in bridge components

AI/ML Technique	Bridge Component(s)	Damage type(s)	Reference(s)
CNN-Based Models			
FCN	Steel bridge girder steel box girders	Fatigue crack	Zhai et al. 2022
CDFFHNet network composed of three main components: (1) VGG-16 feature extraction module fused with the channel attention mechanism, (2) convolution–deconvolution feature fusion module, (3) multiscale feature fusion holistically nested network	Concrete surfaces	Crack	Xu et al. 2022
CAL-ISM, which includes four steps: (1) pretraining of the benchmark classification model, (2) retraining of the semi-supervised active learning model, (3) pixel-level crack segmentation, and (4) crack width measurement	A column pier in the laboratory and a bridge test Mostly piers and under the deck	Crack	Zheng et al. 2022
GNN called SuperGlue Dense image alignment method (known as image registration or RANSAC-flow)	Two steel beams	Corrosion	Bianchi et al. 2022
CNNs and CycleGAN	Various surfaces	Crack, corrosion, and water straining	Munawar et al. 2022
CNN coupled with image visibility optimization techniques	-	Varying damage types (i.e., cracking, weathering, and spalling	Seo et al. 2022
CNN and pixel-based length measurement algorithm	Railing posts, deck, pier cap, column/pier/pile, floor beam	Crack, tilt, split, weathering, paint failure Generally, discoloration, crack, rust, spalling, and efflorescence (can be classified by CNN)	Jeong et al. 2022

AI/ML Technique	Bridge Component(s)	Damage type(s)	Reference(s)
CNNs (including VGG-19, Inception v3, GoogLeNet, and ResNet)	-	Crack	Mirzazade et al. 2022
CBNN	Bridge concrete surface	Crack	Guo et al. 2021
Deep learning model that combines CNN, GRU, and an attention mechanism	38 types of members, including main girders and floor slabs	Multiple forms of damage (27 types of damage) like corrosion, cracks, degradation of anticorrosive on bearings, defects of base mortar, exposed reinforcing bars, leaking, and spalling	Chun et al. 2021
Deep convolutional neural network with transfer learning, GoogLeNet model	Bridge concrete surfaces	Crack Delamination	Savino and Tondolo 2021
CNN - backpropagation stochastic gradient descent method	Concrete surface	Cracks	Qin et al. 2021
CNN of U-Net	Expansion joints	Expansion joint gap	Kim et al. 2021
YOLOv2 network algorithm for crack identification in real-world images	Concrete structures	Crack	Deng et al. 2021
DCNN-based damage locating (DCNN-DL) method using DenseNet architecture	Steel frames	Damaged and undamaged steel bars	Kim et al. 2021
CNNs	Welding joints of a long-span steel bridge	Fatigue crack detection	Quqa et al. 2022
Hybrid ENN-IWO for the type of noise identification, moth-flame optimization algorithm for defect restoration	-	Defects	Abdelkader et al. 2020
Convolutional network and a naive Bayes data fusion (NB-FCN) model	Bridge substructures	Crack	Li et al. 2020
Four feature points algorithms (FAST, ORB, SIFT, and SURF)	-	Fatigue crack	Kong et al. 2020
Cascade crack recognition method including crack region detection, crack semantic segmentation, morphological close operation, and skeleton extraction algorithm DCNNs	U-rib-to-deck weld seams in OSG bridge	Fatigue cracks	Wang et al. 2020
Recurrent neural network modeling Unsupervised data linking algorithm	Decks, superstructures, and substructures	Deterioration like spalling	Liu and El-Gohary 2022
Deep neural network architecture of U-Net	Concrete surfaces	Crack	Bhowmick et al. 2020

AI/ML Technique	Bridge Component(s)	Damage type(s)	Reference(s)
Vision-based method using transfer learning and CNNs	Partial defects on the bridge surface	(1) Spalling, (2) exposed rebar, (3) crack, (4) pockmark	Zhu et al. 2020
YOLOv3, an object detection algorithm based on CNN	High-strength bolts in long-span steel bridges	Fracture	Zhou et al. 2019
Lightweight end-to-end pixel-wise classification called SegNet	-	Crack	Song et al. 2019
Neural networks	Steel bridges	Weathered steel corrosion and coating erosion	Elbeheri and Zayed 2018
CNNs	Honeycomb and concrete bridge structures Aluminum honeycomb core bonded to two aluminum skins	Crack detection	Modarres et al. 2018
Vision-based DCNN	-	Crack	Cha and Choi 2017
Multilayered neural networks (for deterioration prediction) Genetic algorithm (GA) technique (for optimal maintenance plan)	Slab, girder, others	Cracking, cracking, corrosion, spalling, and delamination	Miyamoto 2013
Support Vector Machine and Classification-Based Algorithms			
SVM-based discriminant generation semantic segmentation with Resnet-18 (a CNN with 18 layers of depth)	Concrete surfaces	Cracks	Mir et al. 2022
HML of SVM-based clustering and SVM	Reinforced concrete components	Four types of RC damage: rebar exposure, spalling, efflorescence, and cracking	Fan 2021
SVM	Superstructure, main girder, crossbeam, slab, substructure, bearing, others	Peeling and exposed steel bar, floating, cracking, failure of weather joint, abnormality of transverse prestressing of fix section, exposed anchorage zone, reinforced corrosion, honeycomb, corrosion, free lime, water leakage	Arong et al. 2020

AI/ML Technique	Bridge Component(s)	Damage type(s)	Reference(s)
Semiautomatic object-oriented (OBIA) supervised ML classification using random forests	RPi RGB camera installed upwards on UAV images with an orientation of 45° to the zenith view. A video recording at a resolution of 1029×702 pixels was set to automatically acquire images with a higher frame rate (2 fps)	Five classes: drainage, uncovered metal bar (UMB), oxidized rebar (OR), nondamaged intrados, and nondamaged beam	Belcore et al. 2022
Computer vision algorithms based on image segmentation, feature extraction, and nonlinear regression analysis	RC bridge columns	Column drift, cracking, and spalling patterns	Lattanzi et al. 2016
Automatic crack detection method including a lightweight classification algorithm, a lightweight segmentation algorithm, a high-precision segmentation algorithm, and a crack width measurement algorithm	Not on bridges but can further be applied to bridges as well Experiment on a two-story building and a shaking table test	Crack	Meng et al. 2022
Classification algorithm of learning vector quantization (LVQ)	Concrete slab	Crack	Kusunose et al. 2003
Other Methods			
BMVCI	Concrete structures	Cracks	Liu and Gao 2022
Canny algorithm, which is a pattern recognition technique to recognize the edge pixels in the images	-	Crack	Malek et al. 2022
Computer-vision-based detection algorithm consisting of black hat transform, Canny edge detector, Gaussian blur, and OpenCV functions for preprocessing and identifying defects	Can detect damages in piers, pier caps, decks, beams, etc.	Concrete surface cracks, but it can also be used for concrete section loss, spalling, and delamination	Perry et al. 2020
Tailored point cloud analysis algorithms containing pseudo-algorithm and SfM algorithm	Concrete structures	Cracks	Morgenthal et al. 2019
Hierarchical dense SfM algorithm	-	Connection damage on the west truss, damaged truss chord on east truss, loose bolt on west truss	Khaloo et al. 2018

AI/ML Technique	Bridge Component(s)	Damage type(s)	Reference(s)
SURF-based detection algorithm, which is one of the most commonly used approaches for points of interest (POI) detection	-	Crack	Aliakbar et al. 2016

Several limitations must be considered to ensure the robustness and reliability of automated bridge damage detection systems and to emphasize the need for further research and improvements. One of them is variability in detection performance. The performance of ML models, mostly deep learning approaches, for bridge damage detection varies. High accuracy is therefore very dependent on the quality and diversity of the training images. Poor quality images, for example, those taken in bad light or at low resolution, can badly affect the model's capability to detect the subtle features of damage. This variability therefore has to be dealt with, and high-quality training datasets representative of real-world scenarios must be curated by researchers.

The challenges in classifying bridge damage are also significant. First, the damage types could be complex and varied, such as cracks, corrosion, deformation, and structural defects. Some damage categories really have no clear features to distinguish them from others, and therefore correct classification becomes hard. Although deep learning models are highly capable of feature extraction, they always suffer when the features are blurred or classes are overlapping. For example, it can be difficult to tell different crack or corrosion patterns apart. Research into innovative feature extraction methodologies and class-specific architectures to improve classification is therefore essential.

Moreover, most of the ML algorithms that are currently prevalent are based on curated datasets. Very seldom do they contain in situ images—that is, photographs taken on site during inspections. This can cause a discrepancy between the training data and real bridge damage images. In this regard, researchers must collect and annotate in situ images to ensure that the training data conform to real-world scenarios and environmental conditions.

Environmental factors have a huge impact on the detection of bridge damage. Weather conditions like rain, fog, or snow influence the quality and visibility of images. The image features that show damage might be occluded by raindrops or snow on the camera lens. Seasonal changes can similarly produce variations in lighting and cast shadows in an image to change its contrast. Moreover, bridges come in different designs, materials, and ages, which can lead to further variations in appearance. The variability is such that ML models need to accommodate different structural elements (beams, columns, cables) that exhibit different damage patterns. Research is required in transfer learning so that models are built for varying environmental conditions and bridge types that have an enhanced capacity for generalization.

Future research directions for using AI/ML techniques in bridge damage detection must focus on developing more accurate, robust, and efficient algorithms to handle various types of data and integrating these algorithms with other sensing technologies for more comprehensive damage detection systems. The development of more robust and accurate deep learning models that can process various types of image data, such as multispectral or hyperspectral images, is critical to improve damage detection accuracy. Key capabilities to enable accurate damage detection include specialized neural network architectures to extract relevant spectral features correlated with potential defects, in addition to techniques to handle spectral variability from illumination, the surrounding environment, and sensor noise while retaining damage-related information. Enhanced deep learning models, such as hybrid neural networks that combine CNNs with other architectures like recurrent neural networks (RNNs) or transformers, can leverage both spatial and sequential data for better damage detection. For instance, a hybrid model could use a CNN to analyze the spatial structure of bridge images and an RNN to understand the temporal patterns in a sequence of images captured over time, thus improving the detection of progressive damage such as corrosion. An example implementation might involve using a CNN to detect initial crack formation and an RNN to track the growth of these cracks over time, providing a more dynamic and continuous assessment of bridge integrity.

Another research area in need of attention is the exploration of novel feature extraction methods to enhance the detection of subtle damage patterns in bridge images. While existing image feature extraction techniques have shown promise for bridge damage detection, they struggle to reliably identify subtle or irregular defect patterns. For example, standard methods like SIFT often cannot discern hairline cracks or small spalls from background noise and natural color variations in bridge materials. This capability is essential to avoid missed detections and false positives, especially in real-world applications. Diverse datasets that encompass different lighting conditions, viewpoints, and damage scenarios are essential. Researchers can employ data augmentation techniques (e.g., rotation, scaling, flipping) to create additional training samples. Furthermore, super-resolution techniques can enhance low-resolution images, aiding feature extraction and classification.

Several studies state that future research should focus on generating more comprehensive description sentences from bridge damage images, incorporating details such as the severity and grade of damage. This will improve the efficiency of bridge inspections and reduce subjectivity. Additionally, efforts should be made to refine crack segmentation annotations by using advanced image preprocessing techniques and learning-based background elimination methods to remove non-structural components. This will enhance the accuracy and completeness of crack detection. Expanding image datasets to include more damage types will also facilitate broader applications for identifying various forms of surface damage. Furthermore, developing the capability of frameworks to analyze the location and severity of damage, and exploring the detailed properties and adaptability of these frameworks for in-service bridge damage detection, will be essential for developing comprehensive and practical automated bridge inspection systems.

Moreover, the development of transfer learning approaches that can leverage pretrained models and adapt them to bridge damage detection tasks can be a promising area of research. This approach can help overcome the data scarcity problem, especially for detecting infrequent types of damage. For example, transfer learning models like VGG, ResNet, and Inception pretrained on ImageNet have demonstrated strong performance for crack detection in concrete components. To further enhance the effectiveness of transfer learning in bridge damage detection, specific research directions include fine-tuning pretrained models for specific damage types, such as adapting a model trained on general object recognition to detect corrosion on steel components. Incremental learning can be explored to continuously update the model as new damage types are encountered, preventing catastrophic forgetting. Feature adaptation techniques, like domain adaptation, can be employed to align the features learned from a pretrained model with the specific characteristics of bridge images. Multitask learning can be integrated to simultaneously detect multiple damage types, improving efficiency. Finally, combining transfer learning with other techniques like data augmentation or active learning can create hybrid approaches for enhanced performance.

Developing more explainable and interpretable models is also essential to facilitate the wide reach and practical implementation of AI/ML models. The current models for anomaly detection can be difficult to interpret, making it challenging to understand the specific features or patterns that the models use to detect damage. Developing models that can provide more detailed explanations of their decision-making processes can significantly improve the transparency and trustworthiness of the predictions.

Finally, using AI/ML techniques for real-time damage detection and monitoring can be considered as an emerging area of research. This research area can benefit from developing fast and efficient algorithms that handle large amounts of data in real time and alert bridge owners about potential damage before it becomes critical. Ultimately, the value of automated damage detection processes lies in enabling quantitative condition assessment to further inform preventive and corrective actions. Continued development of automated, vision-based damage quantification strategies is key to realizing this potential. Consistent measurement protocols, reporting standards, and public datasets would further help provide the required capabilities and enhance the condition assessment process.

CHAPTER 3: DIGITAL TWIN MODEL DEVELOPMENT

3.1 Software Products

There are several software products for creating and manipulating 3D models. Photogrammetry is a technique that involves taking measurements from photographs to create 3D models or maps. Each product has its own set of features and capabilities, and the choice often depends on the specific needs and preferences of the user. Three different popular 3D modeling software applications and their capabilities are summarized below.

3.1.1 Autodesk ReCap Pro

Autodesk ReCap Pro is a software application developed by Autodesk for creating 3D models from laser scans and photographs. It is commonly used in the fields of architecture, engineering, and construction for reality capture and modeling purposes. ReCap Pro has the following key features:

1. **Reality capture.** ReCap Pro allows users to import point cloud data from laser scans and photographs to create accurate 3D models of physical spaces and objects.
2. **Registration and alignment.** Users can register and align multiple scans or photographs to create a cohesive and accurate representation of the scanned environment.
3. **Point cloud processing.** The software can handle large datasets of point cloud information, enabling users to process and clean up the data to create more accurate and detailed 3D models.
4. **Annotations and measurements.** Users can add annotations and measurements directly to the 3D models, aiding in collaboration and communication among project stakeholders.
5. **Integration with other Autodesk software.** ReCap Pro is often integrated with other Autodesk software applications like AutoCAD and Revit, allowing users to incorporate reality capture data into their existing workflows.

In short, ReCap Pro is a comprehensive reality capture software application designed to transform physical environments or objects into digital 3D models.

The limitations of using ReCap Pro include the following:

1. **Processing time.** The time required for processing point cloud data and generating 3D models could vary depending on the Autodesk server.
2. **Hardware requirements.** Reality capture software, including ReCap Pro, may have specific hardware requirements. Users need to ensure that their computer systems meet these requirements for optimal performance.
3. **Accuracy and resolution.** The accuracy of the generated 3D models depends on the quality of the input data (e.g., laser scans or photographs). In some cases, the level of detail may be limited by the resolution of the original scans.
4. **Cost.** Autodesk software, including ReCap Pro, typically involves licensing fees.

5. **Software compatibility.** Users may encounter compatibility issues with certain file formats or third-party applications.

3.1.2 Bentley iTwin Capture Modeler

iTwin Capture Modeler offers the highest fidelity and most versatile desktop capabilities for creating reality data to serve as the digital context for design, engineering, construction, and operations workflows. It allows the user to produce reality meshes reliably and quickly at any scale at the best quality on the market by using photographs or LiDAR point clouds. It is available in two versions: iTwin Capture Modeler and iTwin Capture Modeler Center. iTwin Capture Modeler Center enables the user to create unlimited clusters to quickly process projects as large as cities. iTwin Capture Modeler has the following key features:

1. **Reality mesh creation.** The core functionality of iTwin Capture Modeler is centered around creating reality meshes. This involves processing input data, such as photographs or LiDAR point clouds, to generate detailed and accurate 3D representations of structures.
2. **Photogrammetry and LiDAR support.** The software can support both photogrammetry and LiDAR data, allowing users to choose between these data sources based on project requirements.
3. **High fidelity and accuracy.** Given the emphasis on high fidelity and versatility, iTwin Capture Modeler is designed to produce reality meshes with a high level of detail and accuracy.
4. **Versatility in workflows.** The tool offers versatility in supporting various workflows, including those related to design, engineering, construction, and operations.
5. **Ability to work at the PC level.** The offline mode allows users to continue their work even when they are not connected to the Bentley server.
6. **Implementation of AI capabilities.** AI can assist in automatically annotating objects or features in the captured data and can even classify different elements within the reality mesh.

The limitations of using iTwin Capture Modeler could be listed as follows:

1. **Cost.** Licensing costs and subscription fees can be a potential disadvantage.
2. **Hardware requirements.** Users with less powerful hardware might experience limitations in their ability to work with or process data.
3. **Compatibility issues.** There could be compatibility issues with certain file formats or with other software applications used in the same workflow.
4. **Ground sampling distance (GSD).** A lower GSD, achieved with higher-resolution imagery that may not be available to all users, contributes to better accuracy and detail in the final model.
5. **Accuracy and resolution.** The sensors used for capturing data, whether LiDAR scanners or cameras for photogrammetry, have inherent limitations in terms of spatial resolution.

3.1.3 Pix4D

Pix4D is a software suite that specializes in photogrammetry and drone mapping. It is widely used in various industries, including agriculture, construction, surveying, and environmental monitoring. The software allows users to process drone-captured imagery and generate detailed, accurate, and georeferenced 3D models, point clouds, and maps. Below are some features of Pix4D:

1. **Photogrammetric accuracy.** Pix4D is known for providing accurate and high-resolution 3D models and maps through photogrammetric processing of drone-captured imagery.
2. **3D model generation.** Pix4D allows users to create detailed 3D models of structures and landscapes, providing a rich visual representation of the surveyed area.
3. **Drone mapping integration.** The software is specifically designed to work seamlessly with drone-captured images, making it a powerful tool for drone mapping applications.
4. **Multispectral and thermal processing.** Pix4D supports the processing of multispectral and thermal imagery, making it suitable for applications such as precision agriculture and environmental monitoring.
5. **Geographic information system (GIS) integration.** Pix4D integrates with GIS tools, allowing users to incorporate Pix4D-generated data into their existing GIS workflows.

The limitations of using Pix4D are as follows:

1. **High-end equipment/expertise required for large-scale mapping.** While Pix4D can work with consumer cameras and drones, surveying and mapping large areas may require specialized higher-end equipment and skilled operators to achieve the accuracy required for engineering and computer-aided drafting (CAD) applications.
2. **Significant amount of time required for postprocessing.** Depending on project scale, processing the images into a meshed, textured 3D model can take many hours or even days on a PC workstation with large datasets and a high desired accuracy.
3. **Software licensing costs.** While Pix4D does offer trial options, multiseat licensing and purchasing options for commercial use can become quite expensive for long-term access. Subscription costs may also apply.
4. **Optimization required for outputs.** Raw outputs from Pix4D often require importation into other software for optimization and conversion to other CAD/geospatial file formats for utilization in downstream workflows.

3.1.4 Summary

Each of the three software applications caters to specific industry needs and contributes to the evolving landscape of digital modeling and spatial intelligence. Pix4D is best for drone mapping and photogrammetry, transforming aerial imagery into precise 3D models with applications across agriculture, construction, and environmental monitoring. iTwin Capture Modeler, developed by Bentley Systems, focuses on creating high-fidelity reality data through versatile desktop capabilities and produces detailed 3D representations using photographs or LiDAR point clouds, which is particularly beneficial for design and engineering workflows. Autodesk ReCap

Pro specializes in point cloud processing, enabling the generation of detailed 3D models from laser scanning and photogrammetric data, and is prominently used in architecture and construction.

3.2 Data Collection

Utilizing drones for image collection has stood out as a transformative technology in bridge assessment. Specifically, drones with high-resolution cameras offer a unique advantage that facilitates unparalleled data acquisition when applied to bridge mapping. This innovative approach involves meticulous mission planning, where flight paths are strategically designed to capture comprehensive imagery of the bridge and its surroundings. As the drone soars over the structure, it systematically collects geotagged images, providing a detailed and accurate representation of the bridge and its immediate environment. This dataset becomes a foundation for advanced photogrammetric processing, enabling the creation of precise 3D models and point clouds. Integrating drone technology in bridge image collection enhances efficiency and timely and cost-effective assessments of structural integrity, aiding in maintenance planning, structural analysis, and decision-making processes within civil engineering and infrastructure management.

Two types of drones were used to collect the image datasets used in this study, DJI Mavic 2 Pro and DJI Phantom 4 RTK (Figure 3.1)

(a)

(b)

Figure 3.1. DJI drones: (a) Mavic 2 Pro (b) Phantom 4 RTK

Both drones are widely used in various professional fields. The specifications and features for each drone are listed below.

The DJI Mavic 2 Pro has the following specifications and features:

1. **Camera quality.** Mavic 2 Pro can capture 20-megapixel photos and 4K videos at 30 fps, Table 3.1 presents the camera specifications.
2. **Flight time.** Mavic 2 Pro has a maximum flight time of 30 minutes. However, it is important to note that flight time can vary based on factors such as weather conditions, payload weight, flight style, and battery age.
3. **Flight speed.** Mavic 2 Pro offers a maximum flight speed of 44.7 mph. However, a high speed is not needed to allow for detailed data collection. On the other hand, the data collection should be fast enough to cover the target bridge components within a reasonable time window.
4. **Flight mode.** Mavic 2 Pro has different operational modes and settings, such as the following:
   a. **ActiveTrack.** This mode allows the Mavic 2 Pro to automatically follow a subject while keeping it in the frame. It is improved from the previous version with better trajectory prediction and obstacle sensing.
   b. **HyperLapse**. In this mode, the drone captures stable aerial time-lapse videos. Different sub-modes can be chosen, like Free, Circle, Course Lock, and Waypoint, to create dynamic time-lapse footage.
   c. **QuickShots**. QuickShots are preprogrammed flight paths that record short cinematic video clips. Modes include Dronie, Circle, Helix, Rocket, Boomerang, and Asteroid.
   d. **Point of interest (POI)**. The drone circles around a selected subject, keeping it in the center of the frame. This is useful for capturing smooth, circular shots around a point of interest.
   e. **Tripod mode**. This mode reduces the drone's speed and sensitivity, making it easier to get stable, precise shots, especially in tight spaces or when close to the ground.
   f. **Cinematic mode**. Cinematic mode slows down the Mavic 2 Pro's speed and braking for smoother shots and more cinematic footage.
   g. **Terrain follow mode**. This mode allows the drone to maintain a consistent altitude above ground level, which is particularly useful in areas with varying terrain.

Table 3.1. Mavic 2 Pro camera specifications

Camera Specification	Range
CMOS	1”
Megapixels	20
Lens	f/2.8–f/11
FOV	77°
Electronic rolling shutter	8–1/8000 s
Resolution	5472 × 3648
ISO range	100–12,800

The DJI Phantom 4 RTK has the following specifications and features:

1. **Camera quality.** The Phantom 4 RTK is equipped with a high-resolution camera that is 20-megapixel. Table 3.2 presents the camera specifications.
2. **Flight time.** The drone has an approximate flight time of up to 30 minutes under ideal conditions. This duration can vary based on factors like wind conditions, flight speed, and additional payload.
3. **Flight speed.** The maximum flight speed is about 31 mph in P-mode (Positioning mode) and 36 mph in A-mode (Attitude mode). The speed can be adjusted according to the requirements of the mapping or surveying project.
4. **Flight modes.** Phantom 4 RTK has different operational modes and settings, such as the following:
    a. **RTK module.** The integrated RTK (Real-Time Kinematic) module enhances the positional accuracy of the drone, which is essential for precise geotagging of aerial images.
    b. **GS RTK app.** This app allows for intelligent flight planning and is specifically designed to work with the Phantom 4 RTK. It includes features like Photogrammetry and Waypoint Flight.
    c. **Obstacle sensing.** The Phantom 4 RTK can detect and avoid obstacles in its path, which is particularly useful in complex environments.
    d. **Terrain follow.** This mode enables the drone to maintain a consistent height above the ground while adapting to varying terrain, which is crucial for surveying and mapping uneven landscapes.

Table 3.2. Phantom 4 RTK camera specifications

Camera Specification	Range
CMOS	1”
Megapixels	20
Lens	f/2.8–f/11
FOV	84º
Electronic rolling shutter	8–1/8000 s
Resolution	5472 × 3648
ISO range (manual)	100–12,800

3.3 Data Quality and Resolution

The quality and resolution of images captured by drones are regarded as essential factors in the effectiveness of bridge inspections and 3D modeling. For the structural assessment and maintenance of bridges, detailed and high-resolution imagery is necessary for identifying potential issues such as cracks, corrosion, or other structural defects. Conversely, operating the drone at a greater distance ensures safety and provides a broader view of the bridge, which is beneficial for overall structural assessments. However, this may compromise the ability to capture minute details. Therefore, determining the optimal distance is crucial. This distance is often dictated by the drone’s camera specifications, the desired resolution, and the need to balance detailed inspection with operational safety. In Table 3.3, a comparison of the current study with the literature on both resolution and the number of images used in the dataset is presented.

Table 3.3. Number of images and resolution from the literature

Reference	Images in Dataset	Resolution (Pixels)
Cha et al. (2017)	277	4,928 × 3,264
Li and Zhao (2019)	1250	4,160 × 3,120
Feng et al. (2019)	435	7,952 × 5,304
Seo et al. (2018)	-	5,472 × 3,648
Morgenthal et al. (2019)	1250	0.6 mm/pixel
Perry et al. (2022)	250	4,928 × 3,264
Zheng et al. (2022)	175	6,000 × 4,000
Liu and Gao (2022)	150	5,472 × 3,648
Malek et al. (2022)	15	3,904 × 2,196, 2,048 × 1,152
Mir et al. (2022)	-	2,592 × 1,944
Zhai et al. (2022)	240	4,928 × 3,264, 5,152 × 3,864
Deng et al. (2021)	602	5,152 × 3,864, 1,280 × 720
Bao et al. (2021)	458	3,024 × 4,032
Bao et al. (2021)	200	4,928 × 3,264
Present study	177	5,472 × 3,648

The first dataset consisted of 177 images received from the Mavic 2 Pro drone and 111 images received from the Phantom 4 RTK drone. The quality for both datasets was 5,472 × 3,648 pixels. Figures 3.2 and 3.3 present an example from the Mavic 2 Pro, while Figures 3.4 and 3.5 present an example from the Phantom 4 RTK. The Mavic 2 Pro drone flew at a distance of 50 ft from the bridge, while the Phantom 4 RTK drone covered the area from a distance of about 180 ft.

Figure 3.2. Example of the dataset from the Mavic 2 Pro drone

Figure 3.3. Example of an image captured by Mavic 2 Pro drone from a 50 ft distance

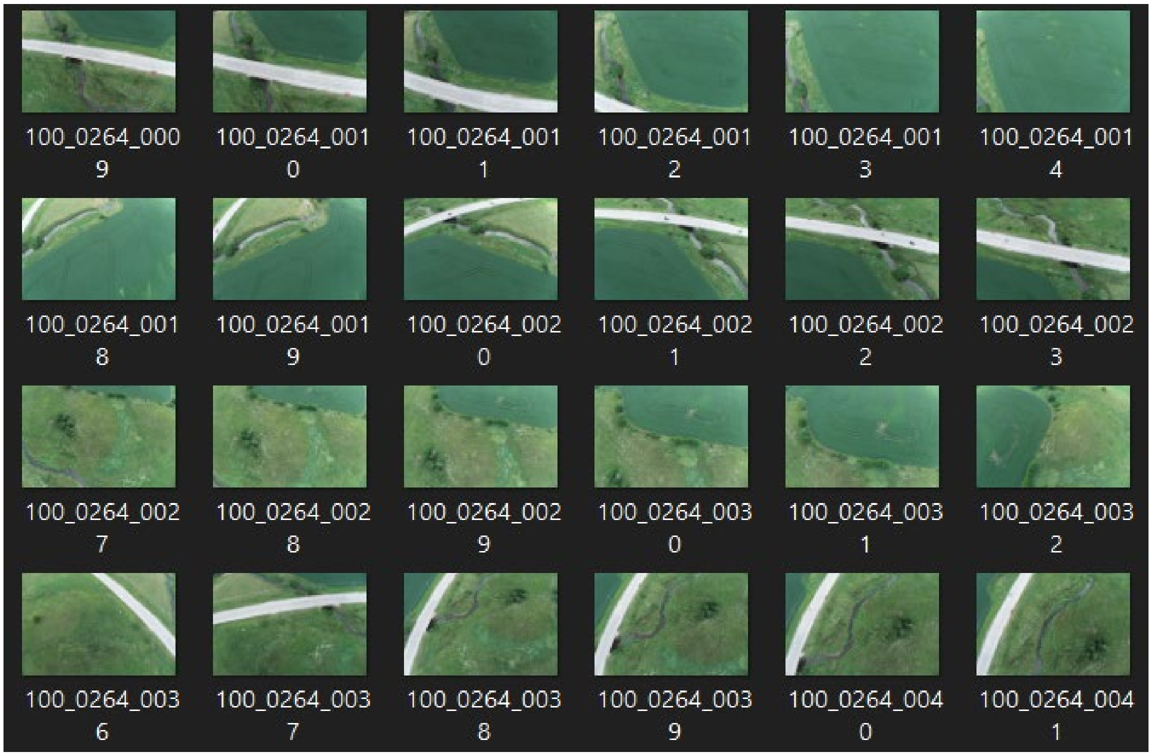

Figure 3.4. Example of the dataset from the Phantom 4 RTK drone

Figure 3.5. Example of an image captured by Phantom 4 RKT drone from a 180 ft distance

The difference in flying distances from the bridge between the Mavic 2 Pro and the Phantom 4 RTK presented a valuable opportunity for comprehensive data collection. Additionally, this difference permitted a meaningful comparison of the quality of the 3D models generated by each drone. By examining how much detail was captured by the cameras at different distances, insights into the precision and level of information provided by each drone could be gained.

The comparison between Figure 3.3 and Figure 3.5 in this study highlights the impact of drone height on the ability to capture defects in a bridge. In Figure 3.3, the closer proximity of the drone to the bridge allowed for more detailed capture of the bridge's structural defects, such as cracks. A contrast is observed when Figure 3.3 is compared to Figure 3.5, where the drone was positioned farther away (180 ft), which resulted in less detailed capture of the bridge defects. The importance of drone positioning in accurately generating and assessing a 3D model is underlined by this difference, which demonstrates that closer aerial flight reveals more accurate and critical details and assists in the generation of an accurate model.

Incorporating the optimal drone distance into an inspection strategy significantly enhances the effectiveness of drone-based bridge inspections and generates precise 3D models. This ensures that the images captured are of high quality and resolution, providing a reliable basis for accurate assessment and informed decision-making in bridge maintenance and safety protocols.

3.4 Generated 3D Models

In this project, the focus was on the 3D modeling of bridges, and by utilizing Bentley iTwin Capture, Pix4D, and Autodesk ReCap Pro, high-quality 3D models derived from the images captured by drones were successfully generated for the bridge in the case study. This integration of classification software not only ensured a more detailed and accurate representation of the bridge's current condition but also enabled a comprehensive analysis of its structural condition. The 3D models were anticipated to provide a multidimensional perspective, allowing a more thorough examination of expected damage and areas requiring maintenance that were missed or were difficult to reach.

The present study focused on the generation of 3D models for the case below. Drones were used on the bridge to take detailed, high-quality images, and then three 3D models of the bridge were created in each software application. This provided a better understanding of the 3D modeling capabilities and how these features could be utilized.

3.4.1 Case Study Description

A bridge characterized by its unique construction and current condition was examined. The bridge, built in 1922, is located 19 miles south of Ames, Iowa. It features a robust design with steel beams supported by high concrete abutments and topped with an RC deck. Spanning 63 ft in length and 44 ft in width, this bridge has been an integral part of the region's infrastructure for 101 years. Despite its age, it maintains a condition rating of fair. In 2021, it was reported to handle an average daily traffic of 6,800 vehicles. However, the bridge shows signs of wear and tear typical of its age and usage, including cracks in its structure, concrete spalling, rusting of steel components, and peeling paint. Figure 3.6 presents images of the bridge examined in this case study.

Figure 3.6. Captured images of the case study bridge

The first software application used to generate a 3D model of the current case study bridge was Bentley iTwin Capture; the software showed a high-quality real 3D model of the bridge, and all details appeared in the model. Moreover, the model exhibited a real view of the bridge with a walk-through feature that facilitated the inspection and damage detection process. Figure 3.7 presents the 3D model from Bentley iTwin Capture.

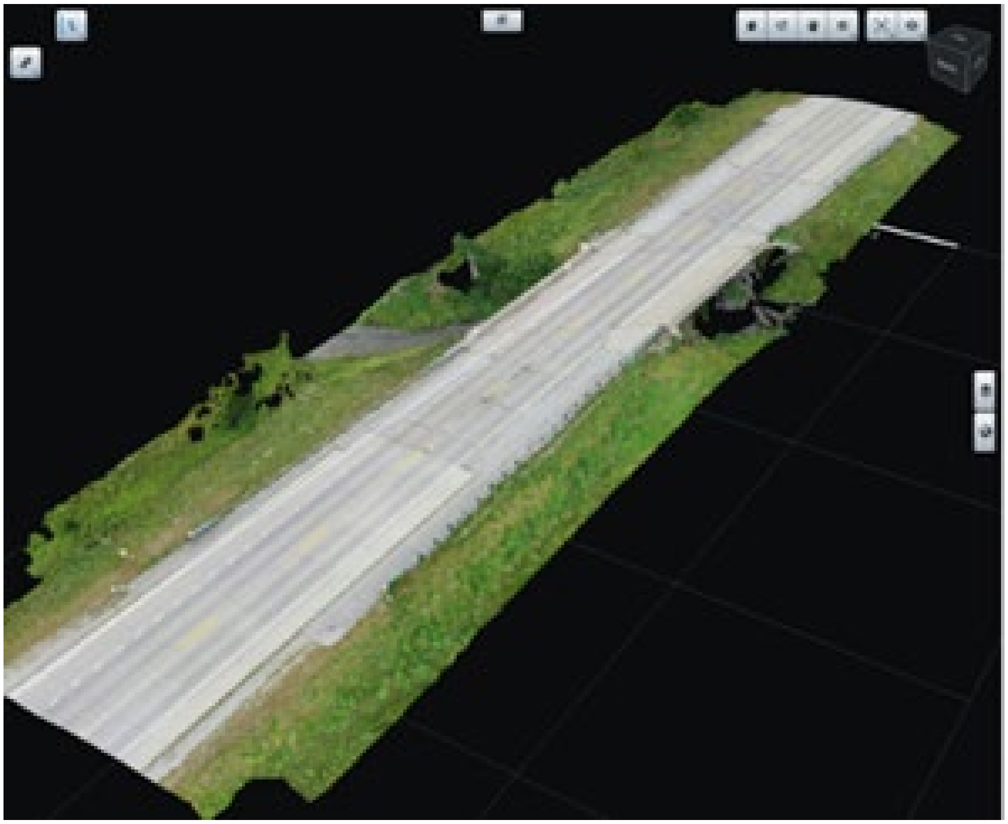

Figure 3.7. 3D model by Bentley iTwin Capture

Bentley iTwin Capture has powerful measurement capabilities for characteristics such as location, distance, area, and volume. Incorporating and utilizing these capabilities with high-quality 3D models allows for a safe and fast inspection and damage detection process. In order to represent the use of these measurement tools in Bentley iTwin Capture, some defects were measured in the generated bridge. Figures 3.8 to 3.11 present examples of the use of measurement tools in Bentley iTwin Capture.

Figure 3.8. Measurement of the depth of a pothole

Figure 3.9. Measurement of the length of a crack

Figure 3.10. Measurement of the area of a defect

Figure 3.11. Measurement of the width of a crack

The second software package used to generate a 3D model was Autodesk Recap Pro. Using this software, we generated another 3D model for the same case study bridge. The model was of lower quality than the model generated by Bentley iTwin Capture, and the resolution and details of the bridge were not as clear as those in the model generated by Bentley iTwin Capture. Figure 3.12 presents the model generated by Autodesk ReCap Pro.

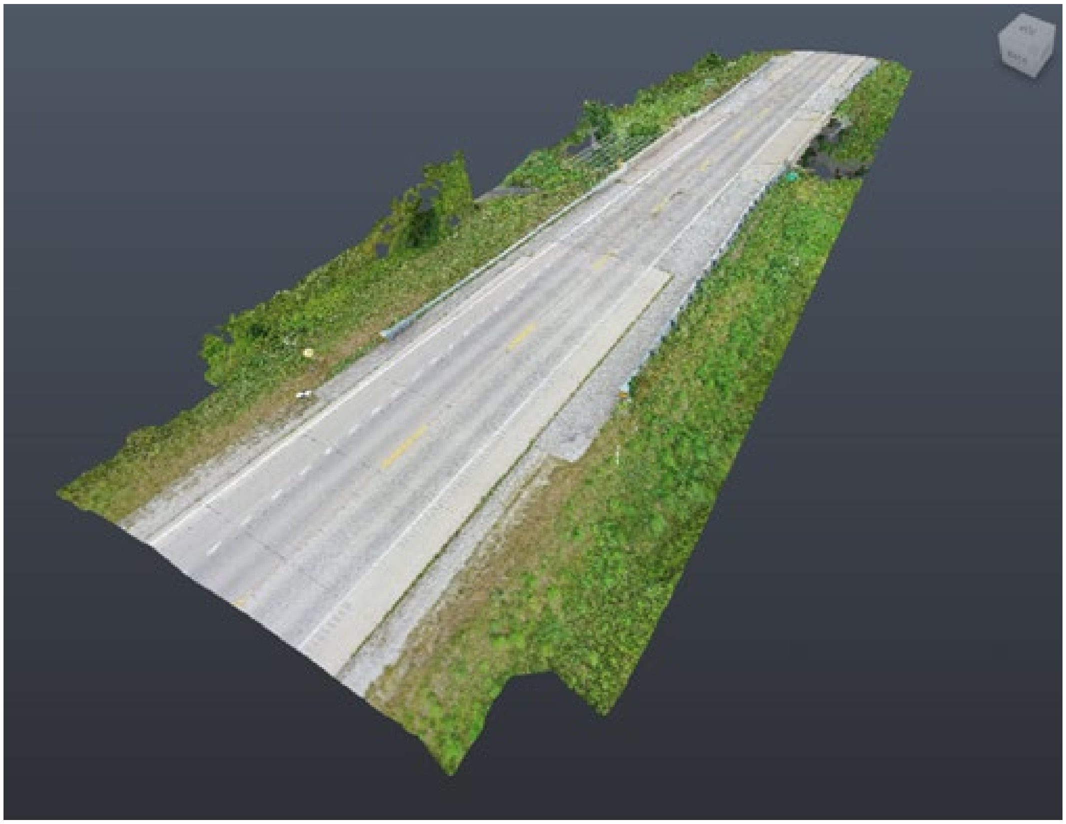

Figure 3.12. 3D model generated by Autodesk ReCap Pro

The third software application utilized to generate a 3D model was Pix4D. The model generated by this software had the lowest quality of all the models generated for the case study. The details of the defects almost vanished, and the model looked like a pixel model. Figure 3.13 presents the model generated by Pix4D.

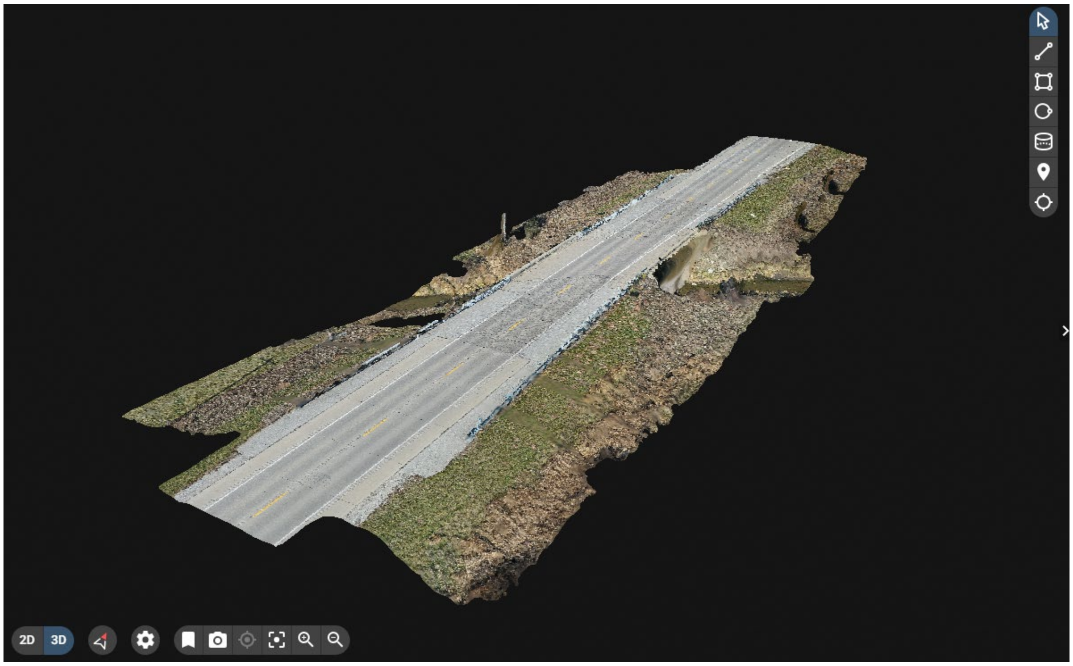

Figure 3.13. 3D model generated by Pix4D

3.4.2 Case Study Results

Figure 3.14 shows a comparison between the 3D models generated by the three software applications for the case study bridge. From Figure 3.14, we can notice the difference in model quality between the three software applications, even though all three used the same dataset to generate their models. Bentley iTwin Capture generated the highest-quality and most accurate model among the three software applications.

(a)

(b)

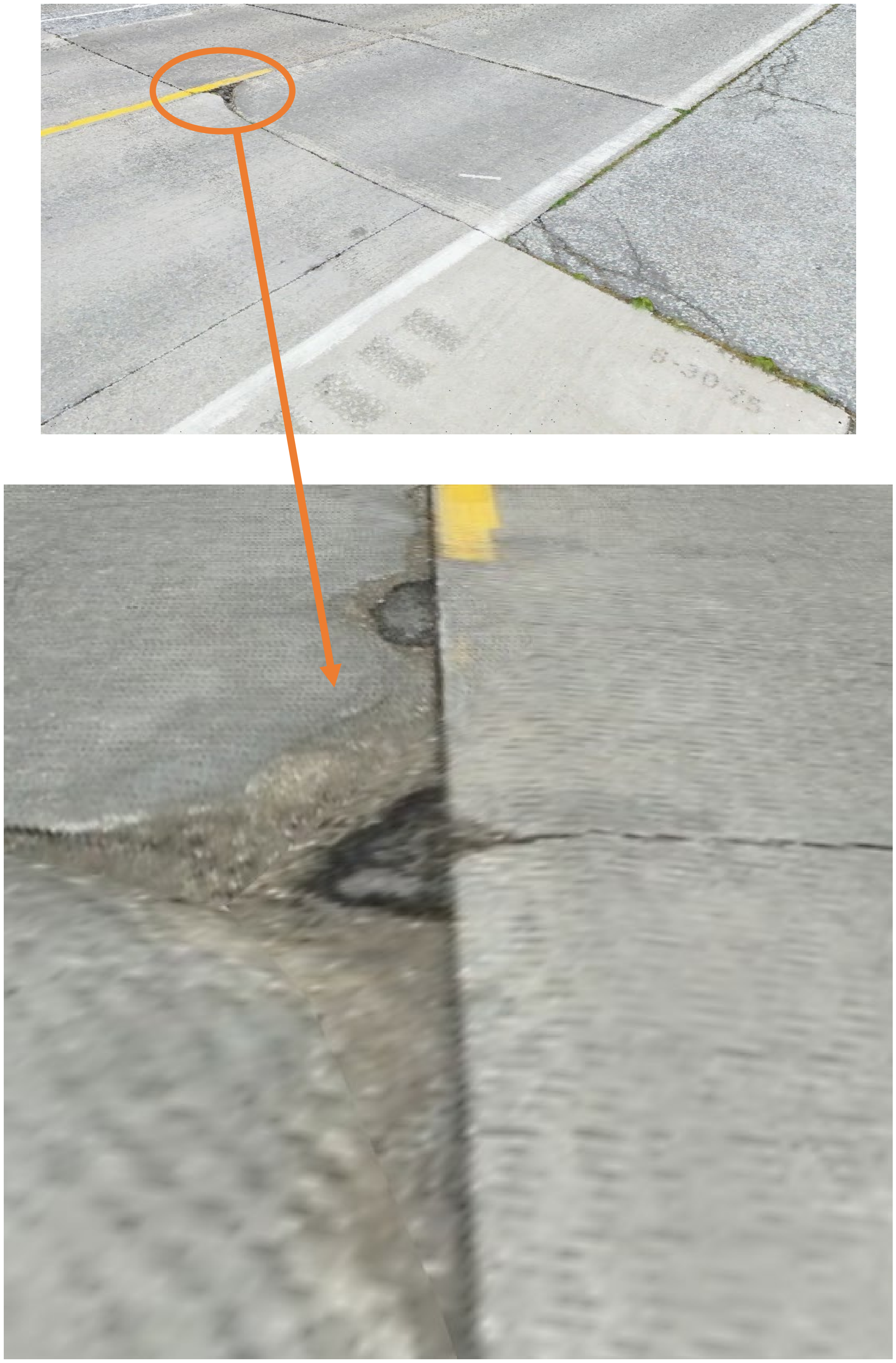

(c)

Figure 3.14. Comparison between (a) Bentley iTwin Capture, (b) Pix4D, and (c) Autodesk ReCap Pro

During the generation of the bridge models, an issue was encountered in the substructure of the bridge, as all three software applications were unable to model this section. The reason for this was attributed to the flying mode of the drones used to capture the image dataset. As mentioned previously, there are several flying modes available for drones. The sequence of the yellow boxes in Figure 3.15 represents the drones flying under automatic mode. In contrast, Figure 3.16 represents the substructure of the bridge, with the orange boxes indicating the images that were not used to generate the 3D model. This occurred because the images in the orange boxes were taken under manual flying mode, where no sequence or overlap between the images was present.

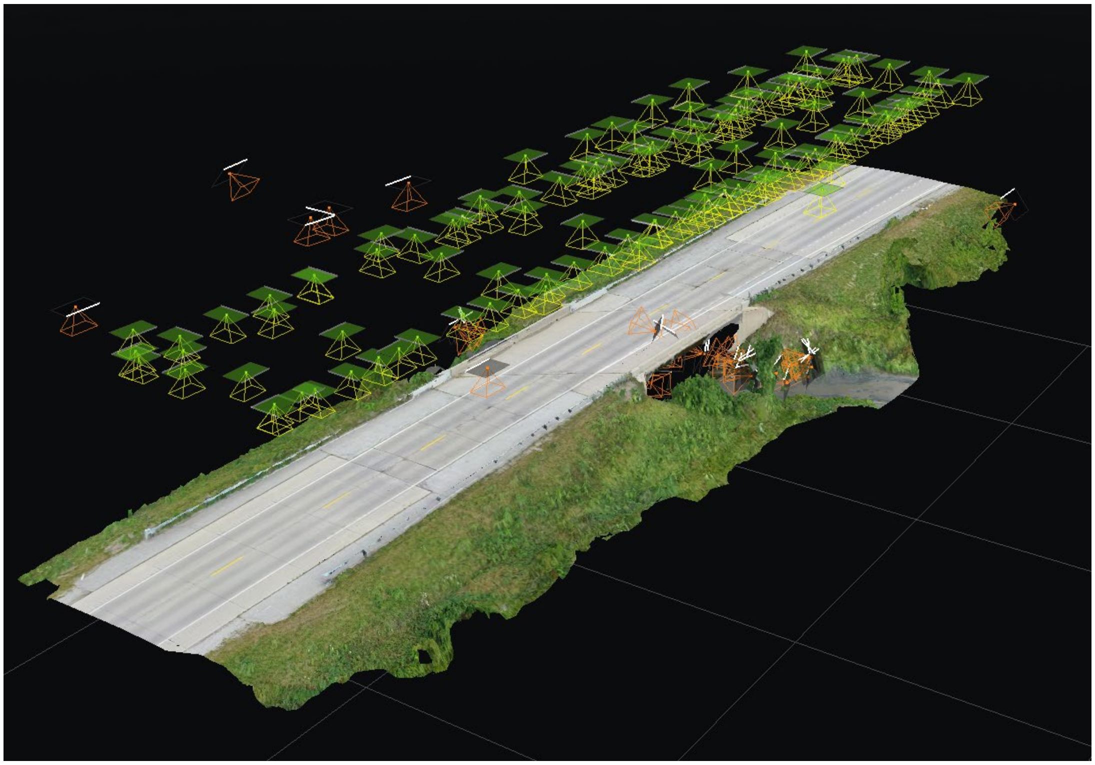

Figure 3.15. Image locations and positions used to generate the 3D model

Figure 3.16. Image locations and positions not used to generate the 3D model

3.5 AI Implementation

The integration of AI technology into Bentley iTwin Capture represents a significant advancement in the field of infrastructure management. By preparing and training AI algorithms, software packages like Bentley iTwin Capture can automate and enhance various aspects of their operations. AI can be utilized for more efficient and accurate feature recognition in captured data, improving the identification of defects and anomalies during inspections. In this study, we applied AI capabilities to detect potholes and cracks in the case study bridge following the steps outlined in the iTwin Context Capture manual. Figures 3.17 and 3.18 illustrate the before and after results of applying the detection model. The software learns from provided pretrained weights to detect cracks (represented by blue lines) and potholes (indicated by green shadows).

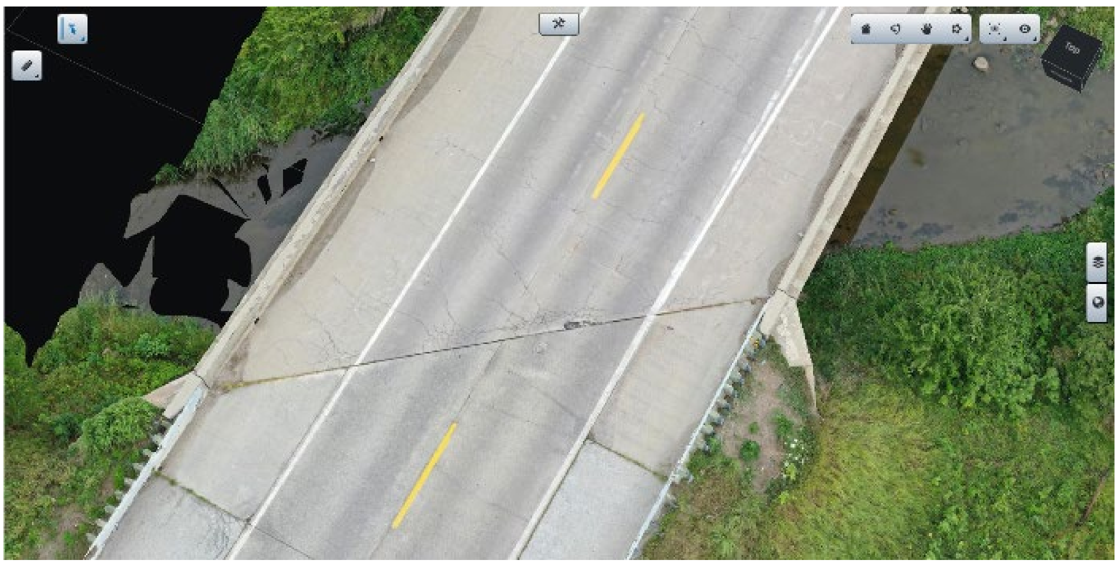

(a)

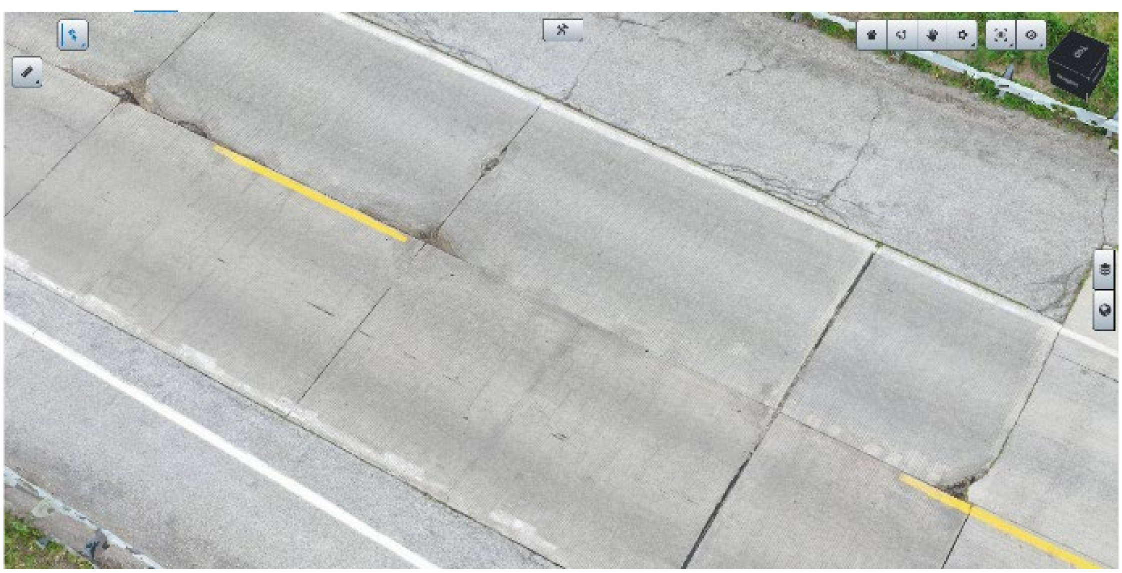

(b)

Figure 3.17. 3D model of the bridge before applying the detection algorithm

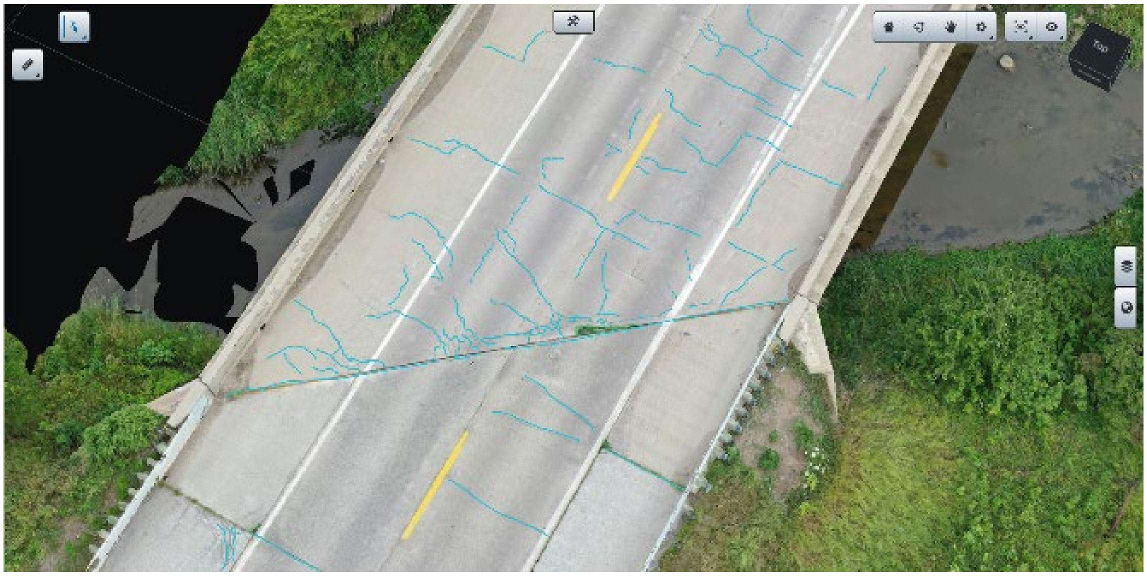

(a)

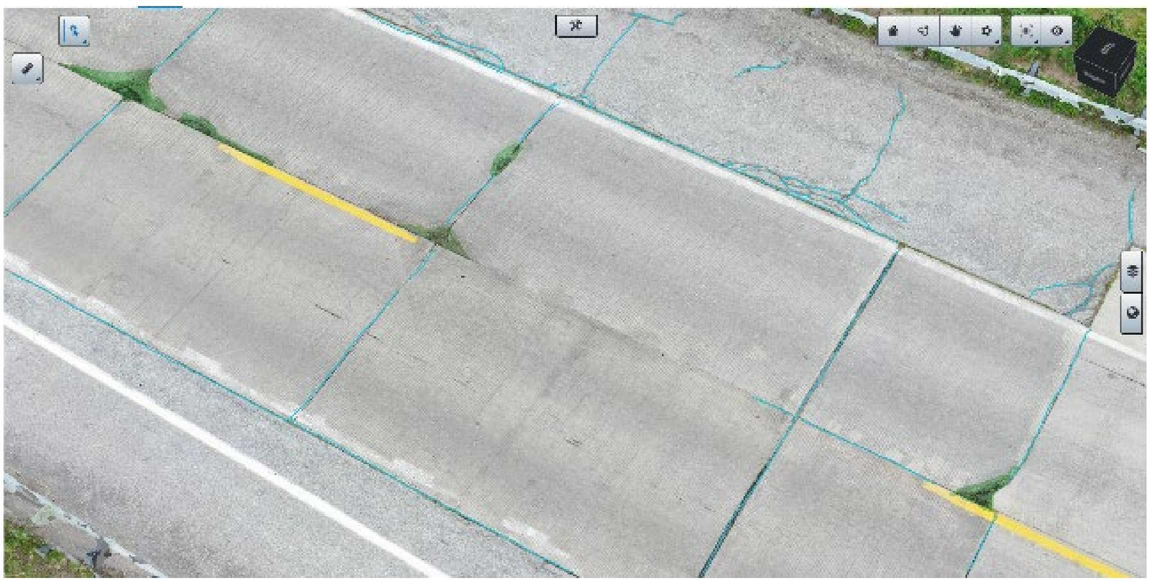

(b)

Figure 3.18. 3D model of the bridge after applying the detection algorithm

The detection method employed in this case study was based on semantic segmentation, a technique that trains the AI to detect and classify each pixel in an image. This approach resulted in high accuracy, as evident in Figure 3.18. The pixel-level detection allowed for precise identification and localization of defects, providing a detailed and comprehensive analysis of the bridge’s condition. This AI-driven approach significantly enhances the inspection process by automating the detection of structural issues that might be overlooked in traditional visual inspections. It not only improves the efficiency of infrastructure management but also contributes to more accurate and reliable assessments of structural integrity, ultimately leading to better-informed decisions regarding maintenance and repairs.

CHAPTER 4: AUTOMATED DAMAGE DETECTION

4.1 Detection Model

Damage detection through the use of automation technology takes place after damage assessment. As mentioned in Chapter 2, researchers have implemented various techniques such as CNN, AI, and ML to predict and highlight defects in images. Furthermore, UAVs are utilized in multiple aspects of the damage detection and assessment process because they can be controlled from a safe distance.

4.2 Data Sources

High-quality images are crucial for damage detection models because they ensure a precise and realistic view of defects, especially in locations with low illumination. In this study, a damage detection model was developed using the same images that were captured by drones for use in the digital twin model. These are high-quality images with a resolution of 5472 × 3648 pixels, and even with zoom-in into the images, the details in the images are still clear.

The bridge images that were available were utilized to annotate different damage types in order to create a customized dataset. Several defects like cracks, concrete spalling, corrosion, peeling paint, etc. were identified. The annotation was performed using the tools available in Roboflow, a software platform designed to assist in the development and optimization of computer vision models. Roboflow provides many tools for annotating images, such as the ability to label objects within images using bounding boxes or other methods. Moreover, Roboflow can automatically augment images (e.g., by changing brightness, cropping, or resizing) to increase the diversity of the dataset.

Using Roboflow to annotate images involved multiple steps. First, the images were uploaded to Roboflow by creating a new project. Then, the type of annotation needed for the project was selected, such as bounding boxes or polygons. Next, each image was manually annotated, for example, by drawing boxes around objects and labeling them with the types of defects. After all of the images were annotated, the annotated data were exported in several formats that suited the needs of this project. This exported data were then ready for training or testing machine learning models. Figures 4.1 and 4.2 present examples of images before and after annotation.

(a)

(b)

Figures 4.1. Example of bridge substructure image before annotation

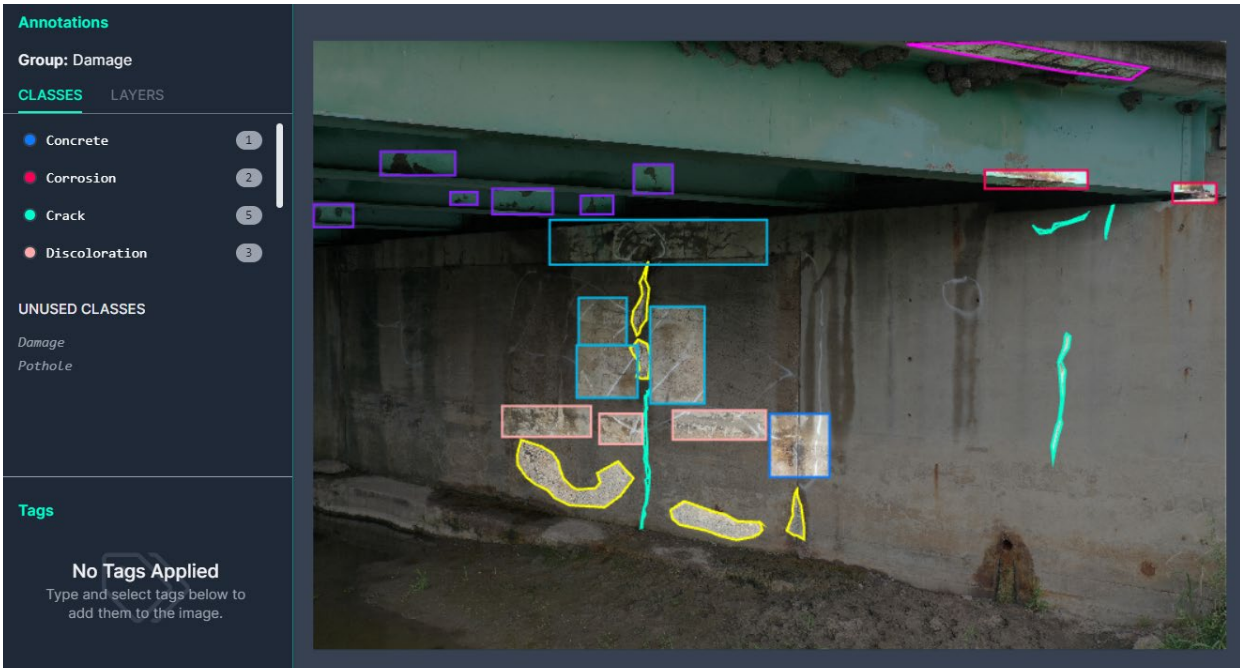

(a)

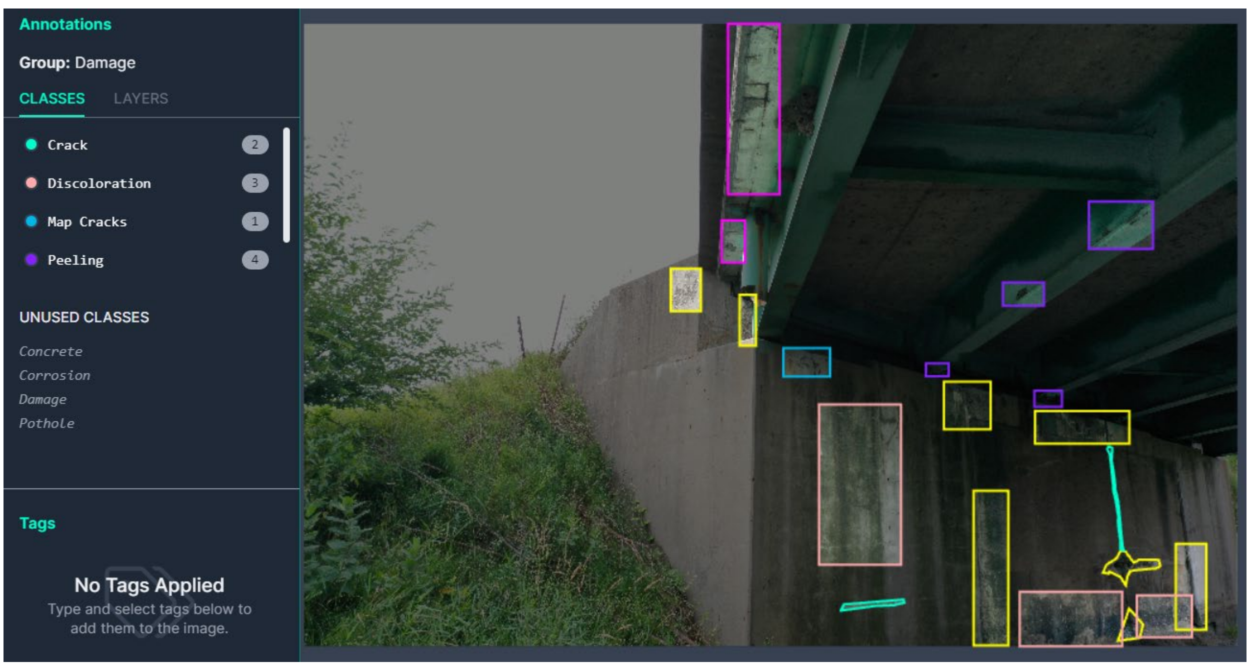

(b)

Figures 4.2. Example of bridge substructure image after annotation

4.3 Model Architecture

4.3.1 YOLOv7

The basis of the model developed in this study was YOLOv7, a fast and accurate object detection model. YOLOv7 is a CNN model that identifies and classifies various elements in a very short period, making it highly important in applications where real-time inspection is critical. This technology is widely used in various fields, such as autonomous vehicles, security surveillance, and, in our case, structural analysis of bridges. Its ability to analyze complex-image and detect defects, such as structural cracks, makes it a valuable tool in ensuring safety and efficiency in various engineering and technological aspects. YOLOv7 features several key components:

1. **Backbone network**. This is used for extracting features from images. Different options are available, each balancing accuracy and speed.
2. **Neck and head**. The "neck" aggregates features of various sizes, while the "head" predicts bounding boxes and object classes.
3. **Anchor boxes**. These are predefined boxes that the model adjusts to fit detected objects, aiding in the recognition of different shapes and sizes.
4. **Spatial pyramid pooling (SPP) and pyramid attention network (PAN) integration**. These enhance feature extraction and improve detection across scales.
5. **Loss function**. This includes components for bounding box regression and class prediction, which are crucial for accurate detection.
6. **Transfer learning**. This often involves pretraining on large datasets and fine-tuning for specific tasks, boosting performance.
7. **Optimizations**. These balance speed and accuracy, making YOLOv7 suitable for real-time applications.
8. **Continuous evolution**. These are regular updates that improve the effectiveness of object detection tasks.

The basic and original network of the YOLOv7 structure is shown in Figure 4.3. Each image uploaded to the model goes through three steps: Initial Processing (Backbone), Feature Extraction (Neck), and Classification of Objects (Head).

1. **Initial Processing (Backbone).** This is the part of the network that performs the initial input image processing. It typically consists of a series of convolutional layers and pooling layers, which are designed to extract features from the image. Here, the backbone processes the input image down from its original through various layers (denoted as Convolution-BatchNorm-ReLU [CBR], Extended Efficient Layer Aggregation Network [E-ELAN], and Max Pooling), reducing the locative dimensions while simultaneously raising the depth of features in the input data.
2. **Feature Extraction (Neck).** This part of the model basically refines the features extracted in the first step and prepares them for the final step, which is detection. It might include additional convolutional layers and often uses techniques to combine features of different scales for multiscale feature learning. In each image, there are operations like Cross Stage Partial Network (CSPNet) and SPP-Block, which is a series of pooling and convolutional

layers, concatenation operations (cat), and finally up-sampling to increase the resolution of the features in the image.

3. **Classification of Objects (Head).** In this step, the head of the network is responsible for making the object predictions. This includes locating and classifying objects in the case of an object detection network. It typically includes convolutional layers (repetitive parameterization of convolutions (Re-ParConv) and outputs the final predictions.

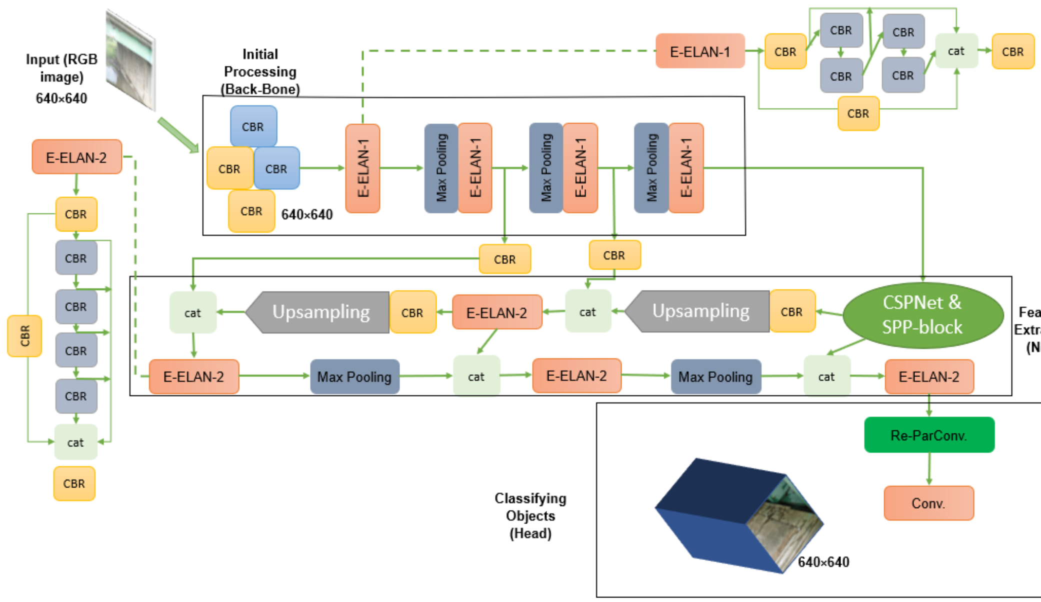

Figure 4.3. Original YOLOv7 network structure

4.3.2 Augmented Damage Detection Model

To address the limitations of existing damage detection models, a new model was needed with the ability to not only detect damage but also quantify its severity. Many current models are effective at identifying structural issues, but they often fall short when it comes to accurately measuring the extent of the damage. This gap in capabilities highlights the need for a more advanced approach, particularly in applications where precise quantification is essential for decision-making and preventive maintenance.

To this end, the capabilities of the YOLOv7 object detection model were successfully improved and extended by modifying and enhancing its architecture to test input images of arbitrary resolutions. Instead of being constrained to processing and analyzing fixed-size 640 x 640 images, the newly modified model is now capable of handling inputs of any image resolution. To achieve this, additional layers were introduced and compiled to dynamically adapt the matrix sizes of the feature maps and tensors propagated through the architecture. These new layers ensure seamless adaptation of the model's internal representations to match the input image dimensions. Furthermore, the model was modified to process inputs with randomly varying resolutions during training and validation. This enhancement allows the model to learn from and make predictions based on images of various resolutions, increasing its practicality for different users.

The second part of the new model determines the quantification of the defects. After detecting and highlighting the defects in the image, the second part of the model determines the number of pixels inside the annotated defects using the region-growing algorithm. The region-growing algorithm, which is also referred to as the tracking algorithm, is implemented to sort the thinned pixels that follow each other within the predicted defect. Figure 4.4 illustrates the tracking algorithm.

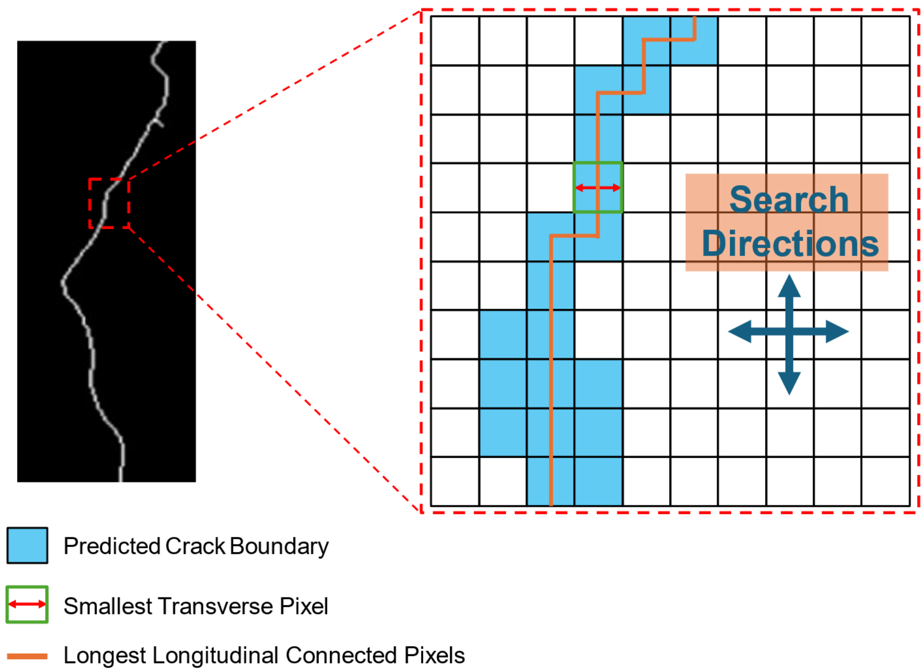

Figure 4.4. Illustration of region-growing algorithm

The search directions play a fundamental role in accurately quantifying the number of pixels within the predicted damage. As illustrated in Figure 4.4, the algorithm explores the defect boundaries in multiple directions: left, right, up, and down. This multidirectional search ensures that all connected pixels within the bounds of the predicted defect are captured accurately. The process includes identifying the smallest transverse pixel and the longest longitudinal connected pixels for the defect.

After finding the number of pixels for the width and the length, the model converts these results through several steps into a real-world dimension, as shown in Figure 4.5. Starting with the camera matrix and properties [K],

$$[K] = \begin{bmatrix} f_x & 0 & c_x \\ 0 & f_y & c_y \\ 0 & 0 & 1 \end{bmatrix} \tag{4.1}$$

$$f_x = f\ \frac{w}{s_x} \tag{4.2}$$

$$f_y = f\ \frac{h}{s_y} \tag{4.3}$$

where f indicates the focal length of the camera in both the x and y directions; s_y and s_x represent the height and the width of the sensor, respectively; h and w represent the height and the width of the image, respectively; and (c_x, c_y) is the principal point (optical center) in pixels.

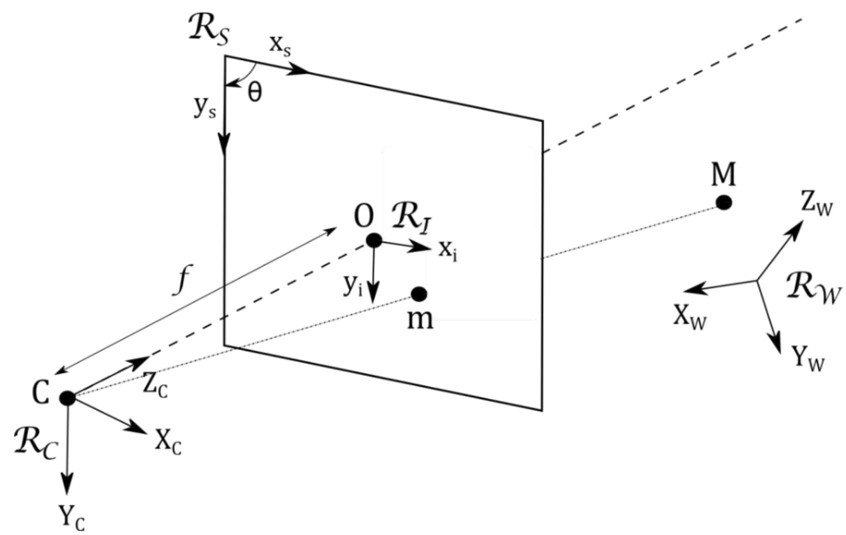

Figure 4.5. Illustration of camera calibration

The normalized image coordinates (x_n, y_n) after the pixel coordinates (u,v) are converted using the camera matrix and properties [K] are as follows:

$$\begin{bmatrix} x_n \\ y_n \\ 1 \end{bmatrix} = \begin{bmatrix} \frac{u-c_x}{f_x} \\ \frac{v-c_y}{f_y} \\ 1 \end{bmatrix} \tag{4.4}$$

Knowing the depth Z_c between the camera and the object in the image, the model uses the normalized coordinates to calculate the camera coordinates as follows:

$$\begin{bmatrix} X_c \\ Y_c \\ Z_c \end{bmatrix} = \begin{bmatrix} Z_c \frac{u-c_x}{f_x} \\ Z_c \frac{v-c_y}{f_y} \\ Z_c \end{bmatrix} \tag{4.5}$$

After obtaining the camera coordinates (X_c, Y_c, Z_c), the model implements the inverse of extrinsic matrix [R|t] to convert the camera coordinates to world coordinates:

$$\begin{bmatrix} R & t \\ 0 & 1 \end{bmatrix} = \begin{bmatrix} r_{11} & r_{12} & r_{13} & t_x \\ r_{21} & r_{22} & r_{23} & t_y \\ r_{31} & r_{32} & r_{33} & t_z \\ 0 & 0 & 0 & 1 \end{bmatrix} \tag{4.6}$$

$$\begin{bmatrix} R^{-1} & -R^{-1}t \\ 0 & 1 \end{bmatrix} = \begin{bmatrix} r_{11} & r_{21} & r_{31} & -(r_{11}t_x + r_{21}t_y + r_{31}t_z) \\ r_{12} & r_{22} & r_{32} & -(r_{12}t_x + r_{22}t_y + r_{32}t_z) \\ r_{13} & r_{23} & r_{33} & -(r_{13}t_x + r_{23}t_y + r_{33}t_z) \\ 0 & 0 & 0 & 1 \end{bmatrix} \tag{4.7}$$

where r_{ij} stands for the rotation of the camera coordinate system and $t_x, t_y, and\ t_z$ represent the translation of the camera in the world coordinate system. Finally, the real-world dimensions are calculated through the world coordinate system:

$$\begin{bmatrix} X_W \\ Y_W \\ Z_W \end{bmatrix} = \begin{bmatrix} r_{11}X_C + r_{21}Y_C + r_{31}Z - (r_{11}t_x + r_{21}t_y + r_{31}t_z) \\ r_{12}X_C + r_{22}Y_C + r_{32}Z - (r_{12}t_x + r_{22}t_y + r_{32}t_z) \\ r_{13}X_C + r_{23}Y_C + r_{33}Z - (r_{13}t_x + r_{23}t_y + r_{33}t_z) \end{bmatrix} \tag{4.8}$$

In summary, the transformation from camera coordinates to world coordinates involves both rotation and translation components, considering the camera's orientation and position in the world space. Thus, the final architecture of the proposed model can be represented as shown in Figure 4.6.

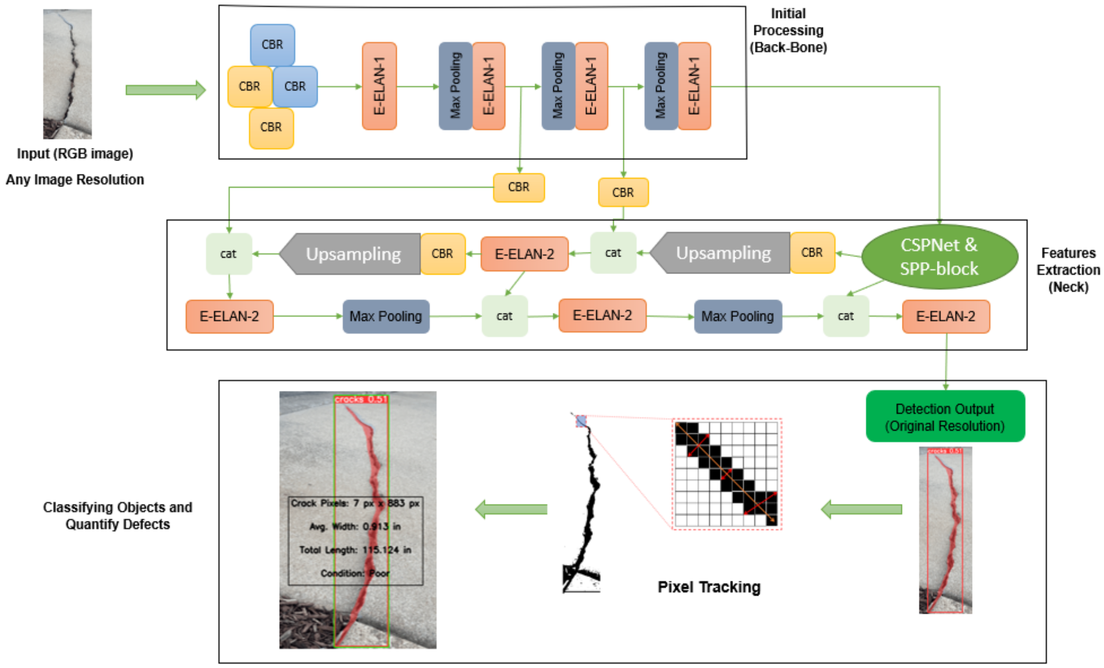

Figure 4.6. New proposed quantification and assessment model

4.4 Training and Validation

In order to substantially augment the capabilities of YOLOv7 for defect detection, a meticulous training regimen was implemented, capitalizing on an extensive dataset. This dataset, comprising over 11,000 images (7,165 images depicting cracks and 4,569 images showcasing spalling defects), was pivotal in encapsulating the nuances of concrete surface damage types. Notably, some images portrayed multiple defect instances, further enhancing the complexity of the training data. Recognizing the constraints of a finite quantity of images, additional relevant images were strategically integrated to augment the dataset. This comprehensive dataset was essential in equipping the enhanced YOLOv7 model with a thorough understanding of diverse defect appearances.

Moreover, due to the limitations imposed by the finite quantity of available images, particularly for certain types of damage, a strategic approach was taken to augment the dataset by sourcing additional images from online sources. This step was instrumental in ensuring that the training model benefited from a broader spectrum of defect presentations, enriching the dataset and providing the YOLOv7 model with a more comprehensive understanding of various manifestations of concrete surface damage.

The dataset, not only vast but also meticulously annotated, included bounding boxes precisely marked around the regions exhibiting defects. This level of detail facilitated a streamlined training process, allowing the model to rapidly assimilate the necessary knowledge for accurate defect detection. The annotations played a pivotal role in accelerating the model's learning curve, enabling quick adaptation to the intricacies of defect identification. Figures 4.7 and 4.8 present pre-annotated images for cracks and spalling in concrete, respectively.

Figure 4.7. Pre-annotated images for cracks in concrete (various backgrounds and distances)

Figure 4.8. Pre-annotated images for concrete spalling (various backgrounds and distances)

A variety of backgrounds, such as concrete, asphalt, and painted walls, were included in the dataset to help the model learn to identify objects irrespective of the background. This approach is crucial for real-world applications where objects are encountered in various settings. The introduction of different backgrounds exposed the model to varying levels of noise and clutter, challenging it to focus on the relevant features of the objects of interest. As a result, the model's ability to distinguish between foreground objects and background was improved, reducing the likelihood of false positives or negatives. Furthermore, as shown in Figures 4.7 and 4.8, images were taken from different distances. The inclusion of images taken at varying distances introduced scale and perspective variations, enabling the model to learn how the appearance of objects changes with distance. This variation is particularly important for tasks that require the recognition of objects of the same class but at different scales or orientations. Figures 4.9 and 4.10 present the annotated images for cracks and spalling in concrete, respectively.

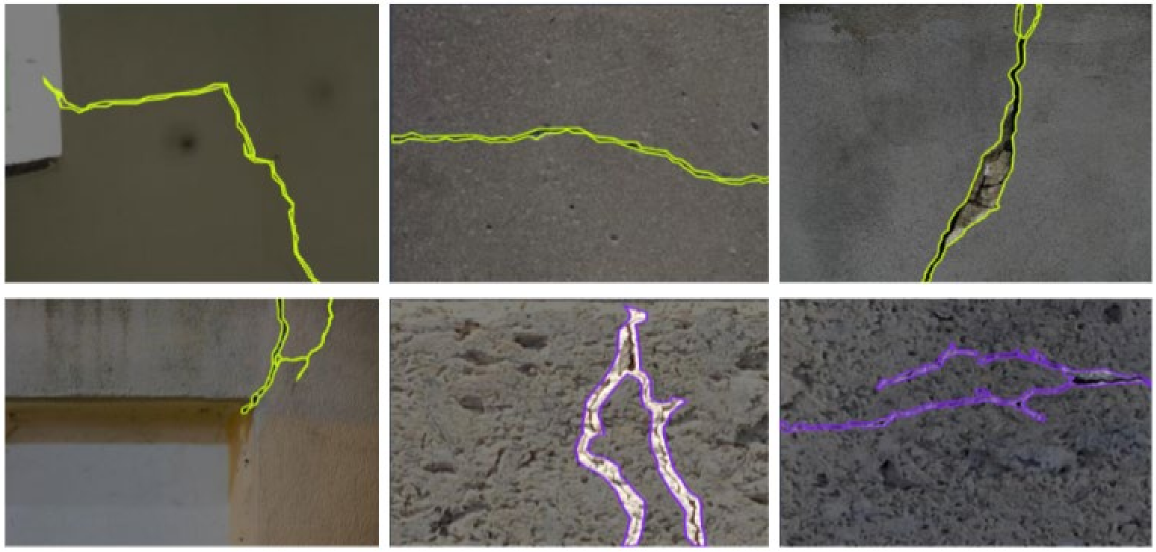

Figure 4.9. Annotated images for cracks in concrete

Figure 4.10. Annotated images for concrete spalling

Significant computing power is required for building and training AI/ML models for image processing, especially when working with high-resolution datasets. Image data are characterized by a much higher dimensionality compared to other data types like text or audio, and computationally intensive operations, such as convolution and backpropagation, are involved in their processing. To train convolutional neural networks efficiently for tasks such as image classification, object detection, and segmentation, access to powerful hardware like high-end graphical processing units (GPUs) or tensor processing units (TPUs) is necessary. Rapid prototyping and research can be dramatically accelerated with a custom-built desktop workstation equipped with multicore central processing units (CPUs) and the latest GPUs, leading to a substantial reduction in training times compared to commodity hardware.

In order to train the developed model, Google Colaboratory (Colab) was utilized (see Figure 4.11). Google Colab Pro, a cloud service based on Jupyter notebooks, provides GPUs and TPUs for accelerated computing. Key features of Google Colab Pro, including access to GPUs for faster training of machine learning models, easy sharing and collaboration on notebooks, and integration with other Google services like Drive and Sheets, were leveraged. Google Colab Pro's GPU resources were accessed through a paid subscription, allowing for efficient training and execution of the deep learning model, with the GPU hardware providing a significant speedup. The flexible Google Colab environment facilitated effective collaboration within the research team, while Google's cloud infrastructure was utilized. The Google Colab Pro subscription offered benefits such as longer runtimes, faster hardware, and higher memory allocations to support the training of the computationally intensive model.

Figure 4.11. Google Colaboratory logo

The new model can successfully detect image defects with high precision and accuracy. To indicate the accuracy of the present model, a confusion matrix is presented in Figure 4.12, which reveals substantial true positive rates for "Cracks" (0.88) and "Spalling" (0.92). These high values signify the model's proficiency in correctly identifying the respective classes. Though minimal, the off-diagonal elements of the matrix draw attention to the comparatively fewer instances where the model confuses one class for another.

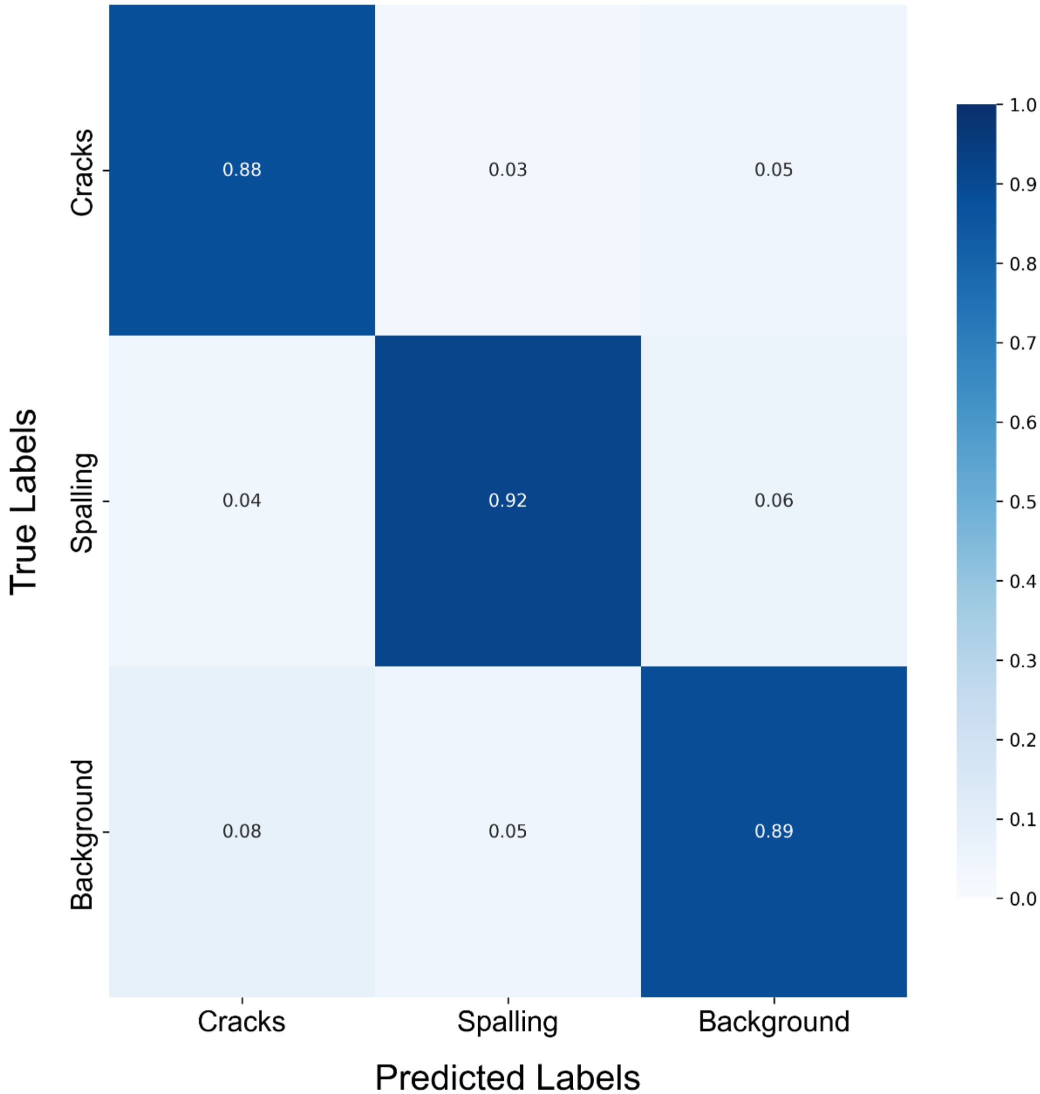

Figure 4.12. Confusion matrix of the developed model

Complementing the confusion matrix, the correlogram of label distributions shown in Figure 4.13 offers additional insights into the model's performance. The distribution of labels across the dimensions, such as the x and y coordinates and the width and height of the detected regions, showcases a concentrated cluster, indicating that the model consistently detects defects within a specific range of features. This correlogram elucidates the relationship between different label attributes and provides an understanding of the geometric characteristics and the locations of detected defects.

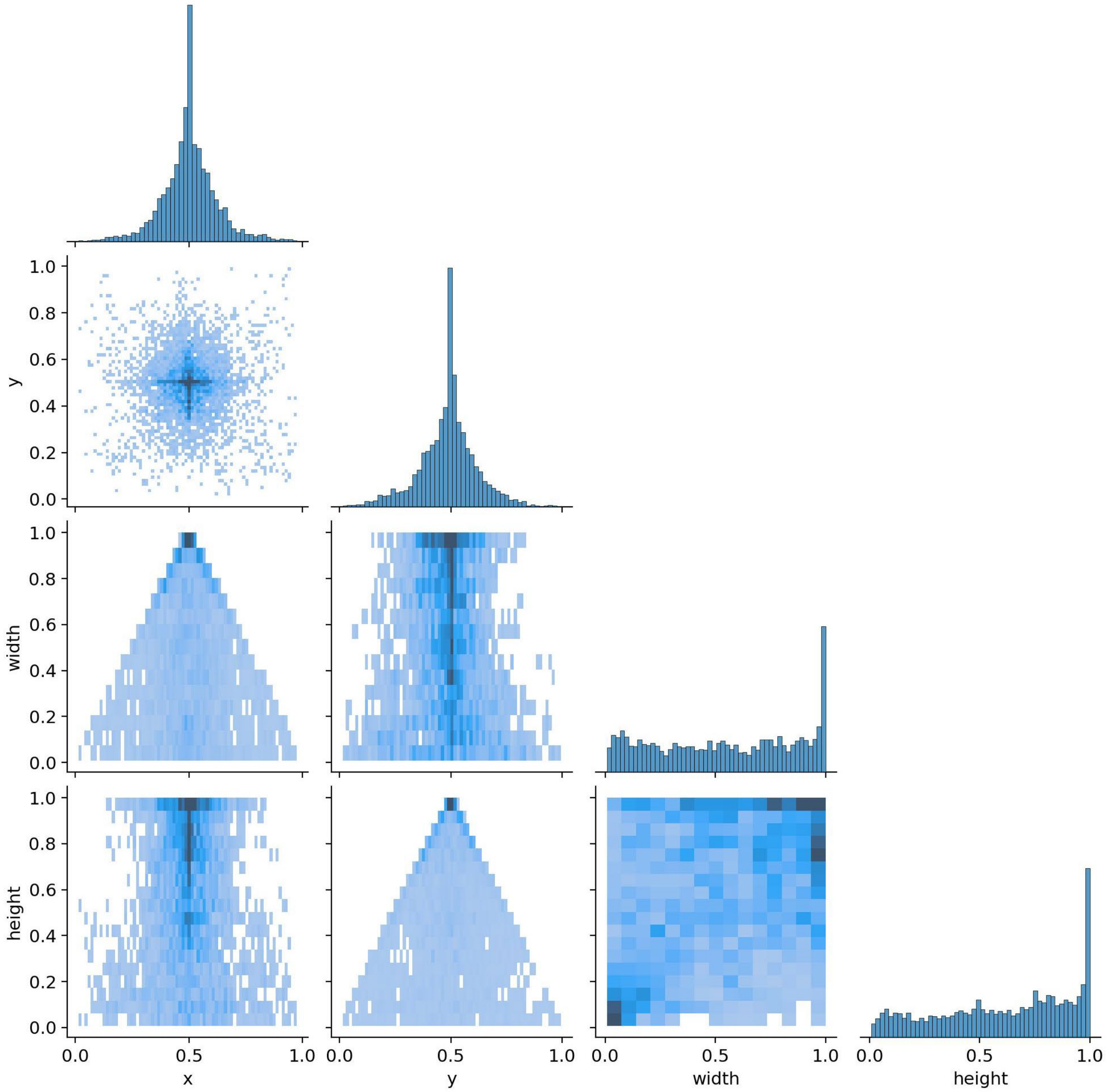

Figure 4.13. Labels correlogram

Together, these tools underscore the model's efficacy. The F1 confidence curves in Figure 4.14 support the confusion matrix in Figure 4.12, demonstrating the model's performance across different classes and indicating a uniform precision in defect detection.

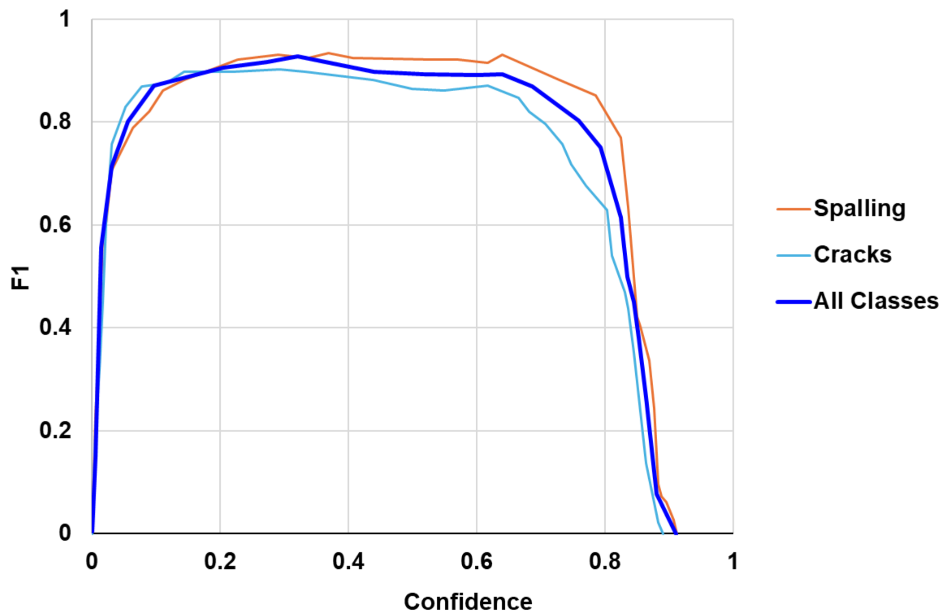

Figure 4.14. F1 confidence curves for the improved Yolov7 model

The F1 confidence curves presented here clearly indicate the model's capacity for distinguishing between defect classes with high fidelity. The curves for "Spalling" and "Cracks" remain tightly bound with little deviation between these classes, which suggests that the model discriminates between them with near-equal accuracy. Meanwhile, the "All Classes" curve, which aggregates the performance across all categories, maintains a trajectory consistent with that of the individual class curves, indicating a uniform performance across the board. As the confidence threshold increases, the F1 score remains consistently high before the inevitable decline as the threshold approaches 1, which is typical due to the reduction in recall. This trend highlights the model's capability to balance precision (the accuracy of positive predictions) and recall (the ability to capture all relevant instances) over a wide range of operational points.

4.5 Results and Discussion

The results successfully obtained from the present model for detecting and quantifying deterioration in concrete structures are presented and analyzed in this section. The performance of the model in detecting structural defects such as cracks and spalling is evaluated across various conditions. The effects of fine-tuning procedures and advanced quantification algorithms on the model's capabilities are assessed. The model's accuracy in damage detection is examined, with a focus on its effectiveness in real-world scenarios (such as variations in illuminance effect, distance, and angle of capture). Improvements achieved through fine-tuning are discussed, and enhanced performance in different contexts is highlighted. The model's ability to quantify detected defects is also evaluated, providing insights into its potential for precise damage assessment.

4.5.1 Damage Detection

When high-resolution images are uploaded to the present model, structural deficiencies, particularly cracks and spalling, within concrete surfaces are detected with remarkable accuracy. Utilizing the new image processing layers, the model successfully identifies even the smallest cracks, such as those as narrow as 0.022 in., as demonstrated in Figures 4.15 and 4.16. The precision and sensitivity of this detection are evident, as the model can highlight cracks that are barely visible. For instance, the images in Figures 4.15 and 4.16 show a concrete surface where, from a distance of 4 ft, the naked eye can barely detect any defect, yet the model accurately marks the fine cracks.

Figure 4.15. Image of concrete cracks before the image is uploaded to the model

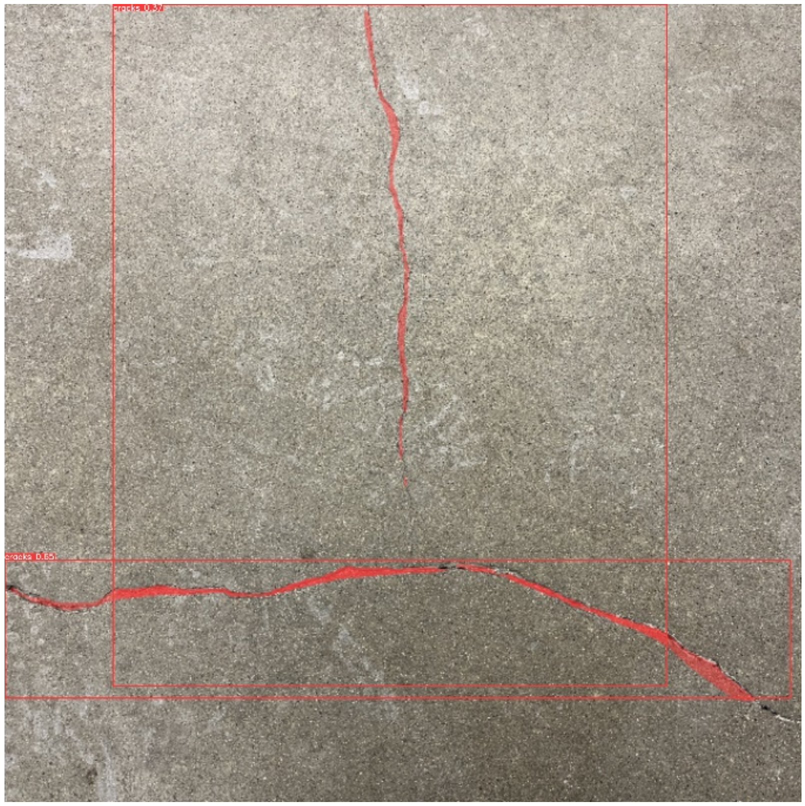

Figure 4.16. Result of concrete crack detection after the image is uploaded to the model

This result demonstrates the model's potential for use in real-time, non-intrusive inspections in field conditions to help ensure the safety and longevity of concrete infrastructure. This capability is instrumental in structural health monitoring, where undetected microcracks can escalate into significant issues. Moreover, Figures 4.15 and 4.16 demonstrate that the model is able to detect defects in smooth concrete surfaces, which is one of the most popular finishes for concrete surfaces, and that the model can calibrate camera properties, such as the distance to the defect, by incorporating those properties into the model's layers.

Figure 4.17 demonstrates the model's advanced detection capabilities from a distance of 15 ft, which exhibits its ability to detect cracks accurately even when the image is taken far from the defects. Moreover, the angle of capture of the image is not directly perpendicular to the crack (not 90 degrees), which highlights the capabilities of the model in processing different distances and angles of capture. The concrete surface in this example is normal concrete, which has a different color and surface texture than the concrete in Figures 4.15 and 4.16. There is also a slightly inclined driveway, which adds to the complexity of detection.

Figure 4.17. Result of concrete crack detection before and after an image is uploaded to the model

Despite these challenges, the model successfully identifies the crack while distinguishing it from other concrete segmentation lines, such as the expansion joints often found between concrete slabs. This precise differentiation illustrates the model's advanced capability to distinguish between the naturally occurring features of concrete surfaces and actual structural defects. The accuracy achieved under these conditions further emphasizes the model's adaptability to diverse concrete surfaces, which can ensure effective monitoring of large-scale structures where perfect angles and close proximity are not always feasible.

Figure 4.18 demonstrates the model's advanced detection capabilities for concrete spalling, accurately identifying areas of damage with precision. The spalling is detected even when the concrete surface has exposed reinforcing steel bars, which adds to the complexity of the detection process and in some cases leads to a different prediction. The image highlights the model's ability to handle real-world degradation scenarios, as spalling often leads to significant structural sensitivity, especially in this case where the steel bars are exposed to corrosion. Despite the surface irregularities and the varying textures of the spalled regions, the model successfully distinguishes between undamaged concrete and areas where spalling has occurred. Additionally, the model maintains high accuracy in segmenting the spalled areas from the surrounding concrete, even in situations where multiple spalling regions are present, as shown in Figure 4.18. This capability underscores the model's potential for real-time structural health monitoring, where detecting spalling early is critical for preventing further deterioration of concrete surfaces.

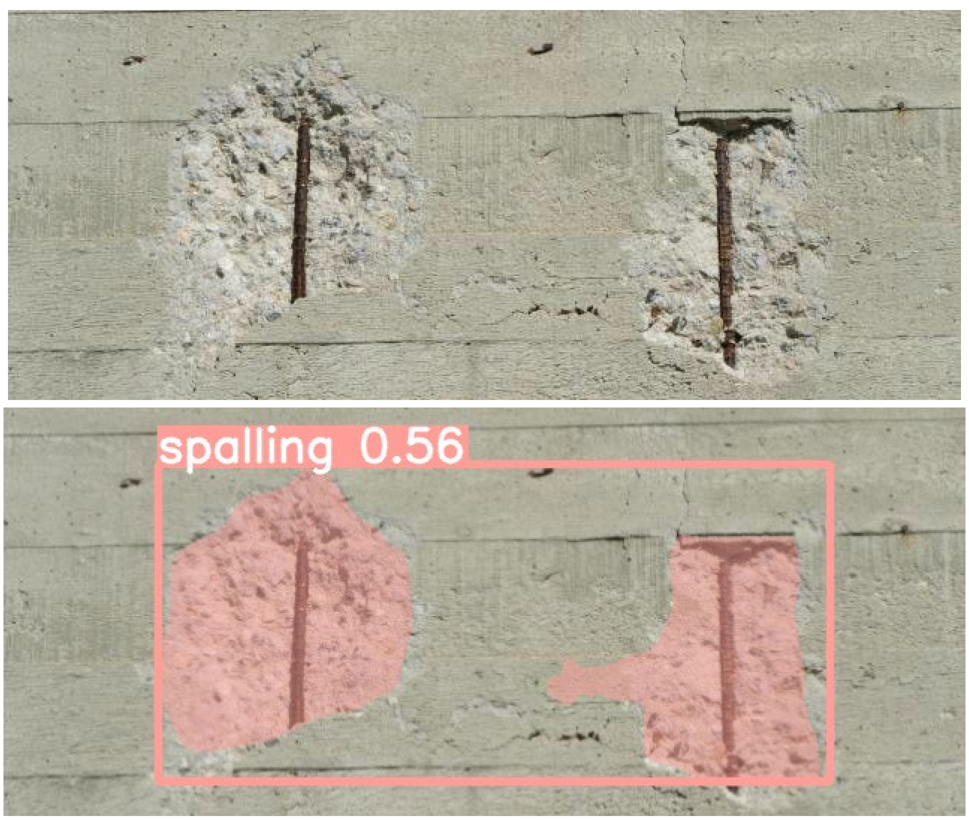

Figure 4.18. Result of concrete spalling detection before and after an image is uploaded to the model (testing for the detection of multiple damage types in one image)

Figure 4.19 showcases the model's ability to detect spalling across varying distances and complex backgrounds. In the top set of images, the top-left and bottom-left images were captured from a closer distance of approximately 7 ft, allowing for precise detection of the spalling around exposed reinforcement bars. The image on the right was captured from a greater distance of approximately 40 ft and presents a vertical column with extensive spalling. The different backgrounds, including smoother surfaces and more intricate textures with exposed rebar, demonstrate the model's adaptability in detecting damage across various conditions. With all these factors and obstacles to detecting damage, the proposed model nevertheless successfully highlights all of the slight curves and edges of the concrete spalling in the figures. The model effectively distinguishes spalling from background features like surface cracks or variations in concrete texture, further emphasizing its capability to handle complex structural inspections.

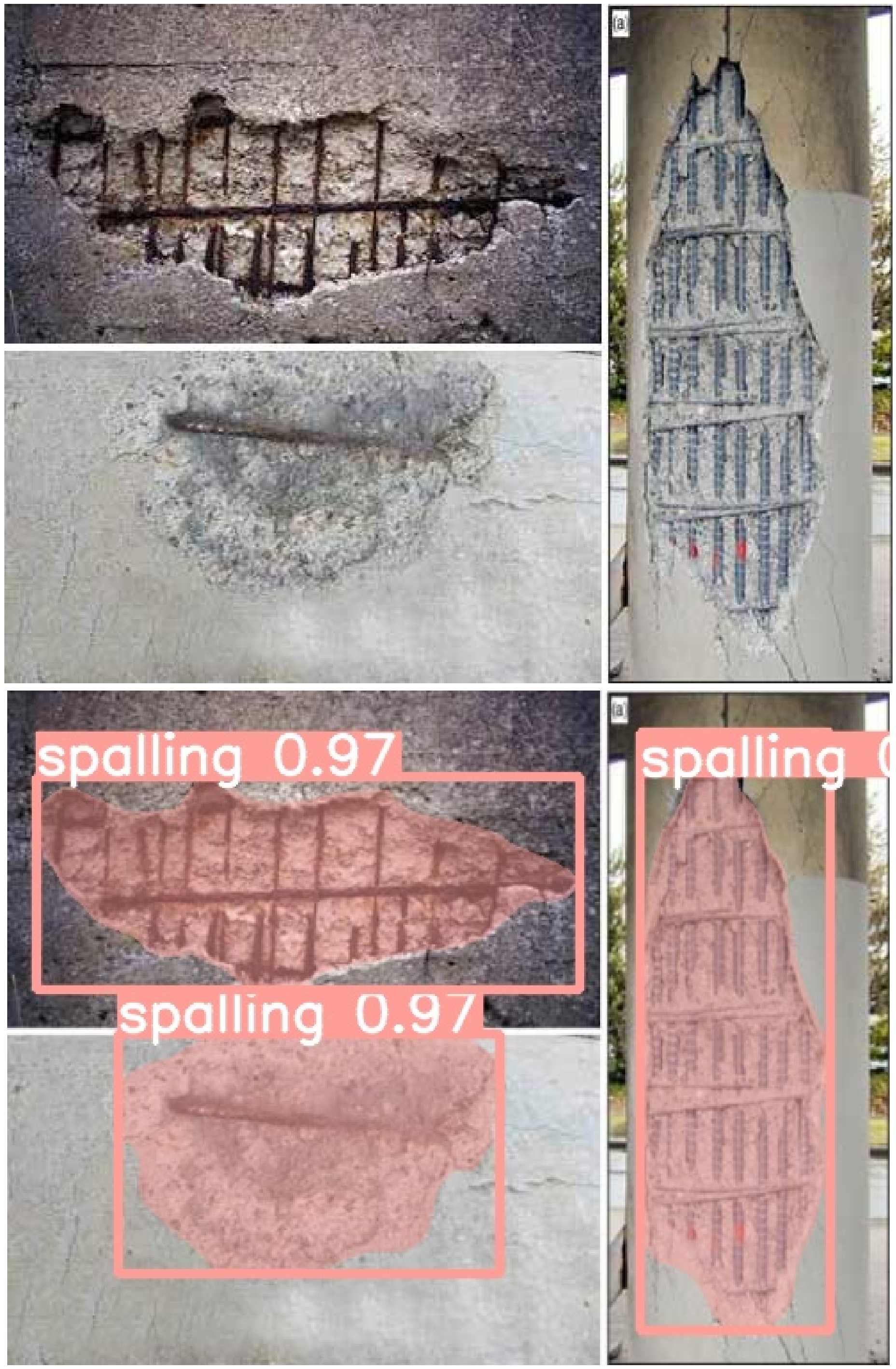

Figure 4.19. Result of concrete spalling detection before and after an image is uploaded to the model (testing for the detection of multiple damage types in different backgrounds)

In Figure 4.20, the developed model successfully detects the pattern of cracks in an image from the case study bridge, which exhibits its ability to identify even the most minor defects that are not visible to the naked eye. As highlighted in the zoomed-in section, the model accurately detects a small crack located in the bottom right corner of the concrete wall. This crack, while barely perceptible without advanced tools, is clearly outlined by the model, demonstrating the model's high sensitivity to minute structural deficiencies. As can be noticed in Figure 4.20, the bridge structure is subjected to environmental factors such as moisture (which causes concrete discoloration) and load stress, which often leads to the development of microcracks that can evolve into more significant issues if left unaddressed. The model's capacity to detect these early-stage cracks is crucial for proactive maintenance and preventing more severe damage.

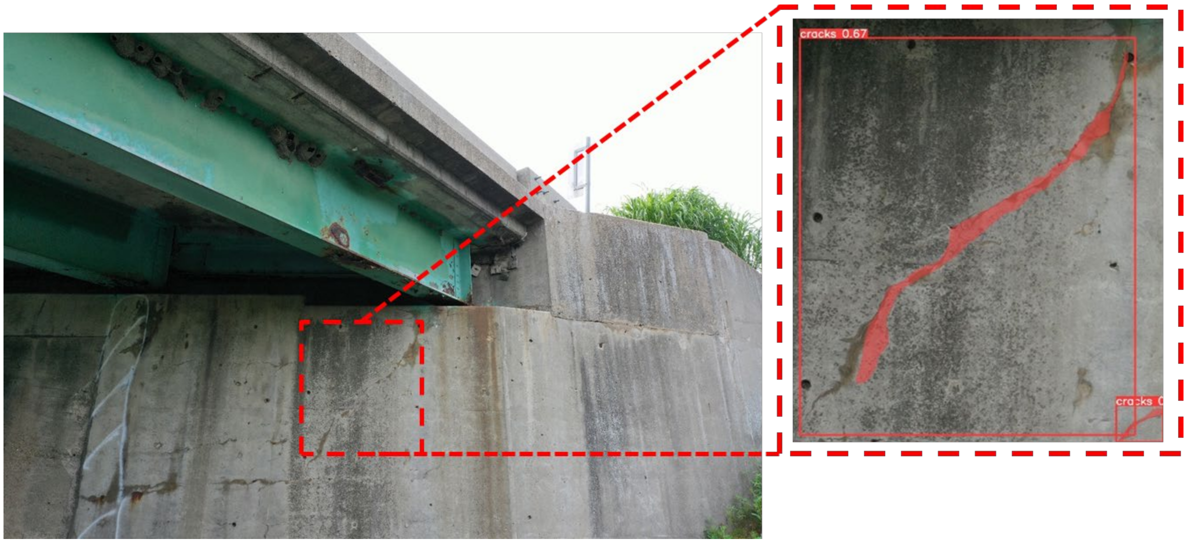

Figure 4.20. Result of concrete crack detection before and after an image is uploaded to the model (image from case study bridge)

4.5.2 Fine-Tuning and Transfer Learning

The process of enhancing the proposed model's predictive capabilities through fine-tuning yielded extraordinary improvements in damage detection. As can be observed from the progression illustrated in Figure 4.21, there was a significant evolution from initial inaccurate detection to highly precise identification of structural defects. This improvement was achieved through a comprehensive and iterative fine-tuning process, which involved carefully adjusting various parameters and training the model with diverse images encompassing a wide range of crack widths and spalling conditions. The use of a diverse and augmented dataset was a key aspect of the fine-tuning process. Different augmentation techniques were applied to increase the variety of the training dataset, including rotation within a range of -15 to +15 degrees, random horizontal and vertical flips, brightness and contrast adjustments, and the addition of Gaussian noise. The training dataset was enriched with images featuring concrete spalling of various sizes and depths as well as cracks of several widths and lengths (ranging from hairline cracks to extensive cracks exceeding 1 in.), as described in Section 4.4. This diversity allowed the model to learn to detect and classify cracks across a broad spectrum of sizes. Similarly, multiple types and severities of spalling were included in the dataset, from minor surface deterioration to extensive concrete loss, enabling the model to accurately identify different stages of spalling.

(a)

(b)

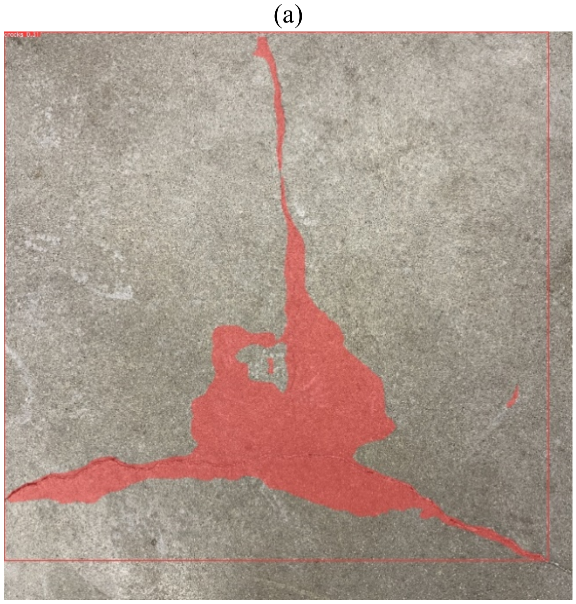

(c)

(d)

(e)

Figure 4.21. Result of fine-tuning in order to improve detection quality

The impact of the fine-tuning efforts is clearly visible in the series of images provided in Figure 4.21. In Figure 4.21a, a concrete surface with subtle, fine cracks that are challenging to detect with the naked eye is shown. This image represents the type of difficult case that the initial model struggled with, often missing these minor defects entirely. As the image series progresses from Figure 4.21a to 4.21e, the increasing accuracy of the model's detection capabilities can be observed.

In Figure 4.21b, the model's improved ability to detect and highlight a significant crack running vertically through the concrete surface is displayed. The red overlay precisely traces the path of the crack, demonstrating the model's enhanced sensitivity to linear defects. This accuracy is attributed to the fine-tuning process, particularly the inclusion of diverse crack widths in the training data.

In Figure 4.21c, a more complex crack pattern, with the defect branching out in multiple directions, is shown. The model's ability to accurately trace this intricate pattern showcases the success of the transfer learning approach. By leveraging weights from the initial model and fine-tuning them on more diverse and challenging datasets, significant improvements in the model's performance on complex defect patterns were achieved.

Figure 4.21d further illustrates the model's improved capabilities, with the accurate detection of a three-way crack junction. This level of precision in identifying complex crack geometries was a notable achievement of the fine-tuning process. The transfer learning approach allowed the model to build upon its basic understanding of linear cracks and extend this knowledge to more intricate patterns.

Finally, in Figure 4.21e, the model's ability to detect both fine cracks and more substantial defects within the same image is demonstrated. The long, horizontal crack is clearly identified, as well as the finer, vertical crack intersecting it. This comprehensive detection capability serves as a testament to the effectiveness of the transfer learning and fine-tuning approach and its role in enabling the model to simultaneously identify defects of varying scales and orientations.

4.5.3 Damage Quantification

A significant breakthrough in quantifying concrete structural defects was achieved after the tracking algorithm was implemented with the developed model. Remarkable accuracy in measuring crack widths and lengths, as well as the dimensions of concrete spalling in high-quality images, was demonstrated by the new model. This advancement is a substantial leap forward in automated structural health monitoring.

The results obtained from the model for the crack shown in Figure 4.22 are impressive. A total crack length of 115.124 in. and an average width of 0.913 in. were estimated. Upon comparing the model's estimations to the actual measurements of 112.2 in. for length and 0.97 in. for width, a length error of about 2.6% and a width error of approximately 6.2% were observed. These minor discrepancies highlight the model's high precision in real-world applications.

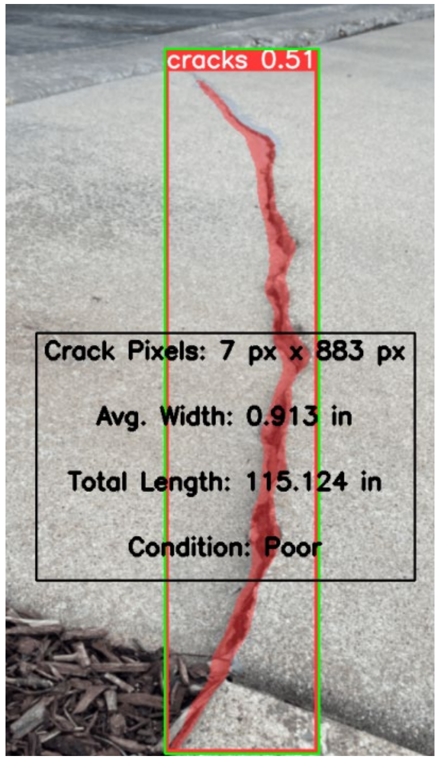

Figure 4.22. Result of crack quantification

The slightly higher error in the width dimension can be attributed to the measurement methodology. Width measurements were taken from different spots along the crack length, and the locations of these spots within the quantification model likely differed from those used for the manual measurements. The bounding box and overlay visible in the image provide further evidence of the model's ability to accurately detect and quantify cracks. The green bounding box encapsulates the entire crack length, while the red overlay traces its path with precision, demonstrating the model's sophisticated edge detection capabilities.

As mentioned above, the evaluation of the crack condition as "poor," based on the guidelines set forth in the *Manual for Bridge Element Inspection*, indicates that both the detected severity and the dimensions of the crack have surpassed critical thresholds. These thresholds are established to assess the structural integrity of the element, and, when exceeded, they signify a level of deterioration that typically requires immediate remedial action. The dimensions and severity of the detected crack suggest that it poses a potential risk to the overall stability of the structure. This classification of "poor" is not only a reflection of the crack's size and extent but also an indication that the defect could compromise the capacity of the bridge components. Therefore, timely intervention, such as structural assessment and potential repairs, would be necessary to ensure that the issue does not escalate into a more significant structural failure.

In Figure 4.23, another case of crack detection and measurement is presented that demonstrates the model's ability to accurately identify and quantify fine cracks in concrete structures. A crack with an actual width of 0.022 in. (0.56 mm) and a length of 56.3 in. (1.43 m) was analyzed using the developed model. The results from this analysis showcase the model's exceptional accuracy in detecting and measuring hairline cracks, which are notoriously difficult to assess using conventional methods due to their minute size and the challenges they pose to visual inspection.

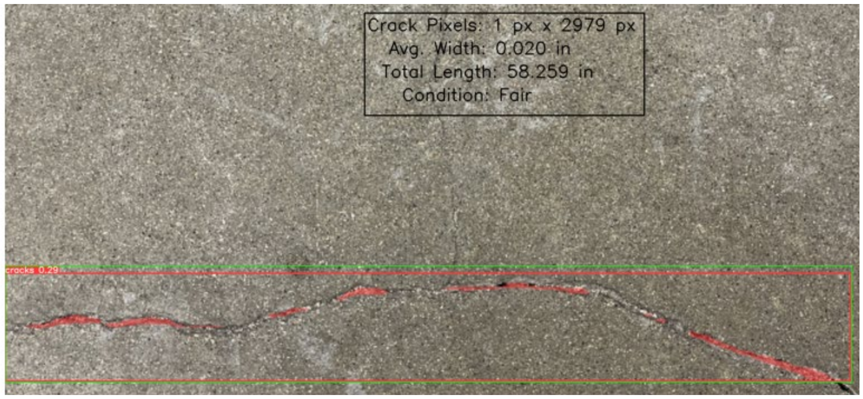

Figure 4.23. Result of crack quantification with different assessment

Upon comparing the model's measurements with the actual dimensions, a width error of approximately 9% and a length error of about 3.5% were observed. Although these errors are slightly higher than those found in other instances, they remain within an acceptable range for practical applications, especially considering the extremely fine scale of the crack width being measured. The difficulty in achieving precise measurements for such small cracks is significantly high, making the model's performance in this scenario particularly noteworthy.

The condition of the crack was classified as "fair" by the model, following the standards set by the *Manual for Bridge Element Inspection*. This automatic assessment was generated based on the quantified dimensions, along with other factors considered by the model's algorithms. The capability of the model to not only detect and measure cracks but also provide a condition assessment aligned with standardized inspection guidelines highlights its value. This functionality can greatly enhance the inspection process by streamlining evaluations, ensuring consistency across different inspectors, and maintaining uniform condition assessments across various locations. The automation of such assessments represents a significant advancement in improving the efficiency and accuracy of structural inspections.

The detection and quantification model accurately identifies and measures spalling in concrete structures, as shown in Figure 4.24. The model calculates the spalling dimensions as 31.943 x 14.700 in. (81.14 x 37.34 cm), resulting in an estimated area of 3.261 ft^2 (0.303 m^2). Comparing this to the actual measured area of approximately 3.05 ft^2 (0.283 m^2), we find a relatively small error of about 6.5%. The discrepancy in measurements likely stems from two main factors: (1) the unhighlighted areas around the edges of the spalling, which the model may have partially included in its calculations, and (2) potential differences in the exact location of measurements between the model and the manual assessment. Despite this minor deviation, the model's ability to quickly and automatically quantify spalling damage demonstrates its potential as a valuable infrastructure inspection and maintenance tool.

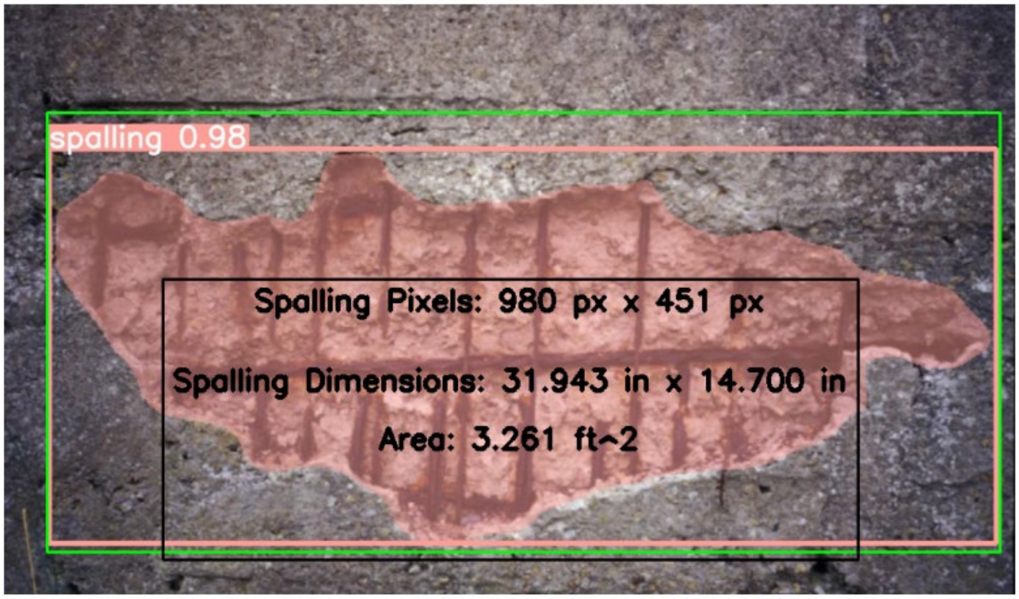

Figure 4.24. Result of concrete spalling quantification

Another key to obtaining an accurate assessment is knowing the camera's properties. Significantly, knowing the camera properties is crucial for exact measurements. The camera's focal length, sensor size, and distance from the subject are essential for converting pixel measurements to real-world dimensions. Without this information, the model's ability to provide precise physical measurements would be compromised, potentially leading to more significant errors in area and dimension calculations.

CHAPTER 5: SUMMARY AND CONCLUSIONS

This research project leveraged and identified opportunities to adopt UAVs to enhance the damage detection, inspection, and 3D modeling of bridge infrastructure. The core objective of the project was to develop an integrated system that combines UAV technology with advanced AI and ML algorithms specifically for bridge inspection and damage detection. By utilizing drones for high-precision data collection and AI/ML for the analysis of structural integrity, the system improved both the accuracy and efficiency of defect identification and to address the limitations of traditional inspection methods, which can be time-consuming and prone to human error. Furthermore, the system was designed to support predictive maintenance by continuously analyzing structural health data over time. This predictive approach allowed for the early identification of potential issues, enabling proactive decision-making and reducing the likelihood of critical failures. In addition to improving safety and reliability, the integration of UAVs, AI, and ML offered the potential for more cost-effective and timely maintenance of bridge infrastructure.

The implementation of UAVs has significantly advanced bridge inspection methodologies. These aerial imaging platforms facilitate the capture of high-resolution, multi-angle imagery of bridge structures. The proximity at which these UAVs operate allows for the detection of microfractures and surface degradation that may elude visual inspection from ground level. The resultant high-fidelity images enable inspectors to identify structural anomalies at an early stage, which is critical for proactive maintenance planning and ensuring the continued structural integrity and safety of the bridge. Furthermore, the accumulation of these high-quality images over time provides a temporal dataset that allows for the quantitative analysis of defect propagation, which is essential for predictive maintenance scheduling and long-term structural health monitoring. In the field of photogrammetry software, the conducted comparative analysis demonstrated the superior performance of Bentley iTwin Capture in generating 3D models from UAV-acquired imagery. Despite the fact that all of the software solutions in this research were assessed utilizing an identical image dataset, Bentley iTwin Capture’s algorithms produced notably more realistic and detailed 3D reconstructions compared to the other software solutions evaluated. The enhanced fidelity of these models was of particular importance, as it enabled virtual inspection from multiple perspectives, analogous to an in situ examination. This level of detail facilitated the identification of latent issues that may not be apparent in two-dimensional imagery, such as defects in complex structural interfaces or areas prone to water accumulation and subsequent deterioration.

The flight path and control methodology of the UAVs used to acquire images were identified as critical factors influencing the quality of the resultant 3D model. Empirical evidence suggested that utilizing preprogrammed, automated flight paths yields superior results compared to manual control. A case study demonstrated that manual operation led to insufficient image capture of the bridge’s substructure, resulting in an incomplete or poorly rendered 3D model. In contrast, automated flight protocols ensured comprehensive coverage of the structure, with images captured from all necessary angles systematically. This methodical approach was found to be fundamental to generating a complete and accurate 3D model, serving as a reliable basis for structural assessment and analysis.

Bentley iTwin Capture's integration of AI capabilities extended its functionality beyond mere 3D reconstruction. The software incorporated advanced measurement tools that leverage AI algorithms to automatically quantify various structural parameters within the 3D model. The accuracy of these AI-derived measurements was validated through comparison with in situ measurements, which demonstrated a high degree of concordance. This functionality enhanced the reliability of the software-generated data, potentially reducing the need for on-site measurements, which can be both hazardous and time-consuming. Moreover, the software's learning capabilities can be trained on custom datasets to recognize specific types of structural defects, such as cracks or corrosion. By training the AI on a comprehensive set of defect images, the system autonomously identified and flagged potential issues in new 3D models. This automated defect detection significantly enhanced the efficiency of the inspection process, allowing inspectors to prioritize areas of concern and allocate resources more effectively.

The implementation of the developed CNN model demonstrated significant advancements in the detection of structural defects, particularly cracks and spalling, in bridge infrastructure. This model achieved comprehensive defect detection with high accuracy across a diverse range of conditions, including varying image resolutions, lighting scenarios, and perspectives. Such robustness enhanced the reliability of damage detection in real-world applications, addressing a critical challenge in automated structural health monitoring. The model's architecture, optimized through iterative testing and validation, incorporated multiple convolutional layers and pooling operations to enable effective feature extraction from complex structural images. Its ability to maintain performance consistency across different environmental conditions was attributed to the diverse training dataset and the implementation of data augmentation techniques. This adaptability was crucial for practical deployment, as it allowed the model to function effectively in the varied and often challenging conditions encountered during bridge inspections. The improved detection capabilities of the proposed model contributed significantly to the field of structural engineering, offering a more efficient and accurate means of identifying potential structural weaknesses in bridge components.

Fine-tuning and transfer learning methodologies played a pivotal role in significantly enhancing the model's performance, enabling it to detect a broader range of defects with greater precision. The fine-tuning process involved careful adjustments to hyperparameters and the selective retraining of specific network layers, which optimized the model for the particular domain of bridge defect detection. Transfer learning, leveraging pretrained weights from large-scale image recognition tasks, allowed the model to benefit from generalized feature extraction capabilities while adapting to the nuances of structural defect identification. By utilizing diverse datasets and augmentation techniques, the model gained the ability to classify different crack widths and spalling severities with high accuracy. This enhanced classification capability was found to be crucial for predictive maintenance and informed decision-making in infrastructure management. The model's improved versatility allowed it to discern between hairline cracks and more severe fractures and differentiate various stages of spalling, providing a nuanced assessment of structural integrity. This solid level of defect categorization enabled infrastructure managers to prioritize maintenance activities more effectively, potentially leading to more efficient resource allocation and improved long-term structural health management strategies.

The developed damage detection model accurately quantified both crack dimensions and spalling area. By incorporating advanced algorithms, including the region-growing technique, the model successfully and accurately translated pixel-based measurements into real-world dimensions. This advancement represented a significant step forward in automating structural health monitoring and improving the accuracy of defect assessments in bridge infrastructure. The region-growing algorithm enabled the model to delineate defect boundaries precisely, allowing for accurate measurement of crack lengths and widths and spalling areas. The conversion from pixels to physical measurements was achieved through careful calibration that involves the consideration of imaging parameters such as distance to the structure and camera specifications. This level of precision in quantification was crucial for assessing the severity of structural damage and informing repair strategies. Moreover, the model's ability to provide consistent and accurate measurements across various environmental conditions enhanced its reliability as a tool for long-term monitoring of structural health. By offering quantitative data on defect progression over time, the model supported more informed decision-making in bridge maintenance and rehabilitation planning.

REFERENCES

Abdelkader, E. M., M. Marzouk, and T. Zayed. 2020. A self-adaptive exhaustive search optimization-based method for restoration of bridge defects images. *International Journal of Machine Learning and Cybernetics*, Vol. 11, No. 8, pp. 1659–1716.

Adel, M., H. Yokoyama, H. Tatsuta, T. Nomura, Y. Ando, T. Nakamura, H. Masuya, and K. Nagai. 2021. Early damage detection of fatigue failure for RC deck slabs under wheel load moving test using image analysis with artificial intelligence. *Engineering Structures*, Vol. 246, Article 113050.

Ai, D., G. Jiang, S. K. Lam, P. He, and C. Li. 2023. Computer vision framework for crack detection of civil infrastructure—A review. *Engineering Applications of Artificial Intelligence*, Vol. 117, Article 105478.

Aliakbar, M., U. Qidwai, M. R. Jahanshahi, S. Masri, and W. M. Shen. 2016. Progressive image stitching algorithm for vision based automated inspection. *International Conference on Machine Learning and Cybernetics, Jeju Island, South Korea*, Vol. 1, pp. 337–343.

Alipour, A., and B. Shafei. 2016a. Assessment of post-earthquake losses in a network of aging bridges. *Journal of Infrastructure Systems*, Vol. 22, No. 2, Article 04015023.

Alipour, A., and B. Shafei. 2016b. Seismic resilience of transportation networks with deteriorating components. *Journal of Structural Engineering*, Vol. 142, No. 8, Article C4015015.

Alipour, A., and B. Shafei. 2022. An overarching framework to assess the life-time resilience of deteriorating transportation networks in seismic-prone regions. *Journal of Resilient Cities and Structures*, Vol. 1, No. 2, pp. 87–96.

Aliyari, M., E. L. Droguett, and Y. Z. Ayele. 2021. UAV-based bridge inspection via transfer learning. *Sustainability*, Vol. 13, No. 20, Article 11359.

Allah Bukhsh, Z., I. Stipanovic, A. Saeed, and A. G. Doree. 2020. Maintenance intervention predictions using entity-embedding neural networks. *Automation in Construction*, Vol. 116, Article 103202.

Murakami, S., H. Ichikawa, and Yiliguoqi. 2020. Utilization of SVM in the soundness evaluation of reinforced concrete slab bridge. *Journal of Japan Society of Civil Engineers*, Vol. 8, No. 1, pp. 59–70.

Ayele, Y. Z., M. Aliyari, D. Griffiths, and E. L. Droguett. 2020. Automatic Crack Segmentation for UAV-Assisted Bridge Inspection. *Energies*, Vol. 13, No. 23, Article 6250.

Azad, S., and B. Shafei. 2025. Performance evaluation of semi-integral abutment bridge ends based on approach slab details. *Journal of Bridge Engineering*, Vol. 30, No. 3, Article 04024117.

Bao, Y., J. Li, T. Nagayama, Y. Xu, B. F. Spencer Jr., and H. Li. 2021. The First International Project Competition for Structural Health Monitoring (IPC-SHM, 2020): A summary and benchmark problem. *Structural Health Monitoring*, Vol. 20, No. 4, pp. 2229–2239.

Belcore, E., V. Di Pietra, N. Grasso, M. Piras, F. Tondolo, P. Savino, D. R. Polania, and A. Osello. 2022. Towards a FOSS automatic classification of defects for bridge structural health monitoring. *Communications in Computer and Information Science*, Vol. 1507, pp. 298–312.

Bhowmick, S., S. Nagarajaiah, and A. Veeraraghavan. 2020. Vision and deep learning-based algorithms to detect and quantify cracks on concrete surfaces from UAV videos. *Sensors*, Vol. 20, No. 21, pp. 1–19, Article 6299.

Bianchi, E. L., N. Sakib, C. Woolsey, and M. Hebdon. 2022. Bridge inspection component registration for damage evolution. *Structural Health Monitoring*, Vol. 22, No. 1, pp. 472–495.

Cha, Y. J., and W. Choi. 2017. Vision-based concrete crack detection using a convolutional neural network. *Dynamics of Civil Structures, Volume 2: Proceedings of the 35th IMAC, A Conference and Exposition on Structural Dynamics,* pp. 71–73.

Cha, Y. J., W. Choi, and O. Büyüköztürk. 2017. Deep learning-based crack damage detection using convolutional neural networks. *Computer-Aided Civil and Infrastructure Engineering*, Vol. 32, No. 5, pp. 361–378.

Chen, J., Y. Liu, and J. A. Hou. 2023. A lightweight deep learning network based on knowledge distillation for applications of efficient crack segmentation on embedded devices. *Structural Health Monitoring*, Vol. 22, No. 5, pp. 3027–3046.

Chun, P. J., T. Yamane, and Y. Maemura. 2022. A deep learning-based image captioning method to automatically generate comprehensive explanations of bridge damage. *Computer-Aided Civil and Infrastructure Engineering*, Vol. 37, No. 11, pp. 1387–1401.

Deng, J. H., Y. Lu, and V. C. S. Lee. 2021. Imaging-based crack detection on concrete surfaces using You Only Look Once network. *Structural Health Monitoring An International Journal*, Vol. 20, No. 2, pp. 484–499.

Dipankar, A., and S. K. Suman. 2023. Pavement crack detection based on a deep learning approach and visualisation by using GIS. *International Journal of Pavement Engineering*, Vol. 24, No. 1, Article 2173754.

Fan, C. L. 2021. Detection of multidamage to reinforced concrete using support vector machine-based clustering from digital images. *Structural Control and Health Monitoring*, Vol. 28, No. 12, Article e2841.

Feng, C., H. Zhang, S. Wang, Y. Li, H. Wang, and F. Yan. 2019. Structural damage detection using deep convolutional neural network and transfer learning. *KSCE Journal of Civil Engineering*, Vol. 23, pp. 4493–4502.

Galdelli, A., M. D'Imperio, G. Marchello, A. Mancini, M. Scaccia, M. Sasso, E. Frontoni, and F. Cannella. 2022. A Novel Remote Visual Inspection System for Bridge Predictive Maintenance. *Remote Sensing*, Vol. 14, No. 9, Article 2248.

Gulgec, N. S., M. Takáč, and S. N. Pakzad. 2019. Convolutional neural network approach for robust structural damage detection and localization. *Journal of Computing in Civil Engineering*, Vol. 33, No. 3, Article 04019005.

Guo, L., R. Li, and B. Jiang. 2021. A cascade broad neural network for concrete structural crack damage automated classification. *IEEE Transactions on Industrial Informatics*, Vol. 17, No. 4, pp. 2737–2742.

Hafiz, A., T. Schumacher, and A. Raad. 2022. A self-referencing nondestructive test method to detect damage in reinforced concrete bridge decks using nonlinear vibration response characteristics. *Construction And Building Materils*, Vol. 318, Article 125924.

Ichinose, L. Kohno, Y. Kitada, T. Matsumura, and M. Matsumura. 2007. Applications of eddy current test to fatigue crack inspection of steel bridges. *Memoirs – Faculty of Engineering Osaka City University*, Vol. 48, Article 57.

Jeong, E., J. Seo, and P. E. J. Wacker. 2022. UAV-aided bridge inspection protocol through machine learning with improved visibility images. *Expert Systems with Applications*, Vol. 197, Article 116791.

Kebig, T., V. H. Nguyen, M. Bender, M. Schäfer, and S. Maas. 2021. Repeatability and precision of different static deflection measurements on a real bridge-part under outdoor conditions in view of damage detection. International Conference on Structural Health Monitoring of Intelligent Infrastructure (SHMII 10), June 30–July 2, Porto, Portugal.

Khaloo, A., D. Lattanzi, K. W. Cunningham, R. Dell'Andrea, and M. Riley. 2018. Unmanned aerial vehicle inspection of the Placer River Trail Bridge through image-based 3D modelling. *Structure and Infrastructure Engineering*, Vol. 14, pp. 124–136.

Khatami, D., B. Shafei, and O. Smadi. 2016. Management of bridges under aging mechanisms and extreme events: A risk-based approach. *Transportation Research Record: Journal of the Transportation Research Board*, Vol. 2550, No. 1, pp. 89–95.

Khatami, D. and B. Shafei. 2021. Impact of climate conditions on deteriorating reinforced concrete bridges in the U.S. Midwest region. *Journal of Performance of Constructed Facilities*, Vol. 35, No. 1, Article 04020129.

Khatami, D., B. Shafei, and B. Bektas. 2023. Data-assisted prediction of deterioration of reinforced concrete bridges using physics-based models. *Journal of Infrastructure Systems*, Vol. 29, No. 2, Article 05023003.

Kim, B., N. Yuvaraj, H. W. Park, K. R. S. Preethaa, R. A. Pandian, and D. E. Lee. 2021. Investigation of steel frame damage based on computer vision and deep learning. *Automation In Construction*, Vol. 132, Article 103941.

Kim, I. B., J. S. Cho, G. S. Zi, B. S. Cho, S. M. Lee, and H. U. Kim. 2021. Detection and identification of expansion joint gap of road bridges by machine learning using line-scan camera images. *Applied System Innovation*, Vol. 4, No. 4, Article 94.

Kong, X., Z. Zhang, L. Meng, and H. Tomiyama. 2020. Machine Learning Based Features Matching for Fatigue Crack Detection. *Procedia Computer Science*, Vol. 174, pp. 101–105.

Kulkarni, A., and B. Shafei. 2018. Impact of extreme events on transportation infrastructure in Iowa: A Bayesian network approach. *Transportation Research Record: Journal of the Transportation Research Board*, Vol. 2672, No. 48, pp. 45–57.

Kun, J., Z. Zhenhai, Y. Jiale, and D. Jianwu. 2022. A deep learning-based method for pixel-level crack detection on concrete bridges. *IET Image Processing*, Vol. 16, No. 10, pp. 2609–2622.

Lattanzi, D., G. R. Miller, M. O. Eberhard, and O. S. Haraldsson. 2016. Bridge column maximum drift estimation via computer vision. *Journal of Computing in Civil Engineering*, Vol. 30, No. 4, Article 04015051.

Li, G., Q. W. Liu, S. M. Zhao, W. T. Qiao, and X. L. Ren. 2020. Automatic crack recognition for concrete bridges using a fully convolutional neural network and naive Bayes data fusion based on a visual detection system. *Measurment Science And Technology*, Vol. 31, No. 7, Article 075403.

Li, S., and X. Zhao. 2019. Image-based concrete crack detection using convolutional neural network and exhaustive search technique. *Advances In Civil Engineering, Select Proceedings of ARICE 2019*. Springer, New York, NY.

Liu, P. C. Y., and N. El-Gohary. 2020. Semantic image retrieval and clustering for supporting domain-specific bridge component and defect classification. *Construction Research Congress,* Reston, VA, pp. 809–818.

Liu, Y., and M. Gao. 2022. Detecting cracks in concrete structures with the baseline model of the visual characteristics of images. *Computer-Aided Civil and Infrastructure Engineering*, Vol. 37, No. 14, pp. 1891–1913.
Mahnert, K.-C., and U. Hundhausen. 2017. A review on the protection of timber bridges. *Wood Material Science and Engineering*, Vol. 13, pp. 1–7.
Malek, K., A. Mohammadkhorasani, and F. Moreu. 2022. Methodology to integrate augmented reality and pattern recognition for crack detection. *Computer-Aided Civil and Infrastructure Engineering*, Vol. 38, No. 8, pp. 1000–1019.
Malekloo, A., E. Ozer, M. AlHamaydeh, and M. Girolami. 2021. Machine learning and structural health monitoring overview with emerging technology and high-dimensional data source highlights. *Structural Health Monitoring*, Vol. 21, No. 4, pp. 1906–1955.
Medhi, M., A. Dandautiya, and J. L. Raheja. 2019. Real-time video surveillance based structural health monitoring of civil structures using artificial neural network. *Journal of Nondestructive Evaluation*, Vol. 38, No. 3, pp. 1–16.
Meng, S., Z. Gao, Y. Zhou, B. He, and A. Djerrad. 2022. Real-time automatic crack detection method based on drone. *Computer-Aided Civil and Infrastructure Engineering*, Vol. 38, No. 7, pp. 849–872.
Mir, B. A., T. Sasaki, K. Nakao, K. Nagae, K. Nakada, M. Mitani, T. Tsukada, N. Osada, K. Terabayashi, and M. Jindai. 2022. Machine learning-based evaluation of the damage caused by cracks on concrete structures. *Precision Engineering*, Vol. 76, pp. 314–327.
Mirzazade, A., M. P. Nodeh, C. Popescu, T. Blanksvärd, and B. Täljsten. 2022. Utilization of computer vision technique for automated crack detection based on uav-taken images. *Lecture Notes in Civil Engineering*, Vol. 200, pp. 713–720.
Modarres, C., N. Astorga, E. L. Droguett, and V. Meruane. 2018. Convolutional neural networks for automated damage recognition and damage type identification. *Structural Control and Health Monitoring*, Vol. 25, No. 10, Article e2230.
Montaggioli, G., M. Puliti, and A. Sabato. 2021. Automated damage detection of bridge's sub-surface defects from infrared images using machine learning. *Health Monitoring of Structural and Biological Systems*, Vol. 11593, pp. 427–435.
Morgenthal, G., N. Hallermann, J. Kersten, J. Taraben, P. Debus, M. Helmrich, and V. Rodehorst. 2019. Framework for automated UAS-based structural condition assessment of bridges. *Automation In Construction*, Vol. 97, pp. 77–95.
Munawar, H. S., F. Ullah, D. Shahzad, A. Heravi, S. Qayyum, and J. Akram. 2022. Civil infrastructure damage and corrosion detection: An application of machine learning. *Buildings*, Vol. 12, No. 2, Article 156.
Nair, A., and C. S. Cai. 2010. Acoustic emission monitoring of bridges: Review and case studies. *Engineering Structures*, Vol. 32, No. 6, pp. 1704–1714.
Naser, M. Z. 2021. Can past failures help identify vulnerable bridges to extreme events? A biomimetical machine learning approach. *Engineering with Computers*, Vol. 37, No. 2, pp. 1099–1131.
Özgenel, Ç. F. 2019. Concrete crack segmentation dataset. *Mendeley Data*, Vol. 1.
Pantoja-Rosero, B. G., D. Oner, M. Kozinski, R. Achanta, P. Fua, F. Perez-Cruz, and K. Beyer. 2022. TOPO-Loss for continuity-preserving crack detection using deep learning. *Construction and Building Materials*, Vol. 344, Article 128264.

Perry, B. J., Y. Guo, R. Atadero, and J. W. van de Lindt. 2020. Streamlined bridge inspection system utilizing unmanned aerial vehicles (UAVs) and machine learning. *Measurement: Journal of the International Measurement Confederation*, Vol. 164, Article 108048.

Perry, B. J., Y. Guo, and H. N. Mahmoud. 2022. Automated site-specific assessment of steel structures through integrating machine learning and fracture mechanics. *Automation in Construction*, Vol. 133, Article 104022.

Qiao, W., B. Ma, Q. Liu, X. Wu, and G. Li. 2021. Computer vision-based bridge damage detection using deep convolutional networks with expectation maximum attention module. *Sensors (Basel)*, Vol. 21, No. 3, Article 824.

Qin, H., F. Huang, and B. Cheng. 2021. Crack identification and measurement of bridges by using CNN models. *Bridge Maintenance, Safety, Management, Life-Cycle Sustainability, and Innovations*. CRC Press, Boca Raton, FL, pp. 123–128.

Quqa, S., P. Martakis, A. Movsessian, S. Pai, Y. Reuland, and E. Chatzi. 2022. Two-step approach for fatigue crack detection in steel bridges using convolutional neural networks. *Journal of Civil Structural Health Monitoring*, Vol. 12, No. 1, pp. 127–140.

Reagan, D., A. Sabato, and C. Niezrecki. 2017. Feasibility of using digital image correlation for unmanned aerial vehicle structural health monitoring of bridges. *Structural Health Monitoring*, Vol. 17, No. 5, pp. 1056–1072.

Sakagami, T., Y. Izumi, Y. Kobayashi, Y. Mizokami, and S. Kawabata. 2014. Applications of infrared thermography for nondestructive testing of fatigue cracks in steel bridges. *Thermosense: Thermal Infrared Applications*, Vol. 9105, pp. 169–176.

Savino, P., and F. Tondolo. 2021. Automated classification of civil structure defects based on convolutional neural network. *Frontiers of Structural and Civil Engineering*, Vol. 15, No. 2, pp. 305–317.

Seo, J., L. Duque, and J. Wacker. 2018. Drone-enabled bridge inspection methodology and application. *Automation In Construction*, Vol. 94, pp. 112–126.

Seo, J., E. Jeong, and J. Wacker. 2022. Machine learning approach to visual bridge inspection with drones. *Structures Congress 2022.* American Society of Civil Engineers, Reston, VA, pp. 160–169.

Shafei, B., A. Alipour, and M. Shinozuka. 2013. A stochastic computational framework to investigate the initial stage of corrosion in reinforced concrete superstructures. *Journal of Computer-Aided Civil and Infrastructure Engineering*, Vol. 28, No. 7, pp. 482–494.

Shafei, B., A. Alipour, and M. Shinozuka. 2012. Prediction of corrosion initiation in reinforced concrete members subjected to environmental stressors: A finite element framework. *Journal of Cement and Concrete Research*, Vol. 42, No. 2, pp. 365–376.

Shi, W., M. Najimi, and B. Shafei. 2020. Reinforcement corrosion and transport of water and chloride ions in shrinkage-compensating cement concretes. *Journal of Cement and Concrete Research*, Vol. 135, Article 106121.

Shi, W., B. Shafei, Z. Liu, and B. Phares. 2020. Longitudinal box-beam bridge joints under monotonic and cyclic loads. *Journal of Engineering Structures*, Vol. 220, Article 110976.

Song, C., L. Wu, Z. Chen, H. Zhou, P. Lin, S. Cheng, and Z. Wu. 2019. Pixel-level crack detection in images using SegNet. *Lecture Notes in Computer Science (Lecture Notes in Artificial Intelligence)*, Vol. 11909, pp. 247–254.

Tang, Y., Z. Huang, Z. Chen, M. Chen, H. Zhou, H. Zhang, and J. Sun. 2023. Novel visual crack width measurement based on backbone double-scale features for improved detection automation. *Engineering Structures*, Vol. 274, Article 115158.

Uesaka, M., Y. Mitsuya, K. Dobashi, J. Kusano, E. Yoshida, Y. Oshima, and M. Ishida. 2018. On-site bridge inspection by 950 keV/3.95 MeV portable X-band Linac X-ray sources. *Bridge Optimization-Inspection and Condition Monitoring*. InTechOpen, London, UK.

Wang, B. S., and Z. C. He. 2007. Crack detection of arch dam using statistical neural network based on the reductions of natural frequencies. *Journal of Sound and Vibration*, Vol. 302, No. 4, pp. 1037–1047.

Wang, D. L., Y. Q. Dong, Y. Pan, and R. J. Ma. 2020. Machine vision-based monitoring methodology for the fatigue cracks in U-rib-to-deck weld seams. *IEEE Access*, Vol. 8, pp. 94204–94219.

Wu, L., S. Mokhtari, A. Nazef, B. Nam, and H.-B. Yun. 2016. Improvement of crack-detection accuracy using a novel crack defragmentation technique in image-based road assessment. *Journal of Computing in Civil Engineering*, Vol. 30, No. 1, Article 04014118.

Xu, S., M. Hao, G. Liu, Y. Meng, J. Han, and Y. Shi. 2022. Concrete crack segmentation based on convolution–deconvolution feature fusion with holistically nested networks. *Structural Control and Health Monitoring*, Vol. 29, No. 8, Article e2965.

Yang, J., L. Zhang, C. Chen, Y. Li, R. Li, G. Wang, S. Jiang, and Z. Zeng. 2020. A hierarchical deep convolutional neural network and gated recurrent unit framework for structural damage detection. *Information Sciences*, Vol. 540, pp. 117–130.

Yang, L., and G. Cervone. 2019. Analysis of remote sensing imagery for disaster assessment using deep learning: a case study of flooding event. *Soft Computing*, Vol. 23, No. 24, pp. 13393–13408.

Zhai, G. H., Y. Narazaki, S. Wang, S. A. V. Shajihan, and B. F. Spencer. 2022. Synthetic data augmentation for pixel-wise steel fatigue crack identification using fully convolutional networks. *Smart Structures and Systems*, Vol. 29, No. 1, pp. 237–250.

Zhang, D., C. Cui, X. Zhang, Z. Jiang, X. Zhang, and Y. Bao. 2023. Monitoring fatigue cracks in rib-to-deck joints of orthotropic steel deck using ultrasonic Lamb waves. *Thin-Walled Structures*, Vol. 189, Article 110922.

Zhang, Q., S. Babanajad, S. Ho Ro, J. Braley, and A. H. Alavi. 2023. Multi-resource fusion of nondestructive evaluation data for bridge deck assessment using discrete wavelet transform and Dempster-Shafer theory. *Measurement: Journal of the International Measurement Confederation*, Vol. 220, Article 113303.

Zhang, S., Z. Fu, G. Li, and A. Liu. 2023. Lane crack detection based on saliency. *Remote Sensing*, Vol. 15, No. 17, Article 4146.

Zhang, Y., and K.-V. Yuen. 2022. Review of artificial intelligence-based bridge damage detection. *Advances in Mechanical Engineering*, Vol. 14, No. 9, pp. 1–21.

Zheng, Y., Y. Gao, S. Lu, and K. M. Mosalam. 2022. Multistage semisupervised active learning framework for crack identification, segmentation, and measurement of bridges. *Computer-Aided Civil and Infrastructure Engineering*, Vol. 37, No. 9, pp. 1089–1108.

Zhou, J., L. Huo, G. Song, and H. Li. 2019. Deep learning-based visual inspection for the delayed brittle fracture of high-strength bolts in long-span steel bridges. *Proceedings of International Conference on Image and Video Processing, and Artificial Intelligence*. International Society of Optics and Photonics, Bellingham, WA, pp. 530–535.

Zhu, J. S., C. Zhang, H. D. Qi, and Z. Y. Lu. 2020. Vision-based defects detection for bridges using transfer learning and convolutional neural networks. *Structure and Infrastructure Engineering*, Vol. 16, No. 7, pp. 1037–1049.